RED BLOOD CELL HEMOLYSIS:

PROTEIN BIOMAKER DISCOVERY FOR PRODUCT QUALITY ASSESSMENT

by

Deborah Chen

B.MLSc., The University of British Columbia, 2012

A THESIS SUBMITTED IN PARTIAL FULFILLMENT OF

THE REQUIREMENTS FOR THE DEGREE OF

DOCTOR OF PHILOSOPHY

in

THE FACULTY OF GRADUATE AND POSTDOCTORAL STUDIES

(Pathology and Laboratory Medicine)

THE UNIVERSITY OF BRITISH COLUMBIA

(Vancouver)

December 2017

Abstract

Red blood cell (RBC) transfusion is a cornerstone therapeutic intervention in contemporary medicine. Stored RBCs undergo multiple biochemical and biophysical changes, collectively referred to as the RBC storage lesions. One of the most prominent alterations is hemolysis, the rupturing of RBC and the subsequent release of hemoglobin-rich cytosolic content. Hemolysis may compromise the red cell concentrate (RCC) therapeutic efficacy with a decrease in viable and functional cells and an increase in bioactive molecules that may disrupt vascular and immune homeostasis. Thus, hemolysis is used as a key surrogate indicator of RCC storage quality; however, this parameter is evaluated at expiry and all RCCs are transfused without knowing their levels of hemolysis. With aims to optimize product quality for transfusion recipients and to improve donor and inventory management efficiency, the identification of predictive markers for storage hemolysis warrants further investigation.

While the molecular mechanism(s) of hemolysis remain elusive, a few factors such as donor characteristics and manufacturing processes are known to influence its development. From a unique donor population composed of repeat donors exhibiting high hemolysis, membrane-associated proteins involved in antioxidant pathways - peroxiredoxin-2, catalase, and 20s proteasome - were identified as potential quality markers using isobaric tag for relative and absolute quantitation. Additionally, in a novel comparative study between RCC subjected to gamma-irradiation and pathogen inactivation (PI), the level of these candidate protein markers displayed robust negative linear relationship with storage hemolysis. These candidate protein markers hint at the role of oxidative damage in product quality deterioration and hemolysis development. While deoxygenation treatment successfully rescued elevated hemolysis in PI-treated RCCs, the application of these protein markers did not yield similar relationship to hemolysis development. This observation suggests that PI-induced damage is heavily reliant on

the presence of oxygen and that the identified protein quality markers may not be specific to oxidative damage alone.

Taken together, the findings presented here propose three potential candidate protein markers for product quality and further support that cumulative oxidative damage contributes to storage hemolysis development. However, the results suggest that there may be additional underlying metabolic and/or molecular mechanisms that are important for hemolysis development.

Lay Summary

Red cell concentrates (RCCs) are one of the most common blood products used in transfusion. The quality of RCCs decreases with time spent in storage; one of the most obvious signs of deterioration is the rupturing of red blood cell (RBC) and the subsequent release of hemoglobin, known as hemolysis. Too much hemoglobin outside of the RBC membrane is dangerous to transfusion recipients. Fortunately, hemolysis can readily be measured and is used as a primary quality control parameter for RCCs. It would be very helpful to have a specific marker that would identify donors whose RCC would not store well at the time of blood collection. As hemolysis development depends on RBC membrane integrity, investigation into the changes of the membrane proteins of RCCs exhibiting high hemolysis may provide insights into what factors affect the product quality. This may also inform the management of blood products and its delivery system.

Preface

Chapter 1 contains contents published in the following review articles: Devine DV, **Chen D**. A fresh look at measuring quality in blood components. ISBT Science Series, 2014. 9: 148–154, and **Chen D**, Serrano K, Devine DV. Introducing the red cell storage lesion. ISBT Science Series. 2016. 11: 26–33. For the review entitled “A fresh look at measuring quality in blood components”, I conducted the appropriate literature review, created a comparative table of the main regulatory guidelines, and drafted the RBC Standards section of the manuscripts. For the review entitled “Introducing the red cell storage lesion”, I conducted the appropriate literature review, drafted and critically revised the manuscript.

Chapter 3 contains material published in a manuscript entitled - Proteomics of red blood cells from donors exhibiting high hemolysis demonstrates a reduction in membrane-associated proteins involved in the oxidative response. (**Chen D**, Schubert P, Devine DV. Transfusion. 2017. 57(9):2248-2256). All of the co-authors conceived and designed the study. I performed all of the research, interpreted the data, drafted and critically revised the manuscript.

A version of Chapter 4 has been published. (**Chen D**, Schubert P, Devine DV. Identification of potential protein quality markers in pathogen inactivated and gamma-irradiated red cell concentrates. Proteomics Clinical Applications. 2017. **11(7-8)**:1600121). All of the co-authors conceived and designed the study. I executed all of the research, interpreted the data, drafted and critically revised the manuscript. Chapter 4 also contains data published in the following articles: Qadri SM*, **Chen D***, Shubert P*, Bhakta V, Devine DV, Sheffield WP. Pathogen inactivation by riboflavin and ultraviolet light illumination accelerates the red blood cell storage lesion and promotes eryptosis. Transfusion. 2017. 57(3):661-673 and Qadri SM*, **Chen D***, Shubert P*, Devine DV, Sheffield WP. Early γ-irradiation and subsequent storage of red cells in

SAG-M additive solution potentiates the storage lesion and susceptibility to apoptotic cell death. Vox Sang. 2017. 112(5):480-483 (**shared first authorship*). I conducted the research, interpreted the data, and critically revised the manuscripts.

Chapter 5 is based on preliminary work conducted in collaboration with New Health Sciences and Canadian Blood Services Centre for Innovation, funded in part by Health Canada. Dr. Peter Schubert kindly provided *in vitro* quality parameters (Schubert P, Culibrk B, Serrano K, *et al.* Improvement of red cell quality upon pathogen inactivation of whole blood using riboflavin/UV light by deoxygenation. Transfusion 2016. **56**:S4; 57A). I performed the western blots, analyzed and interpreted the data.

Materials have been used with permission from applicable sources.

Research Ethics Boards of both Canadian Blood Services and University of British Columbia granted ethics approval for studies presented in Chapter 3 with Protocol Reference # 2013-005 and Certificate # H12-03560, respectively. Studies presented in Chapter 4 and 5 were approved by the Canadian Blood Services Research Ethics Board (Protocol Reference # 2015.004) and were exempted from ethics approval by University of British Columbia Research Ethics Board.

Table of Contents

List of Tables

List of Figures

List of Abbreviations

2, 3-BPG	2, 3-bisphosphoglycerate
AChE	Acetylcholinesterase
ADP	Adenosine diphosphate
AMP	Adenosine monophosphate
ANOVA	Two-way analysis of variance
AS	Additive solution
ATP	Adenosine triphosphate
AU	Arbitrary unit
BC	Buffy coat
CO_2	Carbon dioxide
CLL	Combinatorial peptide ligand libraries
Da	Dalton
DAF	Decay accelerating factor
DEHP	Di(2-ethylhexyl) phthalate
ESI	Electrospray ionization
FDA	Food and Drug Administration
G6PD	Glucose-6-phosphate dehydrogenase
Ghost	Hemoglobin-depleted RBC membrane
GPI	Glycosyl-phosphatidylinositol
GSH or GS-SG	Glutathione
Gy	Gray
HCT	Hematocrit
Hb	Hemoglobin

HH	High hemolyzers
HCD	Higher-energy collisional dissociation
HPLC	High-performance liquid chromatography
HIV	Human Immunodeficiency Virus
H_2O_2	Hydrogen peroxide
iTRAQ	Isobaric tags for relative and absolute quantitation
LR	Leukoreduced or leukoreduction
LTQ	Linear trap quadropole
LC	Liquid chromatography
MS	Mass spectrometry
MS/MS	Tandem mass spectrometry
MALDI-TOF	Matrix-assisted laser desorption ionization-time of flight
MCF	Mean corpuscular fragility
MCV	Mean corpuscular volume
metHb	Methemoglobin
NetCAD	Network Centre for Applied Development
NADH or NAD^+	Nicotinamide adenine dinucleotide
NADPH or $NADP^+$	Nicotinamide-adenine dinucleotide phosphate
NO	Nitric oxide
N_2	Nitrogen
O_2^-	Superoxide
oxyHb	Oxyhemoglobin
pI	Isoelectric point
PI	Pathogen inactivation or pathogen inactivated
PS	Phosphatidylserine

PCM(s)	Post-collection manipulation(s)
QC	Quality control
RCTs	Randomized, controlled clinical trials
ROS	Reactive oxygen species
RBC(s)	Red blood cell(s)
RMV(s)	Red blood cell-derived microvesicle(s)
RCC(s)	Red cell concentrate(s)
$RCC^{Ø}$ or RCC^{Ctrl}	Control or untreated red cell concentrates
RCC^{γ}	Gamma-irradiated red cell concentrates
RCC^{PI}	Pathogen inactivated red cell concentrates
RCC^{WB*}	Red cell concentrates derived from deoxygenated whole blood
RCC^{WB*+PI}	Red cell concentrates derived from deoxygenated whole blood followed by pathogen inactivation,
SAGM	Saline-adenine-glucose-mannitol
So_2	Oxygen saturation
SOD	Superoxide dismutase
Th	Thomson
TA-GVHD	Transfusion-associated graft versus host disease
UV	Ultraviolet
WB	Whole blood
WBF	Whole blood filtration

Acknowledgements

I offer my enduring gratitude to my family and friends, who have been so encouraging, empathetic, and supportive throughout this journey. I owe particular thanks to my supervisor, Dr. Dana V. Devine, whose genuine care, mentorship, and ongoing encouragement to explore various opportunities during my graduate studies expanded my horizons and accelerated my growth as a scientist and beyond. A special thank you to Dr. Peter Schubert, for your penetrating questions and stimulating discussions taught me how to question more deeply and to think more critically. I would also like to acknowledge my fellow lab members, past and present, for their friendship and support made this process enjoyable and gratifying. Moreover, I would like to thank my thesis supervisory committee – Dr. Ed Pryzdial, Dr. Mark Scott, and Dr. Don Brooks – for your guidance and expertise enlarged my vision and appreciation of science. Finally, sincere gratitude to all of the volunteer donors for their generosity and staff at the Network Centre for Applied Development (NetCAD) for their technical support, without whom this work would not be possible.

Dedication

This dissertation is dedicated to: my brain surgeon, Dr. Gary Redekop, whose skilled hands gave my life a new beginning; my rehabilitation team at G.F. Strong - Dr. Derry Dance, Karen Wruck (RSLP), Stacey Anutooshkin (OT), Gillian Coates (PT), and Farida Lalji (SW) – whose expertise, compassion, kindness, and guidance provided me with the right tools and mindset to navigate my recovery; and my partner, Dr. Ryan N. Goldsbury, who had saved my life and whose unconditional love and unrelenting support through my recovery made it possible for me to regain the necessary confidence and strength to complete this work.

Chapter 1: Introduction

1.1 Normal Human Red Blood Cell

Red blood cells (RBCs), or erythrocytes, are the most abundant blood cell type in the circulation. Mature RBCs circulate for approximately 100-120 days before their components are recycled. These anucleated, biconcave discoid cells (~8 μm in diameter) are specialized to traverse narrow capillaries (2-3 μm) and transport oxygen from the outer environment to respiring tissues, through the sophisticated functional properties of hemoglobin (Hb).

The Hb tetramer consists of one pair of α-like globin chains and one pair of β-like globin chains; each globin chain contains a hydrophobic pocket that binds one iron-containing heme molecule, providing a non-polar environment to protect against auto-oxidation of the metal. The heme iron can assume the ferrous or the ferric oxidation state, with only the former being able to reversibly bind oxygen. Dependent on the characteristic protein conformational change with oxygen binding (e.g. positive cooperativity between the oxygen-binding sites), Hb exhibits a sigmoidal oxygenation curve that ensures adequately sensitive oxygen release in response to small fluctuation in oxygen tension. Allosteric effectors, including 2, 3-bisphosphoglycerate (2, 3-BPG), pH, and carbon dioxide, are able to modulate Hb affinity to oxygen.

1.1.1 Red Blood Cell Membrane

The RBC membrane is an asymmetric lipid bilayer, containing w/w 49.2% proteins, 43.6% total lipids (of which 32.5% are phospholipids and 11.1% cholesterol), and 7.2% carbohydrates (of which 4% are neutral sugars, 2.0% hexosamines, and 1.2% sialic acids) [1]. The organization and maintenance of biomolecules at the membrane and the resulting structure afford the RBC its unique property of great deformability - vital for its physiological function.

1.1.1.1 **Membrane Lipids**

The diverse molecular species of phospholipids and cholesterol allows for appropriate packing of biomolecules in the membrane bilayer and governs fluidity and protein-lipid interactions[2]. The glycolipids and most of the choline phospholipids are located in the outer layer, while phosphotidylinositol's and the aminophospholipids (e.g., phosphatidylserine (PS) and phosphatidylethanolamine) are located in the inner leaflet[3].

While the lipids are able to move dynamically across the plane of the bilayer, their dominant organization is not random. Lateral inhomogeneities of lipids species (enriched in sphingolipids and cholesterol) facilitate organization of other membrane components (e.g., flotillins, stomatin, glycosyl-phosphatidylinositol (GPI)-anchored proteins) into local microdomains or "rafts" that are involved in specific physiologic processes, such as signal transduction[4]. Moreover, the asymmetric membrane lipid organization reflects a dynamic equilibrium of transbilayer (flip-flop) motion of lipid species. Again, these movements are not random; they are controlled and regulated by specific proteins (e.g., ATP-dependent flippases, floppases, and translocases) and cytosolic factors, with aims to maintain the asymmetric lipid distribution across the membrane leaflets as it is important for cellular functions[5].

An alteration in this asymmetric lipid distribution could potentiate a physiological event. For example, exposure of PS at the surface has been associated with apoptosis and senescence[6,7]. The recognition of exposed PS by macrophages serves as a signal for the removal of injured apoptotic cells[8]. Furthermore, the restriction of PS to the inner leaflet also inhibits the adhesion of normal RBCs to vascular endothelial cells, thereby ensuring hemostasis and vascular flow[9]. Moreover, when the incorporation of fatty acids in the repair of phospholipids is impaired due to cytosolic alterations and damage in the highly oxidant cytosolic environment, the maintenance of the asymmetric lipid composition could be compromised and may subsequently lead to altered membrane deformability[10]. Taken together, the highly dynamic

organization of the complex mixture of lipid molecules in the membrane is central for RBC to perform their function in the circulation.

1.1.1.2 Membrane Proteins

Lipid composition determines the overall fluidity of the matrix in which transmembrane proteins are embedded, while their interaction with the underlying skeletal protein network determines the overall stability and deformability of the RBC membrane[11]. For example, band 3 macromolecular complexes (e.g., band 3/RhAG and band 3/Glut1) provide crucial membrane cohesion and structural integrity via linkage with principal protein constituents in the spectrin-based membrane skeletal network, including ankyrin, protein 4.1R, adducin, and dematin[12-14], while the dynamic protein-protein interactions within the skeletal network govern RBC membrane stability. Interestingly, lipid-protein interactions also appear to play a role in modulating membrane stability; PS interacts with certain triple-helical repeats of both α- and β-spectrin and may augment membrane stability[15].

Our understanding of the structural organization of the various lipid and protein components of the normal RBC membrane continues to evolve. For example, the recent application of advanced proteomics approaches revealed unexpected complexity of RBC membrane and cytosolic proteomes[16-18].

1.1.2 Cellular Metabolism

Due to the lack of nuclei and other intracellular organelles, mature RBCs are incapable of generating energy via oxidative phosphorylation. Instead, RBCs are reliant on anaerobic conversion of glucose by the Embden-Meyerhof pathway for the generation of high-energy phosphates to maintain a number of vital cell functions (**Figure 1.1**)[19,20].

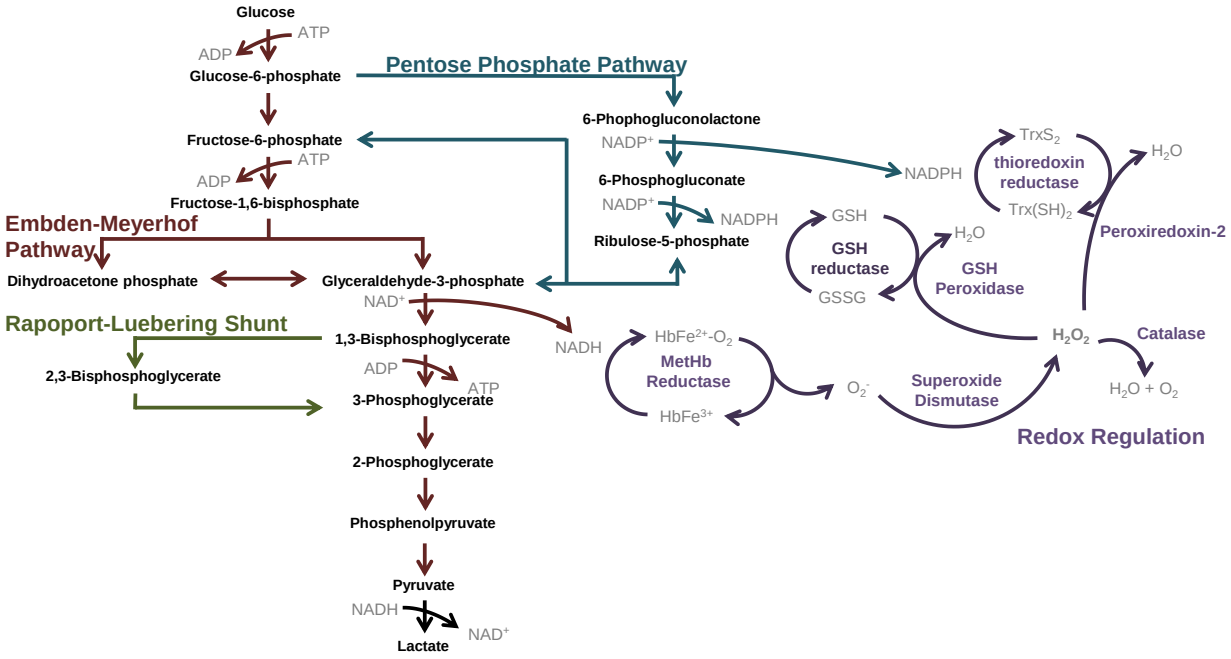

Figure 1.1 Cellular metabolism in RBCs.

The utilization of glucose in RBC via the Embden-Meyerhof Pathway is depicted here, complete with the pentose phosphate shunt and the Rapoport-Luebering shunt. The occurring steady origin of oxidative stress is shown by heme oxidation and the release of superoxide anion. The main antioxidant response pathways are displayed here.

1.1.2.1 Regulation of Ion Transport

Since water movement follows that of cations and anions or is induced by changes in tonicity of the surrounding environment, regulation of ion transport across the membrane is central to the maintenance of RBC osmotic stability and deformability. Aquaporin mediates rapid exchange of water across the hydrophobic membrane[21]. Kuchel and Benga proposed that the high water permeability enabled by the presence of aquaporin allows for an efficient energy-driven membrane undulation by avoiding the displacement of surrounding water[22]. Additionally, aquaporin may also play an important physiological role in maintenance of cell volume, as it

would permit concomitant displacement of water molecules when rapid entry and exit of ions of solutes takes place[22].

Several transport pathways are involved in establishing the dynamic homeostasis of ion content; energy-dependent transport systems (e.g., sodium/potassium ATPase) create necessary concentration gradients that are then utilized by several energy-independent transport systems (e.g., potassium/chloride co-transporter and calcium-activated potassium channel), which may respond to changes in pH, cell volume, and/or membrane integrity. The activity of the sodium/potassium ATPase (with a 3:2 stoichiometry), along with diffusional leaks (inward sodium gradient and outward potassium gradient), is crucial in determining RBC's low sodium, high potassium cellular composition at steady state[23]. For example, the potassium/chloride co-transporter (a passive, gradient-driven transport pathway) utilizes the high potassium intracellular content to extrude potassium and chloride from the erythrocyte; it has been shown to play a role in the pathologic dehydration of sickle erythrocytes, either alone or in conjunction with the calcium-activated potassium channel [24,25], further demonstrating the importance of regulated ion transport for cellular function.

1.1.2.2 **Maintenance of Oxidative Balance**

Paradoxically, oxygen is inherently dangerous to aerobic life. For RBCs, whose primary physiological function is to transport oxygen between the lung and respiring tissues, oxidative stress is inevitable. Thankfully, they are equipped with a repertoire of agents, which work together to prevent, intercept, and repair damage caused by oxygen metabolites[26].

Hb, the specialized oxygen transporter within the RBC, is the most susceptible to oxidative stress. When Hb is oxidized from its ferrous to ferric state, methemoglobin (metHb) does not have the capacity to transport oxygen. The RBC is able to convert metHb into oxyhemoglobin (oxyHb) via both nicotinamide adenine dinucleotide (NADH) and reduced

nicotinamide-adenine dinucleotide phosphate (NADPH) metHb reductase, with the principal reductase using NADH as the cofactor. However, should metHb undergo additional oxidation, protein precipitation and subsequent formation of Heinz bodies may occur, which decreases cellular flexibility and results in premature removal via splenic sequestration[27]; highlighting the importance of efficient oxidative response pathways to maintain vital cellular functions.

Additional antioxidant enzymes also help to minimize damage induced by oxygen radicals (**Figure 1.1**). Perhaps the best known of these enzymes is superoxide dismutase (SOD), which catalyzes dismutation of superoxide (O_2^-) into hydrogen peroxide (H_2O_2). The cellular concentration of cytosolic SOD appears to determine optimal oxidant defense, where elevated SOD activity (as commonly observed in sickle cells) exacerbates oxidation due to the accelerated generation of H_2O_2 [28,29]. Downstream enzymes, including glutathione (GSH) peroxidase, catalase, and peroxiredoxin-2, degrade H_2O_2 by reducing it to H_2O and O_2 to minimize its toxicity.

GSH peroxidases utilize the reducing power of the sulfhydryl moiety of the cysteine residue in the degradation of H_2O_2, in which a disulfide-bond is formed between two GSH molecules (GS-SG). NADPH functions primarily as a cofactor for the reduction of GSH-containing disulfides in the RBC through the mediation of enzyme GSH reductase, which catalyzes the conversion of one molecule of GS-SG back into two molecules of GSH, thus permitting the continuous action of GSH peroxidase[30].

Unlike other mammalian cells, catalase is located in the cytoplasm in the RBC and plays a major role in the scavenging of H_2O_2[31-33]. Similar to GSH peroxidase, catalase appears to also require NADPH for continual operation: Kirkman *et al.* demonstrated that NADPH efficiently prevents the formation of catalase compound II and facilitates the reduction back to its active form (from compound II to compound I) [34,35].

Peroxiredoxin-2, a thiol-dependent homodimer peroxidase, is another important antioxidant within the RBC that effectively competes with GSH peroxidase and catalase in decomposing low levels of H_2O_2[36]. Peroxiredoxin-2 detoxifies H_2O_2 through the oxidation of cysteine residues and is then recycled via the thioredoxin/thioredoxin reductase system[37]. The redox status of peroxiredoxin-2 has been proposed as a potential biomarker for oxidative stress in RBC[38-40]. Its physiological function and importance in erythrocytic oxidative metabolism have been extensively investigated in murine models: peroxiredoxin-2 is essential for RBC survival *in vivo*, as the disruption of peroxiredoxin-2 expression results in marked accumulation of intraerythrocytic H_2O_2 and Heinz body formation, concomitant with compensatory elevated reticulocyte counts and erythropoietin levels[41,42].

Despite the multitude of antioxidant defenses in RBC, oxidative damage is unavoidable and damaged biomolecules must be recognized and removed: the proteasome complex (more specifically, the 670 kDa core or the 20S proteasome complex) is able to degrade oxidatively modified proteins in an ubiquitin- and ATP-independent manner, where the exposure of hydrophobic patches on the surface of oxidized proteins are recognized and serve as binding sequences for the 20S proteasome[43-46].

Proteins involved in the oxidative response pathway, more specifically catalase, peroxiredoxin-2, and 20S proteasome, will be studied and discussed in more detail in the context of RCC storage quality later in this dissertation.

1.1.2.3 **Upkeep of 2, 3-Bisphosphoglycerate**

The Rappaport-Luebering shunt off the anaerobic glycolysis pathway yields 2, 3-BPG for the regulation of Hb oxygen dissociation equilibrium (**Figure 1.1**). The organophosphate preferentially binds to deoxygenated Hb; its interaction with deoxygenated Hb helps to stabilize the low oxygen affinity state and promotes the release of remaining oxygen molecules bound to

the Hb. The upkeep of a high level of 2, 3-BPG is crucial for the ease with which Hb releases oxygen to the respiring tissues.

1.2 Red Blood Cell Storage Lesion

In modern blood component therapy, RBCs are separated from other blood components after whole blood (WB) collection and concentrated with the removal of plasma or collected by apheresis procedures. An essential feature of routine transfusion therapy is the ability to store blood components. Following separation from plasma, RBCs are suspended in an additive solution within a soft-sided plastic storage container and held, normally without agitation, at 4 ± 2°C. The length of storage time - dependent on a combination of local regulation, the composition of the additive solution and the characteristics of the plastic container - ranges between 21 and 49 days, with most countries storing red cell concentrates (RCCs) for between 35 and 42 days[47]. However, the isolation of RBCs and their storage in non-biological containers at non-biological temperatures cause fundamental changes in cellular biochemistry above and beyond the normal ageing processes that they would otherwise undergo in the body[48-50].

Over the allowable RCC storage period, these alterations are apparent in the routine examination of stored cells *in vitro*. With the storage of RCCs in liquid form, changes occurring over time ultimately lead to the inability of the RBC to maintain its integrity, at which point the cell ruptures. The processes, occurring between the initial collection of blood and the lysis of the RBCs, result in a constellation of changes known as the RBC storage lesions.

1.2.1 Metabolic Effects

RBCs depend solely on anaerobic glycolysis for the generation of energy during their lifespan[20]. In this process, RBCs break down one molecule of glucose to produce two molecules of lactate, yielding two molecules of ATP. Coupled to ATP hydrolysis, two protons are

generated, increasing the acidity of the storage solution over time. Although most transfusion recipients have the ability to compensate for this pH change by respiratory and renal mechanisms, massive transfusions may overwhelm these systems and lead to transfusion-induced acid-base abnormalities.

The acidosis that occurs in storage slows glycolysis by the inhibition of the key enzymes, phosphofructokinase and hexose kinase, resulting in reduced ATP production and failure to maintain NADPH through the pentose phosphate pathway[20,50]. Progressive decline in ATP availability during storage may negatively influence RBC *in vitro* quality. ATP concentration is the best metabolic correlate to RBC shape changes throughout storage and to *in vivo* recovery[50]. Stored RBCs have a decreased capability to sustain normal glutathione and peroxiredoxin-2 levels; this may in turn reduce the ability of the RBC membranes to avoid oxidative damage, thereby contributing to further deterioration of RBC function and viability.

Moreover, the decrease in pH also favours the breakdown of 2, 3-BPG. On average, 2, 3-BPG decreases to an undetectable level within 2 weeks of storage[49]. A low level of 2, 3-BPG leads to a left-shifted oxygen disassociation curve, increasing Hb oxygen saturation and affinity. In other words, the degree of hypoxia must be more severe to trigger oxygen unloading in the absence of 2, 3-BPG than that in the presence of 2, 3-BPG. Theoretically, negligible 2, 3-BPG levels in RBCs should not be a major concern in transfusion, as this metabolic alteration is reversible once the RBCs are back *in vivo* post-transfusion. 2, 3-BPG concentration returns to 50% of physiological levels within 24-hours[51] and is fully regenerated within 48 hours[52]. However, in transfusion recipients requiring acute restoration of oxygen releasing capacity or those with reduced compensatory mechanisms, considerations should be given to the regeneration kinetics of 2, 3-BPG.

The major membrane sodium/potassium ATPase is inhibited at low temperature, leading to continuous leakage of intracellular potassium under blood banking conditions[50]. The

accumulation of potassium in the storage solution has been suggested to increase the risk of hyperkalemia-induced arrhythmia or even sudden death in vulnerable patients, such as neonates, patients with renal failure, or those receiving massive transfusions[53,54].

1.2.2 Biomechanical Effects

RBC storage lesions can also be visualized morphologically. The normal resting shape of the RBC is a biconcave disc, which affords RBCs with a maximum surface area to facilitate gas exchange and with the necessary flexibility to travel through the capillary network and the reticuloendothelial system[55]. During storage, RBCs slowly evolve from smooth biconcave discs to spiculated echinocytes to dense spheroechinocytes (**Figure 1.2**). Biomechanical changes occur in parallel with metabolic changes and may be a direct result of metabolic alteration. As mentioned previously, RCC acidification and decrease in ATP concentration affect RBC shape maintenance in storage. Nakao and colleagues induced shape change by ATP depletion and demonstrated that crenated RBC could revert to their original discoid shape with adenine supplementation[56], demonstrating that RBC shape maintenance is dependent on ATP concentration.

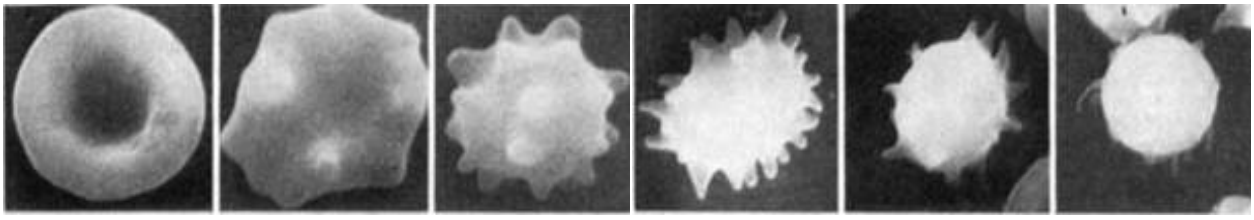

Figure 1.2 Typical stored RBC morphology.

From biconcave discoid to spherocytes. Figure 1 from Usry RT, Moore GL, Manalo FW. Morphology of stored, rejuvenated human erythrocytes. Vox Sang 1975; 28:175-183. Page 178. Adapted with permission from publisher.

While some RBC morphological alterations may be reversible, modification of cell shape and membrane loss via microvesiculation from the tips of echinocytic spines is irreversible[57]. RBC-derived microvesicle (RMV) release is a controlled process, stimulated by pro-apoptotic signals, shear stress, or oxidative damage[58]. RMV formation has been implicated in RBC senescence and proposed as a mechanism to remove damaged cellular components to delay untimely removal of RBCs[48]. RMVs are heterogeneous in size, ranging from 100 to 1000 nm in diameter. They consist of phospholipids, transmembrane proteins, and cytoskeletal proteins but are lacking in spectrin[57]. Moreover, RMVs expose negatively charged phospholipids, providing pro-inflammatory and pro-coagulant surfaces that may increase post-transfusion complications[59] by triggering coagulation through tissue factor signaling, inducing of pro-inflammatory cytokine release, and enhancing cell-cell interaction between platelets and neutrophils[60]. Ultimately, RBC microvesiculation leads to decreased surface to volume ratio and increased cell rigidity, thus contributing to the reduction in RBC deformability. These storage-related shape changes are thought to reduce RBC post-transfusion survival due to their decreased ability to rapidly and adequately adopt their shape according to flow conditions, which may lead to occlusion in capillary beds or even intravascular rupture of RBCs[61,62].

The shape changes of RBC are associated with rheological properties. RBCs stored under blood-banking conditions show significantly enhanced aggregability, adherence to endothelial cells, and decreased deformability by two weeks of storage[63]. The sialic acid content of RBCs decreases with storage[64], leading to reduction of the electrostatic repulsive forces that protect RBCs from aggregation[65]. RBC aggregates may be more resistant to dispersal by blood flow-induced shear stress, thus contributing to blood viscosity and potentially block flow in small vessels with impairment of tissue perfusion. Moreover, PS translocation to the RBC surface increases during storage, adding to the progressive adherence of RBCs to endothelial cells. The role of PS in RBC-endothelial cell interaction was confirmed by demonstrating complete

suppression of adhesion when PS is blocked using annexin V [64]. Elevated interaction between RBC and endothelial cells could potentially cause local turbulent flow, subsequently activating endothelial cells and facilitating unwanted inflammation. Alternatively, adherent RBCs may directly occlude capillaries and cause downstream ischemia. Together, these impaired flow properties induced by storage may contribute to transfusion-related circulatory risk in recipients[66].

1.2.3 Oxidative Effects

Under aerobic storage conditions, RBCs are constantly exposed to a pro-oxidative environment. Normally, RBCs are well equipped with SOD, glutathione, catalase, peroxiredoxin-2, and metHb reductases to repair any oxidative damage[50] in addition to generating NADPH reducing equivalents via the pentose phosphate pathway (**Figure 1.1**). However, all of these protective mechanisms are impaired during storage, the likelihood of hydroxyl radical formation via the Fenton reaction increases and can overwhelm the erythrocyte's antioxidant response pathways.

During storage, RBCs undergo progressive oxidative insult to proteins and lipids. For example, the formation of band 3 oligomers during storage is attributed to protein oxidation and lipid peroxidation[67]. Band 3 clustering due to oxidation is also hypothesized as a mechanism for senescent RBC removal[68]. Spectrin damage by progressive oxidative stress correlates well to RMV formation during storage[69]. Oxidative damage can also cause formation of lysophospholipid, which has been suggested to contribute to transfusion-related acute lung injury[49]. These observations suggest that RBC function and viability deteriorate as the oxidative injury persists over storage.

1.2.4 Clinical Impact of Storage Induced Changes

While the mechanisms of storage lesion development are still not completely understood, *in vitro* studies have demonstrated that this deterioration is linked to a reduction in viability and function of RBCs[61,70]. Such reduction in RBC quality over time has been suggested to correlate to poor *in vivo* efficacy of stored RCC, contributing to adverse post-transfusion events[70]. Concerns have also been raised about the accumulation of bioactive substances in stored RCC that actively perturb immune function[48,70]. However, the clinical impact of RBC storage lesions development remains largely unknown.

As noted above, the RBC storage lesions negatively influence RBC integrity. Metabolic modulation, shape changes, altered rheological properties, and oxidative injury collectively contribute to progressive RBC degradation, resulting in RBC lysis and the subsequent release of cytosolic content and large amounts of Hb, or hemolysis. This is the ultimate manifestation of the RBC storage lesions, as the RBC is no longer viable and can provide no therapeutic benefit to the transfusion recipient.

The release of cytosolic content increases extracellular potassium concentration, further contributing the risk of hyperkalemia-induced arrhythmia in susceptible recipients. Free Hb is a potent inducer of oxidative stress, which can augment the RBC storage lesions development. Gladwin's group observed that the release of both free Hb and RMV upon hemolysis increase the rate of nitric oxide (NO) scavenging by endothelial cells[71,72]. NO is a soluble gas continuously synthesized from arginine in endothelial cells by nitric oxide synthase and acts as an important signal in the regulation of vasodilation and blood flow. Free Hb and RMV have been demonstrated to react with the vasodilator NO at approximately 1000 times faster than intact erythrocytes[73]. The 1:1 NO consumption by free Hb is further accelerated with the concomitant release of cytosolic arginase, which depletes the arginine necessary for NO production by the endothelial cells[74]. This leads to acute vasoconstriction, platelet activation,

and inflammation via activation of toll-like receptors, which could lead to clinically significant outcomes in critically ill transfusion recipients[73,75]. Additionally, transfusion of RBCs results in some degree of immediate clearance from the circulation, as evidenced by elevated serum iron levels. Typically, most RBC clearance occurs within the first hour after transfusion and about 25% of the cells in a transfused unit of RCC are removed by the spleen in the first few passes[76]. This is a significant iron load for the body to manage via the haptaglobin-CD163 scavenger receptor sequester pathway[77] and it is possible to detect non-transferrin-bound iron in the circulation after transfusion. In an autologous transfusion study, Rapido *et al*. demonstrated that 78% of healthy volunteers who received RCCs stored for 6 weeks exhibited significant levels of non-transferrin-bound iron that persisted for 10 hours or more[78]. The downside is that this level of iron load generates ROS, which may in turn cause further production of cytokines and altered immunity[79]. Moreover, free iron is also able to promote the growth of bacteria and increase risk of infection[80-82]. In patients with acute leukemia, circulating non-transferrin-bound iron levels > 2 μM following bone marrow myelosuppression were associated with increased risk of infectious complication[80]. In a canine transfusion model, higher non-transferrin-bound iron levels were associated with enhanced virulence of *Streptococcus aureus*, as evidenced by increased mortality, lung injury, and degree of shock[81]. Moreover, a rapid decline in serum iron and non-transferrin-bound iron was observed with concomitant increase in bacterial load and worsened infection, indicating iron utilization by bacteria to augment growth[82]. Thus, it is important to understand the role of iron in transfusion and the opportunities to minimize unnecessary iron burden for recipients. Increasing concern over the possible role of RMV in transfusion-related immunomodulation has led to ongoing studies that seek to refine the question of the role of the RBC storage lesions in the efficacy of transfusion.

The allowable shelf life of RCCs is determined based on *in vitro* measures of RBC deterioration and measurements of survival in healthy volunteers. It is reasonable to suggest

that there is a limit to RCC storage, beyond which the risk of transfusion outweighs the benefit of the intervention. In order for blood banks to balance product availability and product quality, it is crucial for research to assist in identifying such limits of RCC storage. With the knowledge that RBC changes are inevitable during storage, the scientific community debates the efficacy of transfusion with older RCCs and the benefit of fresh RCCs. Several prospective, randomized, controlled clinical trials (RCTs) in different patient populations have recently been conducted in order to understand the post-transfusion patient outcomes as a function of age of stored RCCs. To date, none of these RCTs has shown a negative effect of the transfusion of older RBCs that are still within their allowable storage window (**Table 1.1**). However, there is a body of literature, mostly composed of retrospective studies, that indicates that the duration of storage of RBCs is an independent risk factor in patient outcome[83]. The results from these RCTs will continue to generate discussion and while the issue is not fully resolved, these results mean that at least for the next while, RBC storage practices are under less pressure to change.

Despite the results of these RCTs and the recognized limitations of retrospective studies, there is a "common" belief that fresh RCCs would provide maximal benefit to patients. However, because the literature contains numerous mostly retrospective clinical studies that provide conflicting results, the total body of evidence cannot support any definitive conclusion at this time[84]. A meta-analysis of 22 observational studies of the association of age of RCCs with adverse post-transfusion outcomes has shown that length of RCC storage is bound to be associated with adverse outcome, because it is associated with the number of units transfused[85]. This is the result of the "first-in-first-out" distribution practice adopted by the blood banks in which the oldest compatible unit is issued from inventory to minimize outdate rate. In other words, the more units a patient requires, the more likely s/he will receive old RCCs. Moreover, the number of units required by a patient is heavily dependent on the severity of his/her medical condition and is the principle confounder in determining the association between

age of blood and adverse post-transfusion outcome. As most blood systems are currently organized, the administration of only fresh RCCs is logistically unrealistic, if not impossible. It would cause a massive shortage in RCC supply and impede many aspects of medical care.

While there is strong consensus regarding the relevance of *in vitro* time-dependent biochemical and cellular changes in stored RBCs within the scientific community, we do not fully understand which of the storage-induced RBC changes are the most clinically relevant. Despite the results of the clinical trials in **Table 1.1**, the debate on whether old RCCs are efficacious continues. Further research is needed to find parallels between RBC storage lesions development and clinical outcomes.

Table 1.1 Recently reported medium to large randomized controlled trials of the effect of RBC storage time on patient outcomes

Updated Table 1 from Chen D, Serrano K, Devine DV. Introducing the red cell storage lesion. ISBT Science Series 2016; 11:26-33. Page 30. Adapted with permission from publisher.

Trial Name	Study Population	Patients Studied	Primary Outcome	Result	References
ARIPI	Pediatric intensive care unit; premature infants (weight <1250g)	377	Composite measure of major neonatal morbidities, e.g.; necrotizing enterocolitis, bronchopulmonary dysplasia, intraventricular hemorrhage, and death	Fresh red cells (≤7 days) did not improve outcomes compared to standard issue red cells	86,87
ABLE	Critically ill intensive care unit patients (≥18 years of age)	2430	90-day all cause mortality	Fresh red cells (≤7 days) did not decrease the 90-day mortality compared to standard issue red cells	88
RECESS	Cardiac surgery patients (≥12 years of age)	1098	Change in Multiple Organ Dysfunction Score (from the pre-operative score through day 7 or time of death/discharge)	Fresh red cells (≤10 days) did not improve primary outcome compared to old red cells (>21 days)	89,90
TRALI2	Critically ill patients whose lungs are mechanically ventilated (≥18 years of age)	100	pulmonary gas exchange as assessed by the partial pressure of arterial oxygen to the fraction of inspired oxygen concentration ratio.	Fresh red cells (≤5 days) did not improve primary outcome compared to standard issue red cells	91
TRANSFUSE	Critically ill intensive care unit patients	5000 (target, ongoing)	90-day all cause mortality	NCT01638416 No published data.	92
INFORM	General population of hospitalized patients who required a RCC (≥18 years of age)	31,497	In-hospital mortality	Fresher blood (freshest available unit) was not superior to standard issue red cells. ISRCTN08118744	93

1.2.5 Moderating the Red Blood Cell Storage Lesions

Efforts to improve the quality of stored red cells have a long history and are anchored in the large number of studies of basic RBC physiology conducted by researchers both within and outside of transfusion medicine. For example, the basic understanding of the requirement for ATP in RBC biochemical processes led to the addition of adenine in today's formulation of RBC

preservative solutions. Thus, the gradual RBC membrane crenation that occurs in parallel with reduced capacity to generate ATP over storage can be moderated by increasing the cell's access to adenine. In addition to the development of additive solutions to preserve red cell viability, improvements were made to the methods of component production. More recent efforts have resulted in a cold rejuvenation process that incubates the RBCs with a solution of pyruvate-inosine-phosphate-adenine at neutral pH in order to at least partly reverse storage-induced RBC shape change[94]. Koshkaryev *et al.* observed significant PS internalization on the RBC surface post-storage rejuvenation treatment, suggesting it is possible to reduce the amount of negatively charged phospholipid on the surface of older RBCs, which should produce a concomitant reduction in storage-induced RBC-endothelial cell adhesion and lead to an improvement in RBC survival in recipients[64]. Furthermore, anaerobic storage decreases RBC hemolysis, ameliorates morphological lesions, and prevents alterations to the cytoskeletal proteome[95,96].

The rate of the RBC storage lesion development is influenced by how RCC are prepared, and notably the properties of the storage containers. The inclusion of di(2-ethylhexyl) phthalate (DEHP) as the plasticizer in polyvinylchloride blood storage bags provided a stabilization of the cell membrane that improved stored RBC quality[97]. While DEHP has fallen out of favour in some jurisdictions owing to theoretical concerns about human teratogenicity and its potential as an endocrine disruptor, it is an example of a storage improvement effected by altering the materials properties of the container.

Regulatory guidelines are in place to ensure blood product quality, based on measures of viability and physical integrity of stored RBCs. Analyses required by regulatory authorities generally differ whether approval is sought for licensure of a novel product or process, or for assessment of quality control (QC) of existing approved component production. For licensure, *in vitro* studies as well as *in vivo* survival studies are often required. The latter involve a

standard measure of viability known as the autologous 24-hour *in vivo* recovery. An aliquot of chromium 51-labeled RBCs obtained at the end of storage is injected into the autologous donor-recipient. The expected percentage of injected cells circulating at 24 hours is typically expected to be greater than 75%. This measurement is sensitive to the presence of injected stored RBCs; however, it does not account for their oxygen carrying capacity. Also, 75% *in vivo* circulation at 24-hour is somewhat arbitrary and may not reflect clinical outcome[98]. For QC measures, the focus is generally on demonstration of sterility and adequate Hb concentration. Hemolysis is often used as a measure of physical integrity of stored RBCs. Hb is released into the additive solution (AS) upon hemolysis and can be easily measured spectrophotometrically [99]. According to the Canadian Standards Association, RCCs must not exceed 0.8% hemolysis at the maximal duration of preservation.

The detrimental effects of RBC storage lesions - biochemical, biomechanical and oxidative changes - have been partially addressed by improvements in component production and in storage conditions.

1.3 Red Blood Cell Proteome

One of the biggest hindrances to comprehensive analysis of protein profiling is the huge dynamic range of proteins present in the typical complex biological sample. In RBC, Hb accounts for more than 90% of the cellular dry weight and approximately 98% of overall cytoplasmic protein content[100], which challenges the detection of low-abundance proteins and results in inevitable losses of information. Investigations on the RBC proteome have made constant gradual progress over the years and the introduction of mass spectrometry (MS) has dramatically altered the research landscape.

The first in-depth RBC membrane proteome identified 102 proteins using both one-dimensional (1D) and two-dimensional (2D) in-gel digestion prior to matrix-assisted laser

desorption ionization-time of flight (MALDI-TOF) MS analysis[18]. Goodman *et al*. applied liquid chromatography-electrospray ionization (LC-ESI) technology to identify 91 membrane and 91 cytosolic RBC proteins in well-characterized membrane fractions, such as the inside-out vesicles[101]. In 2006, Pasini and colleagues generated one of the most comprehensive lists of RBC proteome, identifying 340 membrane and 252 soluble proteins, using a combination of biochemical sub-fractionation techniques with LC-ESI-MS/MS (either quadrupole TOF or Fourier transform)[16]. Differences in sample preparation methodologies and challenge associated with analyzing hydrophobic membrane proteins resulted in inconsistencies of reported findings among different RBC membrane proteome studies. Thus, efforts have been made to create a validated reference web database of RBC membrane proteins for research and diagnostic biomarker development[102].

Resolution was dramatically improved with more sophisticated sample preparation protocols, such as the combinatorial peptide ligand libraries (CLL) technique, which markedly enriched low-abundance RBC soluble proteins and resulted in the identification of 800 unique, non-redundant proteins[103,104]. Moreover, Roux-Dalvai and coworkers were able to elucidate 1578 cytosolic proteins, using two different CLL in series coupled with Orbitrap MS[105]. These proteomics studies revealed striking RBC protein diversity, sparking interest in the examination of interrelationships between proteins. Parallel to the RBC proteome mining efforts, protein-protein interaction network analyses showed that a series of proteins involved in oxidative defense and cellular repair (e.g., peroxiredoxins, catalases, proteasomal subunits, chaperonines, and heat shock proteins) appear to be central to maintaining homeostasis[106-108]. These findings align with our intuition, as RBCs are exposed to continuous oxidative stress and are unable to synthesize new proteins to replace those that are damaged. Furthermore, Bordbar *et al*. curated the expansive proteomic data and integrated experimental literature to reconstruct a metabolism network model, that would allow for systematic analysis and integration of high-

throughput proteomic data in a biochemically meaningful and coherent manner[109]. Their bioinformatics work demonstrated unanticipated complexity of RBC metabolism; the reconstructed network accounted for previously neglected areas of carbohydrate, nucleotide, amino acid, cofactors, and lipid metabolism.

Proteomics technologies advance our understanding of molecular mechanisms of RBC development[110], assessing changes in the cytosol[111] or membrane of RBCs. While there are numerous membrane proteomics investigations of stored RCCs, these reports mainly focused on revealing the diverse complexities of the RBC proteome[16,17,112,113] and were infrequently presented in the context of RCC storage quality[114]. A recent quantitative proteomics analysis of the supernatant of stored red blood cell concentrates revealed novel markers of RBC storage lesions [115]. The introduction of these powerful "-omic" techniques has illuminated the knowledge gap in our current RBC model and will enable us to acquire a much more thorough understanding of its biological complexities.

1.4 Impact of Donor Characteristics on Red Cell Concentrate Quality

While the development of RBC storage lesions does indeed impact RCC quality, focus on storage time as the sole determinant of RCC quality neglects the variability in cell properties that may depend on other factors, such as donor characteristics. The old versus fresh RCCs controversy has made the assumption that all RCCs manufactured and stored according to the same standard operating procedures and regulatory guidelines show a high degree of similarity. However, it appears that the question at hand has been over-simplified and has neglected to account for assorted strategies to improve RBC quality in the manufacturing steps as well as the differential behaviour of the raw material as a function of donor characteristics.

Strong evidence supports that inherent characteristics of a donor determine percentage hemolysis levels and RBC *in vivo* recovery, as these quality parameters tend to be consistent

within a given individual. Ongoing research is focused on delineating these quality determinants, and initial results are both interesting, and at times, surprising. Although the identification of the precise constellation of these characteristics is a source of active research, some features of inter-donor variability and their impacts on RCC quality are well known[116-119].

1.4.1 Donor Genetics

Percentage hemolysis is one of the key surrogate quality indicators for RCCs and a wide range of hemolysis levels is observed between donors under identical manufacturing and storage conditions[118,120]. Using a classic twin study, Van't Erve and coworkers monitored hemolysis levels in RCCs donated by a population of identical and non-identical twins[121]. They demonstrated that genetic factors indeed contribute to the differences in hemolysis levels between individual donors, indicating that donor characteristics may directly impact the quality of blood products.

Despite rigorous donor screening and routine testing, blood donation from individuals with subclinical RBC abnormalities (e.g., mild hereditary spherocytosis and sickle trait) or clinical disease in countries with high incidence (e.g., glucose-6-phosphate dehydrogenase (G6PD) deficiency in persons of African, Asian, and Mediterranean descents and thalassemia in South East Asia) could occur and result in the production of inferior components. These common RBC pathologies lead to destabilization of the membrane, abnormal morphology, and a reduced RBC lifespan, which may subsequently impact RCC quality during storage and circulation residency time in recipient post-transfusion[122]. In addition, there is an interplay between donor characteristics and the manufacturing processes used to prepare red cell components. Due to their altered physiology and rheology, RBCs from donors with sickle trait may not filter adequately at the leukoreduction (LR) step, leading to prolonged or incomplete filtration[123-125].

1.4.2 Donor Age and Sex

Donor age at the time of donation appears to be correlated with the level of percentage hemolysis over storage[118]. Additionally, heterogeneous Hb content of RCCs may be attributed to donor age at the time of donation; it appears that young donors exhibit higher levels of intact Hb per cell compared to those who are older[126]. Donor age at the time of donation not only influences Hb content, but also seems to determine the cellular composition of RCC; those derived from older donors appear to contain an elevated number of reticulocytes[126]. This observation is consistent with the physiological phenomenon of shortened *in vivo* RBC lifespan with increasing age[126]. While there is no direct human evidence of impact of *in vivo* RBC lifespan on transfusion efficacy, shorter endogenous lifespan as a unique donor phenotype seems to reduce post-transfusion recovery in a murine transfusion model[127].

While the collected data do not have enough statistical power to support strong conclusions, the results of a small, longitudinal study point to potential intra-donor variability in mechanical fragility over storage[128]. In addition to normal RBC ageing and accumulation of oxidative damage over storage, a donor's sex and more specifically, menopausal status, alters the susceptibility of stored RBCs to mechanical stress and hemolysis[129]. Raval and colleauges observed that RBCs collected from post-menopausal women are more prone to RBC membrane injuries than those obtained from pre-menopausal women throughout storage, clearly demonstrating a relationship between donor characteristics and RCC *in vitro* quality parameters.

1.4.3 Donor Lifestyle Preference and Behaviours

In addition to donor genetics and demographics, the lifestyle preferences and behaviours of donors also seem to impact the quality of donated blood products. Elevated dietary intake of lipid and the consequent lipemia appear to alter the fragility of RBCs and

induce hemolysis in a dose-dependent manner in both animal models and in human[130-132]. Moreover, triglyceride-rich chylomicrons appeared to play a significant role in hemolysis development *in vitro*[133]. These reports provide further evidence that donor dietary choices and the elapsed time between a donor's last meal and donation appointment may heavily influence the hemolysis level. Increased donation frequency has also been suggested to impact hemolysis levels as frequent donors may exhibit insufficient erythropoiesis due to depleted iron stores over time. While no correlation was observed between ferritin level and storage hemolysis, increased donation frequency is associated with increased resistance to oxidative hemolysis[134].

1.4.4 Donor Biochemistry

Other biochemical differences, such as lipid composition and protein concentrations, among donors may also influence RCC quality in storage. Dinkla *et al.* demonstrated that the PS exposure level varies from donor to donor and that a donor's endogenous PS exposure level predicts the percentage hemolysis over storage and RBCs' susceptibility to osmotic stress[135]. Moreover, underlying pathologies could influence PS exposure; individuals with diabetes mellitus type 2, especially those who developed chronic renal diseases as a long-term complication, exhibit elevated endogenous PS exposure[136]. Interestingly, levels of PS exposure positively correlated with increased oxidative damage to membrane lipids[136], providing further evidence for the potential utility of PS exposure level as a marker for RBC's susceptibility to oxidative damage and osmotic stress.

Additionally, donors exhibiting increased membrane bound peroxiredoxin-2 in fresh RBCs showed high lipoperoxidation level in storage[38], supporting that inter-donor biochemical differences may impact RBCs' susceptibility to oxidative effects of RBC storage lesion. Moreover, in a small paired fresh versus old stored RCC study, Tzounakas *et al.* showed that

many RBC quality parameters change predictably over storage and are dependent on donor-related pre-storage attributes, notably fetal Hb concentration[119]. Other biomarkers that predict the quality of a donated unit of blood will emerge from ongoing clinical and laboratory studies applying the techniques of genomics, proteomics, metabolomics and lipidomics. This information will ultimately allow us to manage both donors and product inventory in a more sophisticated manner that minimizes the impact of the RBC storage lesions.

1.5 Impact of Production and Manufacturing Processes on Red Cell Concentrate Quality

Although much has been accomplished to improve and to standardize production and manufacturing processes of blood components over the years, the procedures used to collect and process WB into different components enhance risk of hemolysis and cannot be fully mitigated.

1.5.1 Standard LR-SAGM Red Cell Concentrate Production

In Canada, blood products are routinely processed by one of the two production methods: buffy coat (BC) and WB filtration (WBF) methods, where one key difference is the timing of LR during the manufacturing process (see **Chapter 2.1**). The BC method removes most of the white blood cells, platelets, and plasma from the RBCs prior to LR while the WBF method subjects the WB through an in-line LR filtration. While both component-processing methods yield standard LR saline-adenine-glucose-mannitol (SAGM) RCCs satisfying the regulatory requirements, units manufactured using BC process exhibited lower average hemolysis values at expiry compared to those produced by the WBF method[118]. Additionally, hemolysis levels in units produced using WBF method appeared to display greater degree of

variability. These observations are likely attributed to the additional mechanical force exposed to the RBCs during the WBF centrifugation step.

Hemolysis could occur at any of the various stages in the manufacturing of LR SAGM RCC, including exposures to high centrifugation speed during component separation, damage from excessive shear through cannulas, rapid resuspension of packed RBCs in additive solution, and LR filtration. Moreover, temperature during production could also play a role in final product quality.

1.5.2 Gamma-Irradiation

Transfusion-associated graft versus host disease (TA-GVHD) occurs when viable donor T-lymphocytes proliferate and engraft in susceptible individuals after transfusion[137]. TA-GVHD results in significant morbidity and mortality in approximately 90% of individuals so affected and there is currently no effective treatment[138]. Thus, efforts are focused on prevention of TA-GVHD prior to transfusion. While all RCCs are LR, residual white blood cells are still present in the unit. The current and only approved strategy to prevent TA-GVHD is gamma-irradiation.

Canadian Blood Services employs irradiators containing a Cesium-137 source to deliver a gamma-irradiation dose of 25 Gy. The ionizing radiation readily penetrates nucleated cells and damages nuclear DNA either directly or by generating ions and free radicals that have biological actions. The damage to T lymphocyte DNA prevents post-infusion proliferation that abrogates the potential for TA-GVHD[139,140].

However, gamma-irradiation causes a significant reduction in RCC *in vitro* quality parameters and RBC survival. Reactive oxygen species (ROS) generation and the deterioration of membrane integrity are evidenced by lipid peroxidation, potassium leakage, increased hemolysis, and defective ATP metabolism[140-145]. Increased hemolysis challenges the product's adherence to regulatory guidelines and may render the unit less therapeutically effective, with a

reduction in viable and functional cells as well as an accumulation of bioactive molecules that perturb immune function. Increased potassium concentration may escalate risk of post-transfusion hyperkalemia and subsequent cardiac complications in neonates or in patients requiring massive transfusions. Furthermore, the observed decrease in RBC *in vitro* quality may diminish post-transfusion recovery and lead to potential adverse post-transfusion outcomes.

Armed with this knowledge, the current US Food and Drug Administration (FDA) gamma-irradiation guidelines, which are also used in Canada, were implemented to account for these changes in product quality. The guidelines state that irradiation may be performed at any time during RCC storage. Irradiated RCC may be stored until the end of allowable shelf life based on the type of storage container, but no longer than 28 days after irradiation. However, the impacts of length of RCC storage before and after gamma-irradiation on hemolysis and extracellular potassium levels were not fully understood by the transfusion community. To bridge the gap, Serrano *et al*. investigated the effect of timing of gamma-irradiation on hemolysis and observed that hemolysis increased with storage time, both before and after irradiation[144]. RCC irradiated in their fourth week of storage and subsequently stored for 15-21 days exhibited the highest level of hemolysis. In the same study, extracellular potassium level was measured in a smaller subset of samples. Extracellular potassium levels increased rapidly following gamma-irradiation and plateaued within one week of storage, regardless of the unit age when irradiated, and they all exceeded the level of normal non-irradiated units at day 42. This further suggests that gamma-irradiation compromises RBC membrane integrity, possibly directly affecting sodium/potassium ATPase function. In assessing both hemolysis and extracellular potassium levels, the timing of gamma-irradiation seems to significantly impact unit quality. This finding highlights one of blood bank operators' biggest challenges in balancing product safety and product quality. Continued research in this area will help to inform regulatory guidelines and inventory management strategies.

1.5.3 Pathogen Inactivation Technologies

Emerging pathogens and increased international travels pose a great risk to the safety of the blood supply. In order to minimize potential risk of transfusion-transmitted diseases, routine screening and rigorous testing are implemented and performed. However, blood operators can only screen and test for known infectious risks and agents (e.g., hepatitis B virus, hepatitis C virus, human T-cell leukotrophic virus I/II, HIV, and West Nile virus); though not all known pathogens have tests available or are being routinely tested (e.g., babesiosis, variant Creutzfeld-Jacob disease, hepatitis A virus, human herpes virus 8, chikungunya virus, Chagas disease, and malaria) and have been shown to adversely affect the blood supply. Additionally, limits to the sensitivity of bacterial cultures and turnover time also pose further limitations to product testing effectiveness and efficiency. Furthermore, commercially available tests may not be able to reliably detect the presence of infection in a donor during the "window" or incubation period, which consequently compromises transfusion safety. The current reactive strategy of surveillance, identification, test development, and screening may allow a pathogen to disseminate widely even before clinical disease is recognized; such was the case in the tainted blood scandal of HIV in the early 1980s, which undermines public confidence in the blood supply.

Without a robust strategy to estimate risks of an emerging transfusion-transmitted pathogen, the blood operators and transfusion communities are looking for a more proactive approach to ensure a safe and readily available blood supply. This need drove the development of pathogen inactivation (PI) technology, which aims to inhibit pathogen proliferation and to prevent the likelihood of disease transmission, while preserving adequate cellular and protein quality in the blood product to improve transfusion recipient outcome[146].

Currently, the manufacturers of the Mirasol Pathogen Inactivation Technology (riboflavin/ultraviolet (UV) illumination centred at 313 nm; Terumo BCT, Lakewood, CO) are

collecting the clinical data required for a submission to Health Canada to request licensure for platelet products due to the fact that their storage conditions are favourable for bacterial growth. However, RCCs are not free of infectious risk. For example, human babesiosis, caused by the intraerythrocytic protozoan parasite *Babesia microti*, is transmissible by transfusion and is increasingly recognized as posing risk to the blood supply safety[147,148]. While most healthy individuals do not exhibit symptoms, the parasite could potentially lead to hemolytic anemia or even death in susceptible, immunocompromised patients. While RCC would benefit from PI, direct application of this technology to RCC was technically challenging due to inherent viscosity of the RBCs and to the absorption spectrum of Hb (400-450 nm)[149]. Therefore, this PI technology is currently being adapted to WB units [150,151] (see **Chapter 2.4.2**).

An alternative PI technology, Intercept Blood System (Cerus Corporation, Concord, CA), sidesteps the technical challenge of absorbency of light by Hb via the use of a nucleic acid-targeted alkylator, S-303, and is applied directly to RCCs[152]. This PI process is performed in the presence of GSH to quench extracellular reaction of S-303 with other neucleophiles, such as phosphates and proteins. As Intercept does not require an external energy source for treatment and involves an additional step to replace treatment solution with storage solution after PI process, it appears to retain various RBC *in vitro* quality parameters compared to standard AS-5 RCCs: Intercept-treated RCCs exhibit reduced extracellular potassium levels, higher glucose levels and lower lactate accumulation derived from metabolism of glucose[153]. While percentage hemolysis was significantly higher in Intercept-treated RCCs compared to standard AS-5 RCCs, mean percentage hemolysis remained well below the acceptable limit of < 0.8% at all time-points[153]. Early phase III clinical studies of the first-generation Intercept PI system for RBC were suspended when patients in the chronically transfused trial developed alloantibodies against S-303 after several transfusions[152]. Phase III clinical studies of the second-generation Intercept PI

system for RBC are underway in the European Union to evaluate therapeutic efficacy of Intercept-treated RCC compared to standard RCCs.

As a collective, the transfusion medicine community, including blood bankers, governmental regulators, and the private sector, sees the benefit in a shift towards the new paradigm of preemptively implementing new approaches in improving microbiological safety and must collaborate to gain a more comprehensive understanding of the impact of emerging PI technology on product quality and patient safety[154].

1.5.4 Deoxygenation Treatment

Numerous *in vitro* studies unequivocally demonstrated that oxidative damage accumulates with time spent in storage and contributes significantly to RBC storage lesions development. Hemanext is developing a technology to enable the storage of RBCs under anaerobic conditions; the elimination of the primary substrate for ROS-generating Fenton reaction, oxygen, at the beginning of and maintained throughout storage would directly reduce oxidative damage. The deoxygenation process was accomplished by first equilibrating the RBC suspension with argon gas repeatedly over a period of 1 hour to reduce oxygen saturation (So_2) to below 4% prior to storage in a standard blood bag inside an anaerobic canister filled with argon and helium (9:1); a palladium catalyst was included to further deplete oxygen during storage. Independent research groups have also explored the use of other gases (e.g., argon, nitrogen, and helium) to displace oxygen with aims to alleviate many of the signs associated with RBC storage lesions; the deoxygenation approach has been shown to successfully protect against morphological, biomechanical, and biochemical changes during storage[95,155-157]. In addition, metabolic modulation mediated by competitive binding of deoxygenated Hb and glycolytic enzymes to the N-terminal cytosolic domain of band 3 promotes high energy phosphate synthesis via the Embden-Meyerhof pathway[158,159]. Moreover, metabolomics

assessment of RBC responses to hypoxia revealed beneficial effects of anaerobic storage on energy metabolism[160]. The newest product design by Hemanext simplifies the deoxygenation process by removing the gas equilibration step: the Anaerobic Storage System (Hemanext; Bethesda, MA) utilizes a membrane oxygenator to reduce oxygen to 5% So_2 under gentle agitation and maintains anaerobic environment for refrigerated RCC storage[161]. Deoxygenation treatment could also be explored as a strategy to minimize deleterious effect of other post-collection manipulations, such as PI treatment.

1.6 Hypothesis and Specific Aims

RCC quality depends on complex interplays between many variables, such as storage time, donor characteristics, and manufacturing processes. Using the resources of Canadian Blood Services, a unique population of repeat donors has been identified that exhibit "high" levels of spontaneous hemolysis. Analysis of these donors may yield biomarkers that can be used to both evaluate donor and to uncover underlying mechanisms in RBC storage lesion development. As differences in hemolysis development are related to the differences in RBC membrane integrity, we hypothesize that *alterations in the RBC membrane protein profile may identify specific membrane-associated protein biomarkers for product quality*. To test this hypothesis, our experimental approaches were as follows:

1. **Inherent donor variations - delineating impact of donor characteristics on hemolysis and identifying candidate protein biomarkers for RCC quality.** Multidimensional interaction between various donor characteristics and RCC storage quality warrants further investigation and may inform our effort in quality biomarker identification. *In vitro* quality parameters and ghost fractions derived from repeat donors exhibiting high hemolysis were assessed and compared to those obtained from their respective age- and sex-matched control donors, with aims to detect alterations in the

membrane proteome that may attribute to the differences in hemolysis development during RCC storage.

2. **Post-collection manipulations – investigating process-induced hemolysis and verifying candidate protein quality biomarkers in pathogen inactivated and gamma-irradiated RCC.** Additional component processes, such as PI and gamma-irradiations, are known to exacerbate RBC storage lesions development, which may serve as a model for investigating the hemolysis development in RBC. The effect of process insult on *in vitro* quality parameters and membrane protein profiles was appraised in relations to the untreated matched control RCC under standard blood banking conditions.
3. **Hemolysis modulation – application of candidate protein quality biomarkers in deoxygenated RCC.** Variation in processing method has been demonstrated to modulate hemolysis development. Utility of potential candidate protein quality biomarkers in predicting development of hemolysis was evaluated in alternatively prepared RCC.

Chapter 2: Materials and Methods

2.1 Production of Red Cell Concentrates

WB collection and LR-SAGM RCC production (**Figure 2.1**) were carried out by Canadian Blood Services local Production and Distribution Centres (Vancouver, British Columbia; Calgary, Alberta; Regina; Saskatchewan; Winnipeg, Manitoba; Brampton, Ontario; Ottawa, Ontario, Canada) and Network Centre for Applied Development facility (Vancouver, British Columbia, Canada).

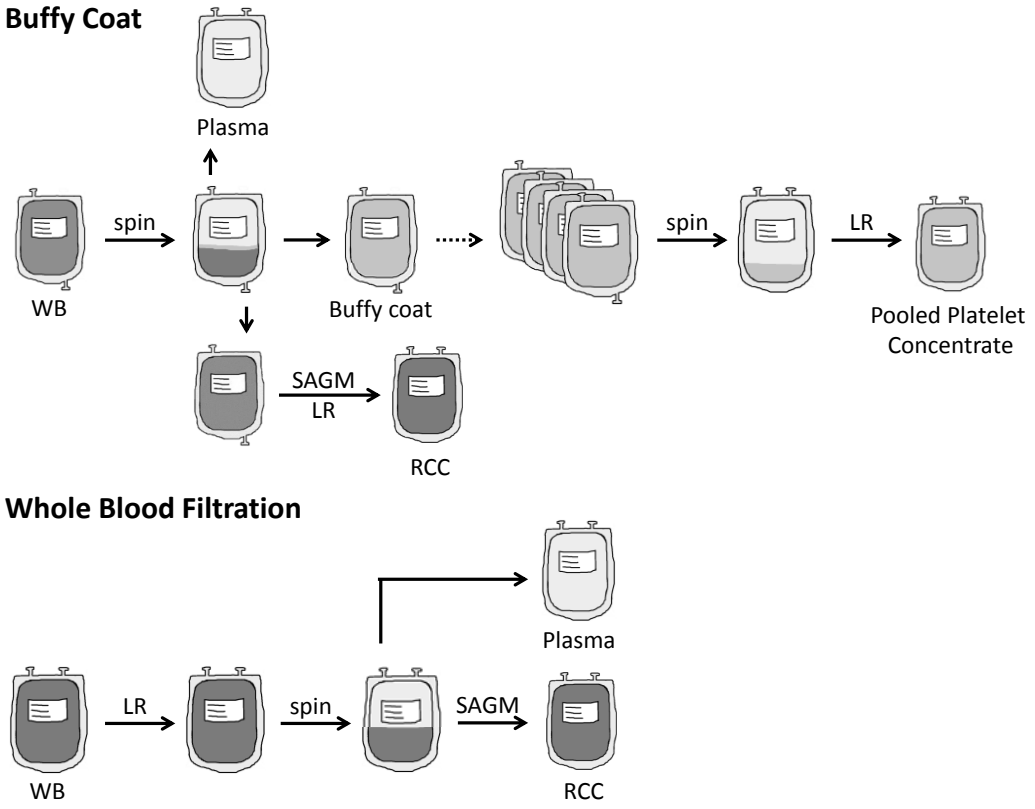

Figure 2.1 Schematic representation of RCC manufacturing process

LR-SAGM RCC may be produced by either the buffy coat or the whole blood filtration production method at Canadian Blood Services. (LR=leukoreduction; RCC = red cell concentrate; SAGM = saline-adenine-glucose-mannitol; WB = whole blood)

2.1.1 Buffy Coat Method

WB units were held overnight on a butane-1, 4-diol cooling tray (CompoCool, Fresenius Kabi, Bad Homburg, Germany) prior to RCC production using the buffy coat method. Briefly, a WB unit was subjected to centrifugation (Sorvall RC3BP with a HBB-6 Rotor, Thermo Scientific, Ottawa, Ontario, Canada) at 3493 x g for 11 minutes and separated into its components (CompoMat G4 Extractor, Fresenius Kabi). SAGM (110 mL) was added to the RBC with thorough mixing prior to gravity filtration via an in-line LCR-Diamond LR filter (Macopharma, Tourcoing, France) into the final RCC storage bag.

2.1.2 Whole Blood Filtration

WB units were cooled in insulated shipping containers and LR by filtration via an in-line MTL1 WB filter (Macopharma) in the refrigerator within 72-hour of the stop-bleed time. The filtered WB units were centrifuged (Sorvall RC 3BP with a HBB-6 rotor, Thermo Scientific) at 4552 x g for 6 minutes. A Compomat G4 was used to extract plasma from the WB unit, and SAGM (100 mL) was added to the RCC.

2.2 Storage and Transportation of Red Cell Concentrates

All RCCs were stored upright for 42 days at 4 ± 2°C, according to standard blood banking conditions. RCC were transported using J-82 shipping boxes containing ice packs and temperature monitors in a validated packing configuration designed to ensure maintenance of an acceptable temperature range (1-10°C) during transit time.

2.3 Identification and Recruitment of High Hemolyzers

One percent of all collected RCCs are assessed as part of the routine QC at outdate. Between 2011-06-10 and 2013-10-23, a total of 20,818 RCCs were assessed for QC purposes.

Within this QC database, forty donors who donated RCC exhibiting hemolysis level exceeding 0.8% at expiry on more than one occasion (high hemolyzers) were identified.

All forty high hemolyzers identified from the QC database were invited through the medical offices of their local CBS blood collection clinics and ten donors were successfully recruited (9 male and 1 female; 48 ± 14 years). Age- and gender-matched repeat donors with no history of elevated hemolysis were identified and recruited through the CBS NetCAD facility (Vancouver, Canada) to act as controls. Each donor provided one RCC unit.

2.4 Post-Collection Modification

For selected experiments, ABO compatible WB or RCC were pooled and split to generate identical units for comparison, with one RCC kept untreated as a control.

2.4.1 Gamma-Irradiation

RCC were subjected to gamma-irradiation (25 Gy; Gammacell 1000 Elite, Best Theratronics Ltd., Ottawa, Ontario, Canada) immediately following production (day 1). Rad-Sure blood irradiation indicator labels (Ashland, Mississauga, Ontario) were applied to the RCC to verify that an adequate radiation dose has been delivered.

2.4.2 Riboflavin / Ultraviolet Illumination Treatment

WB units were subjected to the pathogen inactivation (PI) treatment procedure (Mirasol Pathogen Reduction Technology System, Terumo BCT); addition of 35 mL of riboflavin solution (500 µmol/L) followed by UV illumination at a dose of 80 J/mL$_{RBC}$, according to manufacturer's protocol. The duration of UV illumination was calculated by the device using hematocrit (HCT) obtained by manual microcapillary centrifugation (HAEMATOKRIT 210, Hettich Zentrifugen, Tuttlingen, Germany) and the weight of the WB unit. Treated WB units were held overnight on a

butane-1, 4-diol cooling tray (CompoCool, Fresenius Kabi) prior to RCC production using the buffy coat method, which resulted in WB PI-treated RCC (RCC^{PI}).

2.4.3 Deoxygenation Treatment

WB units were subjected to deoxygenation treatment prior to the PI process. WB was transferred in a sterile recirculation reservoir bag (New Health Manufacturing, Avon, Massachusetts), connected to a neonatal membrane oxygenator (Sorin D100, LivaNova PLC, London, UK). Blood was continuously circulated through the membrane oxygenator by a Cobe Century peristaltic pump (Cobe Cardiovascular, Arvada, Colorado) at 700 mL/min as continuously monitored by SONOFLOW Flow Sensor series CO.55/080 (Sonotec USA Inc., Islandia, New York), while 5% carbon dioxide (CO_2) + 95% nitrogen (N_2) purging gas was supplied at 2.5 L/min controlled by Precision Gas Mass Flow Controllers (MC-5SLPM-D) with Flow Vision MX Gas Blending Station Software (Alicat Scientific, Tucson, Arizona). So_2 of circulating blood was measured periodically by sterilely removing samples from the circulation bag via a septum port for So_2 analysis by a cooximeter (ABL90 FLEX, Radiometer, Copenhagen) until recirculating blood reached the target So_2 value of 3-5% (30-45 min depending on the initial So_2 of the blood), yielding RCC^{WB*} or RCC^{WB*+PI}. In order to minimize re-oxygenation of anaerobic blood after transfer from the recirculation bag, oxygen content of PI treatment processing bag, as well as final storage bags for anaerobic units were purged by repeatedly flushing the bags with N_2 through a sterilely attached 0.2 µm filter. Anaerobic units were stored in air-tight canisters (Difco Scientific, BD Biosciences) at 4°C. Oxygen content of the canister was purged by flushing with N_2 gas and RCC were stored with 2 packs of oxygen sorbent (Ageless S200, Mitsubishi Gas Chemical USA, New York, New York) after processing in day 1 and after sampling.

2.5 Red Blood Cell *in vitro* Quality Parameters

While the final proof for RCC quality is still the post-transfusion clinical outcome, RBC *in vitro* parameters can offer insights into product quality.

2.5.1 Sampling Procedure

Samples were collected on days 5, 14, 21, 28, and 42 aseptically via insertion of a sampling site coupler (EPE1016AU, Macopharma) in a biosafety cabinet. Briefly, the units were gently and thoroughly mixed and the volume required for testing (10 mL) was withdrawn with a syringe and a sterile needle.

2.5.2 $pH_{22°C}$

$pH_{22°C}$ was determined manually on a 500 µL RCC with a ROSS Ultra Semi-Micro pH probe (Thermo Scientific) at room temperature (22°C).

2.5.3 Red Blood Cell Count and Mean Corpuscular Volume

RBC count and mean corpuscular volume (MCV) were obtained using a hematology analyser (Advia 120, Siemens Healthcare Diagnostics Ltd, Oakville, Ontario, Canada). All RCC samples were manually aspirated into the analyser without further dilution. QC was performed daily using Advia 120 TESTpoint Haematology Control Normal (Siemens).

2.5.4 Extracellular Potassium Concentration

Extracellular potassium concentration was measured on supernatant (diluted 1:50 in potassium ionic strength adjuster solution) with a 9719BNWP Potassium Combination Electrode (Thermo Scientific). Supernatant was extracted without interrupting the pellet interface after a

centrifugation spin (Beckman GS-6R Centrifuge, Beckman Coulter, Mississauga, Ontario Canada) at 2060 x g for 10 minutes at 4°C, unless otherwise specified.

2.5.5 Percentage Hemolysis

Percentage hemolysis was calculated using the following formula:

$$\%\ Hemolysis = \frac{(1-HCT)\ x\ Hb_S}{Hb_T} \quad [1]$$

, where

HCT = haematocrit (L/L)

Hb_S = supernatant haemoglobin concentration (g/L)

Hb_T = total haemoglobin concentration (g/L).

HCT was obtained by manual microcapillary centrifugation (HAEMATOKRIT 210) and total and supernatant Hb determined by Harboe direct spectrophotometric method [162]. Briefly, RBC and supernatants were diluted 1:10 in distilled water and incubated at room temperature for 30 minutes to lyse RBCs. Lysed RBC were further diluted 1:100 in distilled water. The absorbance was read at 380, 415, and 450 nm against a distilled water blank in an SpectraMax 190 Microplate Reader (Molecular Devices, Sunnyvale, CA) and converted to corrected Hb concentration using the following formula[163]:

$$Hb\ \left(\frac{g}{L}\right) = (167.2\ x\ A_{415} - 83.6\ x\ A_{380} - 83.6\ x\ A_{450})\ x\ \frac{1}{1000}\ x\ \frac{1}{dilution\ in\ dH_2O} \quad [2]$$

2.5.5.1 Red Blood Cell-Derived Microvesicles

Microvesicles are fragments of plasma membrane. RMV in the supernatant were defined as events smaller than 1 µm.

2.5.5.2 **Quantification**

RMV were labeled with RPE-conjugated monoclonal mouse anti-human CD235a (glycophorin A, clone JC159, Catalog No. R 7078, Dako; Agilent Technologies, Markham, ON) and enumerated using flow cytometry (FACSCanto II, BD Biosciences, Mississauga, ON, Canada). An unstained sample was acquired to detect the sample auto-fluorescence and to adjust the forward scatter channel threshold to reduce background noise. Quantification was achieved with addition of a known concentration of fluorescent beads (Fluoresbrite YG Microspheres 1.00µm, Polysciences, Inc., Warrington, PA) to the samples. RMVs were identified by relative size as informed by the forward and side scatter channels in reference to the fluorescent beads (1 µm). Sample acquisition was discontinued when the number of reference fluorescent beads in the relative region reached 10,000 events. The concentration of RMV/µL of supernatant was calculated using the following formula:

$$\frac{RMV}{\mu L\ Supernatant} = RMV\ Events\ \times \frac{\left(\frac{Beads\ in\ tube}{10{,}000\ beads\ counted}\right)}{Supernatant\ Volume} \quad [3]$$

2.5.5.3 **Size Determination**

The mean size of RMV was determined using photon correlation spectrometry (N4 Plus, Coulter International Cooperation, Miami, FL). Briefly, supernatants were diluted with twice-filtered PBS to ensure accurate detection in the linear range ($5 \times 10^4 \sim 1 \times 10^6$ counts/second). The samples were allowed to equilibrate and to achieve uniform Brownian motion at room temperature for a minimum of 30 minutes prior to analysis. For each sample, acquisition was performed at a 90° angle at 22°C for 1 minute in triplicate.

2.5.6 Perchloric Acid Extraction

RBCs were washed with phosphate-buffered saline (PBS, pH 7.4) and then acidified with 60 µL perchloric acid (70% weight/volume). Extracts were incubated on ice for 10 min prior to centrifugation (Microfuge 22R Refrigerated Microcentrifuge, Beckman Coulter) at 6000 x g for 5 min at 4°C. One ml of protein-free supernatant was neutralized with 56 µl 5N potassium carbonate and stored at -80°C. Samples were thawed, homogenized, and centrifuged to remove potassium perchlorate precipitates prior to analysis.

2.5.6.1 2, 3-Bisphosphoglycerate

2, 3-BPG concentration was determined spectrophotometrically (SpectraMax 190 Microplate Reader, Molecular Devices) using a commercially available kit (Roche Diagnostics, Laval, Quebec, Canada).

2.5.6.2 Adenosine Nucleotide Levels

Adenine nucleotide levels were evaluated using reverse-phase high-performance liquid chromatography (HPLC; Alliance 2695, Waters, Mississauga, Ontario, Canada) and adenosine monophosphate (AMP), adenosine diphosphate (ADP), and adenosine triphosphate (ATP) standards as described previously [164]. Briefly, gradients were prepared with two degassed solvent mixtures. Solvent A was 0.1M potassium dihydrogen phosphate (Fisher Scientific, Ottawa, Ontario, Canada), pH 8.0; Solvent B was 0.1M potassium dihydrogen phosphate and 10% volume/volume methanol (Fisher Scientific), pH 8.0. Degasification was performed using an ultrasonic bath for 30 minutes to reduce the level of dissolved gas below the natural equilibrium level. The perchloric acid extract was resolved with a reverse-phase column (Supelcosil LC-18-T column; Sigma-Aldrich, Oakville, Ontario, Canada) using the elution program: initial conditions 100% A, from 0-4 minutes, linear gradient step to 100% B in 9

minutes, linear gradient to 100% A in 1 minute, and isocratic step at 100%A for 6 minutes; flow rate of 1.3 mL/min. Adenosine nucleotides were identified by their retention time and their concentrations were calculated by comparison with a calibrated triple nucleotide external standard solution (100 µM ATP, 50 µM ADP, 25 µM AMP). The Empower 3 Chromatography Data Software system (Waters) was used for the analysis and peak integration.

2.5.7 Morphology

RBC gross morphology was assessed using a 6-stage grading system[165] by microscopic examination (Nikon Labophot, Tokyo, Japan) of glutaraldehyde-fixed blood smears at 1000x magnification.

2.5.8 Osmotic Fragility

Osmotic fragility was determined using a series of saline solutions with concentrations ranging from 0.0 g/L to 9.0 g/L. Briefly, RBC were diluted 1:10 in appropriate saline solutions and incubated at room temperature for 30 minutes. Lysed RBC were then subjected to centrifugation (Microfuge 22R Refrigerated Microcentrifuge, Beckman Coulter) at 18,000 x g for 1 minute. The resultant supernatants were further diluted 1:10 or 1:100 in distilled water. The absorbance was read at 380, 415, and 450 nm against a distilled water blank in a SpectraMax 190 Microplate Reader (Molecular Devices) and corrected Hb (g/L) calculated using formula [2]. The sodium chloride concentration that produced 50% hemolysis was reported as mean corpuscular fragility (MCF).

2.5.9 Phosphotidylserine Exposure

RBC were washed twice in Ringer's solution containing 125 mM sodium chloride, 5 mM potassium chloride, 5 mM glucose, 32 mM HEPES, 1 mM magnesium sulphate, and 1 mM

calcium chloride (pH 7.4) prior to flow cytometry analysis. RBCs were stained with Annexin-V-FITC (1:200; ImmunoTools, Friesoythe, Germany) in Ringer's solution containing an additional 4 mM calcium chloride for 15 min at 37°C. Fluorescence intensity was measured in the FL1 channel with an excitation wavelength of 488 nm and an emission wavelength of 530 nm using an EPICS XL-MCL (Beckman Coulter) flow cytometer.

2.5.10 Cytosolic Calcium Activity

Similar to the assay conditions for the measurement of PS exposure, RBCs were stained with Fluo3/AM (2 µM in Ringer's solution; Biotium Hayward, CA, USA) for 15 min at 37°C for the determination of cytosolic calcium activity.

2.6 Membrane Protein Related Assays

2.6.1 Hemoglobin-Depleted Red Blood Cell Membrane Fraction Preparation

Hb-depleted RBC membrane (ghost) fractions were isolated using Dodge's method[166]. Briefly, 2 mL of each RBC sample was washed 3 times with 10 mL normal saline and reconstituted to starting volume. Each hypotonic RBC lysis cycle consisted of incubation with 25 mL of ice-cold 5 mM sodium phosphate buffer (pH 8.0) containing phenylmethylsulfonyl fluoride (Fisher Scientific) on ice for 10 minutes, centrifugation at 15,000 x g at 4°C for 10 minutes, and removal of supernatant. Five hypotonic RBC lysis cycles were performed and the ghost fraction was white in appearance. The final ghost fraction volume was again adjusted to the starting volume and aliquoted into microcentrifuge tubes prior to storage at -80°C.

2.6.2 Isobaric Tags for Relative and Absolute Quantitation

Selected ghost fractions were evaluated using a quantitative proteomics approach based on iTRAQ labeling, high pH reverse phase fractionation, and liquid chromatography-tandem

mass spectrometry (LC-MS/MS) analysis. This technique was selected for its ability to multiplex several samples for simultaneous protein quantification with simplified analysis and increased analytical precision and accuracy[167]. As well, iTRAQ can be used to identify and quantify proteins across functional categories and diverse molecular weight and isoelectric point (pI) ranges[167]. The isobaric mass design of the iTRAQ reagents allows for differentially labelled peptides to appear as a single peak in MS scans, reducing the probability of peak overlapping. When iTRAQ-tagged peptides are then subjected to MS/MS analysis, fragment ion peaks observed at higher *m*/*z* are specific for peptide amino acid sequence and are used for peptide identifications while isotope-encoded reporter ion peaks are used to provide relative quantitative information.

2.6.2.1 **Sample Preparation**

Protein concentrations were determined using a Bradford Protein Assay (Bio-Rad, Mississauga, Ontario, Canada). Samples (100 µg) were solubilized in triethylammonium bicarbonate and 0.2% sodium dodecyl sulfate. Proteins were reduced with tris-(2-carboxyethyl) phosphine at 60°C for one hour and alkylated with methyl methanethiosulfonate. Proteins were then in-solution digested with N-tosyl-L-phenylalanine chloromethyl ketone treated trypsin (Ab Sciex, Concord, Ontario, Canada) overnight at 37°C and labeled with appropriate iTRAQ label (Ab Sciex). iTRAQ labeled peptides were then combined and subjected to stage-tip sample cleanup [168].

2.6.2.2 **Acquisition**

Purified peptides were analyzed using a linear trap quadropole (LTQ)-Orbitrap Velos (Thermo Scientific) on-line coupled to an Agilent 1290 Series HPLC using a nanospray ionization source (Thermo Scientific), including a 2-cm-long, 100-µm-inner diameter fused silica

trap column and a 50-µm-inner diameter fused silica packed emitter tip analytical column. The trap column was packed with 5 µm-diameter Aqua C-18 beads (Phenomenex, www.phenomenex.com), while the analytical column was packed with 3.0 µm-diameter Reprosil-Pur C-18-AQ beads (Dr. Maisch, www.Dr-Maisch.com). Buffer A consisted of 0.1% aqueous formic acid, and buffer B consisted of 0.1% formic acid and 80% acetonitrile in water. Samples were re-suspended in buffer A and loaded with the same buffer. Standard linear gradients were run. The HPLC system included Agilent 1290 series Pump and Autosampler with Thermostat. The LTQ-Orbitrap was set to acquire a full-range scan at 60,000 resolution from 350 to 1500 Th in the Orbitrap to simultaneously fragment the top 5 peptide ions by collision-induced dissociation and top 5 by higher-energy collisional dissociation (HCD; resolution 7500) in each cycle in the LTQ (minimum intensity 1000 counts). Parent ions were then excluded from MS/MS for the next 30 seconds.

2.6.2.3 **Analysis**

Raw files were processed with Proteome Discoverer v. 1.4 (Thermo Scientific). The search was performed with the Mascot algorithm against a database comprised of the human protein sequences from Uniprot (www.expasy.org) using the following parameters: peptide mass accuracy 10 parts per million; fragment mass accuracy 0.6 Da; trypsin enzyme specificity, fixed modifications - carbamidomethyl, variable modifications - methionine oxidation, deamidated N, Q and N-acetyl peptides, ESI-TRAP fragment characteristics. False discovery rate was limited to 1% at the peptide level. For all analyses, low confidence peptide identifications were discarded, and the peptide IDs were placed in protein groups. Protein groups were reported if they contained 2 or more peptides identified, with at least one unique peptide. Quantification was then performed at the peptide level on HCD scans of identified peptides using the iTRAQ 4-plex quantitation method built into Proteome Discoverer.

2.6.2.4 Immunoblot Validation

Ghost fractions were separated by sodium dodecyl sulfate-polyacrylamide gel electrophoresis gels and transferred onto nitrocellulose membranes (Bio-Rad). The membranes were blocked with 5% bovine serum albumin (Sigma-Aldrich) dissolved in PBS containing 0.1% Tween 20 overnight at 4°C. Membranes were probed with primary antibodies against peroxiredoxin-2, catalase, pan-20S proteasome, stomatin, (Abcam, Cambridge, MA), α- and β-spectrin, or β-actin (Sigma-Aldrich), followed by incubation with their respective secondary antibodies (Licor, Lincoln, NE). Protein bands were visualized on a bioimaging system (Li-COR, Licor) and their intensities were quantified by densitometry using the imaging analysis software (Odyssey, Licor).

2.7 Statistical Analysis

Normality of distribution of data was first tested using Minitab statistical software (Minitab, Inc. State College, PA). Johnson transformation was performed on non-normal distributions. Group means were compared using two-way analysis of variance (ANOVA) with repeated measures, followed by Tukey-Kramer post-hoc test for further pair-wise comparisons. Categorical variables were compared using the Fisher's exact test. Stepwise logistic regression analysis was employed to project hemolysis level at expiry by more than one continuous predictor variable. Multivariate regression analysis was performed to estimate the relationships among continuous variables. Pearson correlation was employed to determine the strength and direction of the linear relationship between two continuous variables. For all statistical analysis, a p-value < 0.05 was considered significant. Sample size calculations assumed a significance level of 5% and a power of 80% to detect a potential difference in the *in vitro* quality variables between RCC^{HH} and RCC^{Ctrl}.

Chapter 3: Inherent Donor Variations - Delineating the Impact of Donor Characteristics on Hemolysis and Identifying Candidate Protein Biomarkers for Red Cell Concentrate Quality

3.1 Introduction

Despite standardized product manufacturing procedures and storage conditions, RCCs exhibit considerable variability in hemolysis during the allowable storage period due to inherent differences in donor characteristics[117,118,122], including but not limited to genetics [127,169], iron status [134,170], age at donation [126], sex and menopausal status [129]. Moreover, membrane PS exposure level has been shown to vary among donors [171]; its ability to predict hemolysis over storage as well as the RBC's susceptibility to osmotic stress suggests an interplay between RBC *in vitro* quality parameters and donor-specific membrane integrity. Currently, the development of hemolysis is generally accepted as a result of loss of Hb in RMV[172], increasing mechanical rigidity and cumulative oxidative damage with time spent in storage[173], though the molecular mechanism(s) still remain poorly understood. Thus, the multidimensional interaction between various donor characteristics and RCC storage quality warrants further investigation.

In the present study, we recruited ten healthy volunteer donors whose donations exceeded the acceptable level of hemolysis at outdate on more than one occasion (referred to as high hemolyzers in this study; RCC^{HH}) within the Canadian Blood Services QC database, as these individuals may offer new insights into unique donor characteristics or molecular commonalities that impact RCC storage quality. Control donors (RCC^{Ctrl}) matching the respective age- and sex- characteristics of those high hemolyzers were also recruited for a comprehensive comparative analysis of *in vitro* quality parameters, donor characteristics (e.g., ABO distribution, frequency of donations), and membrane proteomic profiles. This study aimed to investigate why some donors store more poorly than others by analyzing differences in the

membrane protein profiles using quantitative proteomics, with the goal to better understand RCC product quality and to inform strategies in improving both donor and RCC inventory management.

3.2 Results

3.2.1 Red Cell Concentrate *in vitro* Quality Parameters

Donation frequency in the past 12 months, donor age and sex, RCC volume, and production methods were comparable between two study populations (**Table A.1**), confirming that some known confounders of RCC storage quality were appropriately controlled in this study. As shown in **Table 3.1**, temporal effects on various *in vitro* quality parameters were evident in both donor populations as previously observed[50,173,174]. Despite having comparable pH during storage, high hemolyzer RCC contained significantly less 2, 3-BPG content compared to those of control RCC ($p < 0.01$) at all time-points measured. The typical biconcave discoid RBC shape seemed less prevalent in high hemolyzer RCC than in that of control RCC ($p < 0.01$) at early time points (days 5 and 14). While under our experimental conditions, only two high hemolyzers exhibited levels exceeding 0.8% hemolysis at expiry, hemolysis levels of high hemolyzer RCC were significantly elevated compared to those of control RCC for all time-points measured ($p < 0.01$). RMV release followed a similar trend with that of hemolysis. Observed alterations in membrane maintenance and integrity appeared to parallel with high hemolyzer RCC's reduced ability to resist changes in osmotic pressure compared to that of control RCC ($p < 0.01$), though the magnitude of such difference did not change with time spent in storage ($p > 0.05$). The alterations in these *in vitro* quality parameters seem to hint at differences at the RBC membrane between the two donor populations.

Table 3.1 Comparative *in vitro* measurements for RCC^{HH} and RCC^{Ctrl} over storage (mean ± S.E.M; n = 10).

All parameters show data from days 5, 14, 21, 28 and 42 of storage, except 2, 3-BPG which was measured on days 5, 14, and 21 and MCF which was measured on days 5, 28 and 42 of storage. (* = no significant change over storage; † = $p < 0.05$ between two donor populations at all measured time points). Table 1 from Chen D, Schubert P, Devine DV. Proteomic analysis of red blood cells from donors exhibiting high hemolysis demonstrates a reduction in membrane-associated proteins involved in oxidative response. Transfusion 2017; 57:2248-56. Page 2252. Adapted with permission from publisher.

Storage Day / *In Vitro* Parameters	Day 5		Day 14		Day 21		Day 28		Day 42	
	RCC^{HH}	RCC^{Ctrl}	RCC^{HH}	RCC^{Ctrl}	RCC^{HH}	RCC^{Ctrl}	RCC^{HH}	RCC^{Ctrl}	RCC^{HH}	RCC^{Ctrl}
pH	7.02 ± 0.03	7.12 ± 0.03	6.88 ± 0.02	6.89 ± 0.03	6.77 ± 0.02	6.80 ± 0.02	6.71 ± 0.02	6.70 ± 0.01	6.64 ± 0.03	6.60 ± 0.02
HCT *	0.60 ± 0.01	0.60 ± 0.01	0.60 ± 0.005	0.61 ± 0.01	0.60 ± 0.01	0.61 ± 0.01	0.59 ± 0.005	0.61 ± 0.01	0.59 ± 0.006	0.60 ± 0.01
Extracellular Potassium (mM)	12.39 ± 1.56	12.05 ± 1.18	24.62 ± 1.81	27.42 ± 1.49	33.76 ± 2.15	35.74 ± 1.88	38.71 ± 1.85	42.31 ± 1.83	51.88 ± 1.84	52.17 ± 1.89
2,3 – BPG (µmol/g Hb) †	0.95 ± 0.30	2.07 ± 0.23	0.36 ± 0.11	0.82 ± 0.15	0.14 ± 0.07	0.36 ± 0.10				
Morphology Score (AU)	76.2 ± 2.0†	92.3 ± 1.6	70.2 ± 2.9	75.9 ± 4.1	65.7 ± 2.2	67.9 ± 3.4	62.1 ± 2.1	63.9 ± 2.8	57.2 ± 2.4	58.0 ± 2.8
ATP (µmol/g Hb)	4.34 ± 0.19	4.21 ± 0.12	4.08 ± 0.23	3.98 ± 0.14	3.67 ± 0.21	3.68 ± 0.14	3.20 ± 0.18	3.29 ± 0.11	2.30 ± 0.15	2.30 ± 0.11
ADP (µmol/g Hb)	0.54 ± 0.17	0.33 ± 0.11	0.66 ± 0.21	0.62 ± 0.19	0.75 ± 0.25	0.82 ± 0.26	0.77 ± 0.24	0.85 ± 0.27	0.68 ± 0.22	0.81 ± 0.26
AMP(µmol/g Hb) †	0.11 ± 0.04	0.08 ± 0.02	0.19 ± 0.06	0.14 ± 0.04	0.26 ± 0.09	0.20 ± 0.06	0.33 ± 0.11	0.28 ± 0.09	0.41 ± 0.13	0.43 ± 0.14
Hemolysis (%) †	0.075 ± 0.025	0.031 ± 0.004	0.123 ±0.030	0.058 ± 0.006	0.198 ±0.048	0.080 ± 0.008	0.274 ± 0.052	0.111 ± 0.012	0.599 ± 0.079	0.201 ± 0.028

In Vitro Parameters \ Storage Day	Day 5		Day 14		Day 21		Day 28		Day 42	
	RCC^{HH}	RCC^{Ctrl}	RCC^{HH}	RCC^{Ctrl}	RCC^{HH}	RCC^{Ctrl}	RCC^{HH}	RCC^{Ctrl}	RCC^{HH}	RCC^{Ctrl}
RMV Count (count/µL supernatant) †	4545 ± 1437	1015 ± 321	9093 ± 2875	2498 ± 771	14227 ± 4742	4437 ± 1403	28040 ± 8867	7089 ± 2242	74510 ± 23562	20258 ± 6406
RMV Mean Diameter (nm) *	137.8 ± 16.1	148.2 ± 12.3	158.8 ± 12.3	162.7 ± 15.3	176.0 ± 8.1	176.8 ± 15.1	178.4 ± 8.3	180.0 ± 11.3	185.6 ± 5.6	192.0 ± 11.4
MCF (% NaCl) *,†	0.462 ± 0.006	0.434 ± 0.011					0.473 ± 0.007	0.437 ± 0.013	0.484 ± 0.011	0.439 ± 0.012

3.2.2 Proteomic Analysis of Ghost Fractions of Red Cell Concentrates Derived from High Hemolyzers and Controls During Storage

To further decipher differences between two donor populations at the membrane level, we applied a quantitative proteomics approach using iTRAQ on the two high hemolyzers exceeding the acceptable upper limit of 0.8% and their respective age- and sex-matched controls to assess the protein changes in ghost fractions as a function of storage (RCC^{HH} D5, RCC^{HH} D42, RCC^{Ctrl} D5, and RCC^{Ctrl} D42). This approach identified 108 proteins (**Table A.2**), with 63 shared between two independent experiments. This level of peptide overlap between two independent experiments lies in the range of technical replicates showing 35-60% repeatability [175] and is additionally impacted by the donor-to-donor variability. In order to detect biologically significant alterations, we applied selection criteria of a fold change of protein level of either < 0.5 or > 1.5, resulting in 15 proteins that fulfilled the requirements of consistency, significance, and confidence criteria [176]. There were no marked membrane protein changes over storage in control RCC. While alterations appeared variable and inconsistent for high hemolyzer RCC over storage (RCC^{HH} D5 and D42), a number of reproducible membrane-associated protein changes were displayed with respect to control RCC at early time point (**Table 3.2**).

Table 3.2 iTRAQ-identified levels of protein candidates exhibiting differences in ghost fractions collected from donor pairs #3 and 8.

Changes in membrane-associated protein levels of RCC^{HH} on days 5 and 42 and RCC^{Ctrl} on day 42 are displayed with respected to RCC^{Ctrl} on day 5. Underlined proteins were verified by immunoblot analyses (see **Figure 3.1**). Table 2 from Chen D, Schubert P, Devine DV. Proteomic analysis of red blood cells from donors exhibiting high hemolysis demonstrates a reduction in membrane-associated proteins involved in oxidative response. Transfusion 2017; 57:2248-56. Page 2253. Adapted with permission from publisher.

	High Hemolyzer #3			High Hemolyzer #8			Average		
Protein Name	RCC^{HH5}	RCC^{HH42}	RCC^{Ctrl42}	RCC^{HH5}	RCC^{HH42}	RCC^{Ctrl42}	RCC^{HH5}	RCC^{HH42}	RCC^{Ctrl42}
Catalase	0.169	0.139	1.193	0.068	0.135	0.360	0.118	0.137	0.777
Fructose-bisphosphate aldolase	1.947	1.250	0.948	4.008	1.809	1.718	2.977	1.530	1.333
Heat shock cognate 71 kDa protein	0.445	0.822	1.590	0.531	1.166	0.843	0.488	0.994	1.217
Peroxiredoxin-2	0.041	0.035	1.051	0.040	0.157	0.419	0.040	0.096	0.735
Proteasome activator complex subunit 1	0.070	0.059	0.952	0.031	0.285	0.379	0.050	0.172	0.665
Proteasome subunit alpha type	0.118	0.090	0.905	0.167	0.406	0.506	0.143	0.248	0.706
Proteasome subunit alpha type-5	0.180	0.198	0.921	0.119	0.371	0.466	0.150	0.284	0.694
Proteasome subunit beta type-1	0.567	0.285	0.941	0.114	0.350	0.436	0.341	0.318	0.688
Proteasome subunit beta type-2	0.112	0.089	0.894	0.042	0.339	0.380	0.077	0.214	0.637
Proteasome subunit beta type-4	0.133	0.095	0.744	0.097	0.345	0.481	0.115	0.220	0.612
Proteasome subunit beta type-7	0.191	0.156	0.926	0.133	0.369	0.455	0.162	0.262	0.690
Sorbitol dehydrogenase	1.023	0.733	0.846	2.516	1.972	1.146	1.769	1.352	0.996
Protocadherin-1 (Fragment)	0.180	0.248	0.612	0.701	0.822	0.593	0.441	0.535	0.602
Transitional endoplasmic reticulum ATPase	0.106	0.083	0.946	0.121	0.426	0.428	0.114	0.255	0.687
Tropomyosin 1 (Alpha), isoform CRA_m	0.463	0.451	0.908	0.326	0.500	0.424	0.395	0.476	0.666

3.2.3 Immunoblot Verification of Proteomic Findings

Various factors, such as ratio compression[177] and reporter ion dynamic range[178], could result in an underestimation of change in relative abundance of proteins across samples. Thus, alterations in the levels of selected membrane proteins were assessed in ghost fractions to confirm iTRAQ-identified protein changes. Membrane-associated protein candidates that have been previously proposed as RCC quality biomarkers and also identified in this proteomics study were selected for orthogonal validation[179]: catalase, peroxiredoxin-2, 20S proteasome. In addition to the two high hemolyzer RCC donor pair (#3 and #8) samples assessed by iTRAQ, immunoblot analyses on the remaining eight donor pairs demonstrated similar membrane-associated protein patterns with marked differences between ghost fractions of RCC derived from high hemolyzers and controls and inconsistent alterations with storage (between day 5 and 42); representative immunoblots (**Figure 3.1A-1C**) confirmed significant differences between ghost fractions of RCC derived from high hemolyzers and controls as determined by iTRAQ. Protein levels for spectrin, actin, and stomatin, which were unchanged between the two donor populations (**Table A.2**), were also evaluated via immunoblots (**Figure 3.1D-1F**) to further verify the proteomic results.

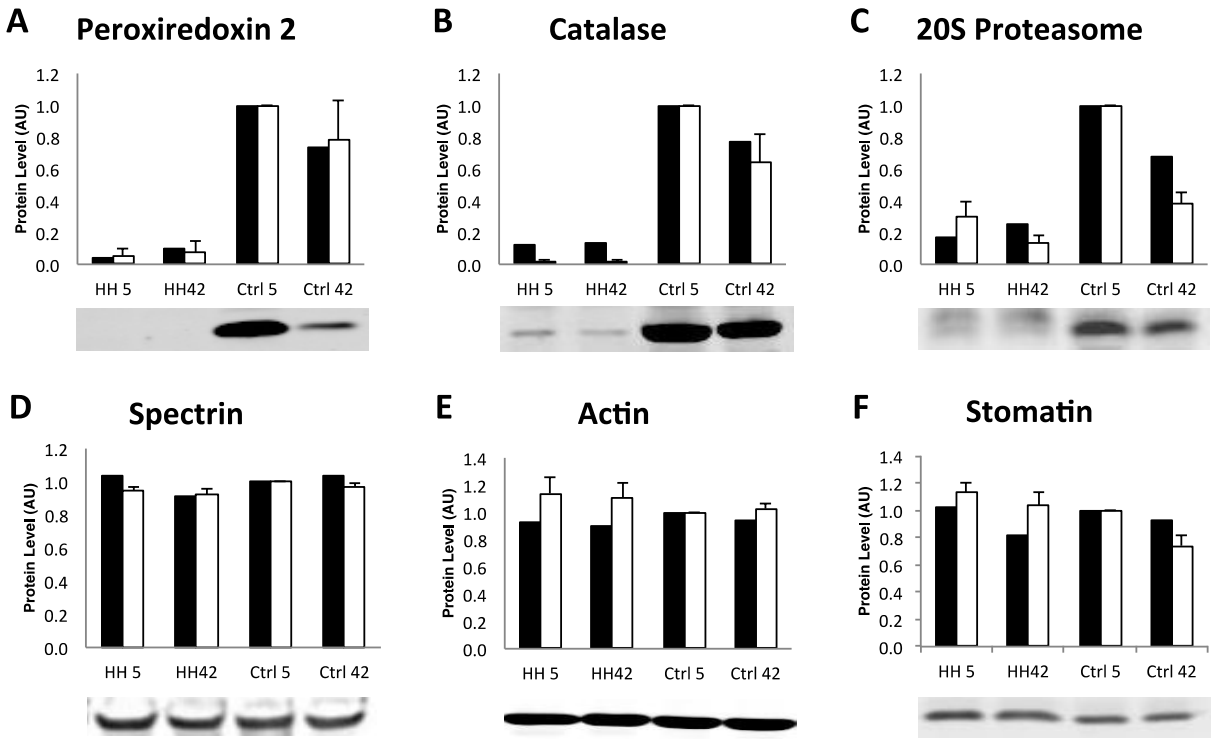

Figure 3.1 Immunoblot verification of selected iTRAQ-identified protein candidates.

Column graphs displaying the ratio of protein changes with respect to RCC^{Ctrl} day 5 ghost fractions. (Solid bars = mean iTRAQ ratio change, n=2; open bars = mean ± S.E.M of immunoblot densitometry analyses, n=10). Representative immunoblots on selected iTRAQ-identified protein candidates, including peroxiredoxin-2 (A), catalase (B), pan-20S proteasome (C), spectrin (D), actin (E), and stomatin (F). Figure 1 from Chen D, Schubert P, Devine DV. Proteomic analysis of red blood cells from donors exhibiting high hemolysis demonstrates a reduction in membrane-associated proteins involved in oxidative response. Transfusion 2017; 57:2248-56. Page 2254. Adapted with permission from publisher.

3.3 Discussion

While blood component production aims to provide optimal quality through process standardization, the influences of inherent donor-to-donor variability on product quality are often difficult to evaluate and to utilize for donor and inventory management purposes. In order to glean insights into relevant impacts of donor characteristics on RCC quality during storage, we

identified an otherwise healthy volunteer donor population exhibiting high hemolysis RCCs on repeated donations and analyzed various quality indices, donor characteristics (including ABO distribution and frequency of donations), and alterations in the membrane proteome of these donors compared to their respective age- and sex-matched control donors with aims to generate potential protein quality makers for inventory monitoring and management.

Aligned with previous reports [173,174], time-dependent storage lesions development was evident in both donor populations (**Table 3.1**). While only two high hemolyzer RCC (donors #3 and #8) exceeded the upper acceptable limit of 0.8%, high hemolyzer RCC exhibited elevated hemolysis compared to control RCC at all time-points measured and were higher compared to the Canadian Blood Services historical QC average of 0.29% at expiry[118]. This observation may also be due to differences in methodology; in the QC setting, hemolysis is calculated using HCT and total Hb obtained from ADVIA-120, and supernatant Hb determined by a HemoCue low Hb system (HemoCue Corporation, Brea, CA). RMV release appeared to parallel hemolysis development, with high hemolyzer RCC producing significantly more RMV during time spent in storage compared to control RCC. Osmotic fragility, a surrogate indicator of membrane integrity, also seemed to suggest notable differences between the two donor populations, with the membrane of high hemolyzer RCC being significantly less resilient compared to that of the control RCC. While MCF increased marginally with time spent in storage, these changes were insignificant and did not offer an explanation for the marked elevation observed in hemolysis and RMV release. These membrane changes were mirrored in RBC morphology, with high hemolyzer RCC displaying more features of crenation and containing more echinocytes compared to control RCC. However, despite similar adenine nucleotide metabolism between RCC derived from high hemolyzers and controls, the differences in morphology score disappeared with time spent in storage. Given that only intact cells are assessed for their shape, this observation could possibly be attributed to an inherent feature of the method of morphology

evaluation. While genetic abnormalities were not directly assessed in the study, baseline morphology and osmotic fragility were evaluated by a practicing hematologist and all donations appeared normal. Interestingly, 2, 3-BPG levels were markedly reduced in higher hemolyzer RCC compared to control RCC, suggesting potential reduction in Hb stability and therefore increased risk of oxidative damage. However, these parameters were not assessed in this study. Alternatively, the observed differences in 2, 3-BPG levels may reflect the slight difference in pH, which may be related to unit handling and logistics, as all high hemolyzer RCC units were shipped to NetCAD while control RCC units were produced at NetCAD. Taken together, these observations suggest that high hemolyzers are indeed a subpopulation exhibiting unique membrane characteristics within the general donor pool. Thus, we looked to the membrane proteome for clues that may account for the differences in *in vitro* quality indices. Ghost fractions from two donor pairs were assessed via iTRAQ to further delineate potential donor characteristics that may impact product quality. While *in vitro* parameters displayed similar trends previously reported, time-dependent alterations in membrane proteome profiles as identified by iTRAQ appeared to be inconsistent with some existing reports. Previous membrane proteomic investigation of normal RCC revealed time-dependent alterations, such as increased membrane accumulation of peroxiredoxin-2 [38], degradation of cytoskeletal components[180], decrease in various glycolytic enzymes, small G proteins, chaperone proteins (e.g., T complex protein-1), and components of the proteasome[17,112,113] which has been shown to be released during blood bank storage [115,181]. More recent studies identified the role of oxidative protein modifications in RBC metabolism during their blood bank storage, including glyceraldehyde 3-phosphate dehydrogenase and hemoglobin [182,183]. However, in this study in depth immunoblot analyses on selected membrane-associated protein candidates derived from proteomic analyses, peroxiredoxin-2 for example, on all donor pairs suggests inconsistent change with

storage (**Figure 3.1A**). The observed inconsistency may possibly be attributed to the differences in methodology during ghost fraction preparations.

The proteins identified in **Table 3.2** are mostly cytosolic proteins that are membrane-associated. This may be attributed to the target residues for tryptic cleavage (i.e., lysine and arginine) are preferentially found in the hydrophilic part of transmembrane proteins and membrane-associated proteins. While peroxiredoxin-2, glycolytic enzymes, heat shock cognate 71 kDa protein, protocadherin, transitional endoplasmic reticulum ATPase have been previously identified in RBC membrane fractions[107,108], most of them were not further investigated as their physiological functions are poorly understood in the context of RBC storage quality. Peroxiredoxin-2 has recently drawn attention as a candidate biomarker for oxidative stress levels in stored RCCs[38,40]. A molecular mechanism is suggested between the oxidized hemoglobin on Cys93 and peroxiredoxin-2[184].

Proteomic data revealed marked reduction in candidate membrane-associated protein levels at early time point between higher hemolyzer RCC and control RCC, which hints at a possible impact on product quality during storage. The significant reduction in proteins involved in oxidative defense may explain the elevated hemolysis and impaired membrane integrity observed in high hemolyzer RCC. As *in vitro* parameters and proteomic findings both display distinct differences between the two donor populations, we sought to investigate how selected predictors at early time point contribute to the category membership of high hemolyzer RCC or control RCC at day 42. In an effort to better understand the donor characteristics predictive of hemolysis development over storage, we have performed a stepwise logistic regression of continuous variables that have been previously suggested to be associated with RCC quality, such as donor age at time of donation, Day 5 hemolysis, Day 5 ATP level, and levels of candidate protein quality markers. The three main predictors, in descending order of importance, for hemolysis development over storage were Day 5 hemolysis ($p < 0.01$), Day 5

peroxiredoxin-2 protein level ($p < 0.01$), and donor age at time of donation ($p = 0.15$). However, given the small sample size, we hesitate to place emphasis on the identified association between these parameters and hemolysis level at expiry without further cross-validation in a larger sample population.

Other factors may influence the quality of RCC and possibly the results of this study. While the RCC production method is known to impact hemolysis and was not specified for the purpose of minimizing workflow interruption in this study[118], it was comparable between the two groups (**Table A.1**). The ABO distribution between the two populations was significantly different (p <0.01). Routine RCC QC is performed on 1% of total collections, but these are primarily group AB donations. Due to the small proportion of AB donors and the high outdate rates of AB RCCs, repeat donors have a reasonably high probability of appearing more than once in the QC pool. However, there is no suggestive evidence that ABO group influences RCC quality[185]; our in-house unpublished data show that ABO distribution does not impact hemolysis levels at expiry (n = 219, p = 0.88). The frequency of donation has been implicated in RCC quality, as it alters the iron status of the donor over time and may result in impaired/iron-deficient erythropoiesis. While high hemolyzers #3 and #8 donated twice more than their respective controls, no significant difference in the number of donations in the past 12 months, including the donation in study, between the two donor populations was detected.

Taken together, our findings suggest that proteins involved in oxidative response pathways at the red cell membrane at early time points may be predictive of storage quality. More specifically, membrane-bound peroxiredoxin-2 may offer potential utility as quality monitoring tool to inform inventory and donor management strategies.

Chapter 4: Post-Collection Manipulations – Investigating Process-Induced Hemolysis and Verifying Candidate Protein Quality Biomarkers in Pathogen Inactivated and Gamma-Irradiated Red Cell Concentrates

4.1 Introduction

Blood banks are challenged to balance blood product safety and quality. Rigorous donor screening, routine product testing, and standardized manufacturing procedures ensure overall safety and quality of blood transfusion products, while post-collection manipulations such as gamma-irradiation and PI technology aim to further enhance product safety for vulnerable recipient populations[146,186,187]. However, these RCC post-collection manipulations often improve safety at a cost to product quality, as previously mentioned in **Chapter 1.5.2** and **1.5.3**.

Briefly, TA-GVHD, resulting from the engraftment of allogenic donor leukocytes, is effectively prevented with gamma-irradiation[139,140]. However, gamma-irradiation causes a significant reduction in RCC *in vitro* quality parameters and RBC survival. ROS generation and the deterioration of membrane integrity are evidenced by lipid peroxidation, potassium leakage, increased hemolysis, and defective ATP metabolism[140-145]. Due to the loss of RCC quality, the length of storage time of gamma-irradiated RCC is normally reduced. PI technologies are a proactive approach to mitigate the transmission of pathogens by blood products[146]. One PI technology (treatment with riboflavin and UV illumination) has been adapted to WB treatment[150,151] and is an effective way to prevent TA-GVHD[188]. However, RCCs derived from PI-treated WB had poorer *in vitro* quality compared to that of untreated controls[189], as evidenced by marked increased hemolysis. The exact biochemical mechanisms of storage-dependent development of hemolysis and its exacerbation by post-collection manipulations remain largely unknown.

Therefore, to understand the impact of RCC post-collection manipulations, we investigated the biochemical alterations induced by RCC post-collection manipulations. We

found significant correlations between hemolysis as a primary RCC quality measure and the concentration of certain membrane-associated proteins, including peroxiredoxin-2, catalase, and 20S proteasome, suggesting their utility as protein biomarkers for standard RCC quality and their potential application for fine-tuning blood-banking strategies in balancing product safety and quality.

4.2 Results

4.2.1 Red Cell Concentrate *in vitro* Quality Parameters

The concentration of RBCs and pH were comparable between untreated ($RCC^{Ø}$), PI-treated (RCC^{PI}), and gamma-irradiated ($RCC^{γ}$) RCC throughout storage ($p > 0.05$; data not shown), confirming that the pool-and-split design yielded RCCs with comparable cellular contents (**Figure 4.1**).

PI-treated RCC exhibited an elevated HCT compared to both gamma-irradiated and untreated RCC by day 28 of storage ($p < 0.01$; **Figure 4.2A**). This observation is consistent with increased MCV over storage ($p<0.01$), with PI-treated RCC exhibiting the highest MCV and gamma-irradiated RCC displaying a moderate increase compared to that of untreated RCC ($p < 0.01$; **Figure 4.2B**). Extracellular potassium levels increased with time spent in storage ($p < 0.01$). Both post-collection manipulations accelerated initial potassium leakage, while potassium levels steadily increased in untreated RCC with increasing storage time (**Figure 4.2C**). Hemolysis continuously increased during storage for all three arms ($p < 0.01$). The development of hemolysis was considerably higher in PI-treated RCC ($p < 0.01$) and consequently these samples exhibited elevated hemolysis compared to both gamma-irradiated and untreated RCC for all time-points measured (**Figure 4.2D**). Notably, the development of hemolysis in PI-treated RCC was marked after 21 days of storage.

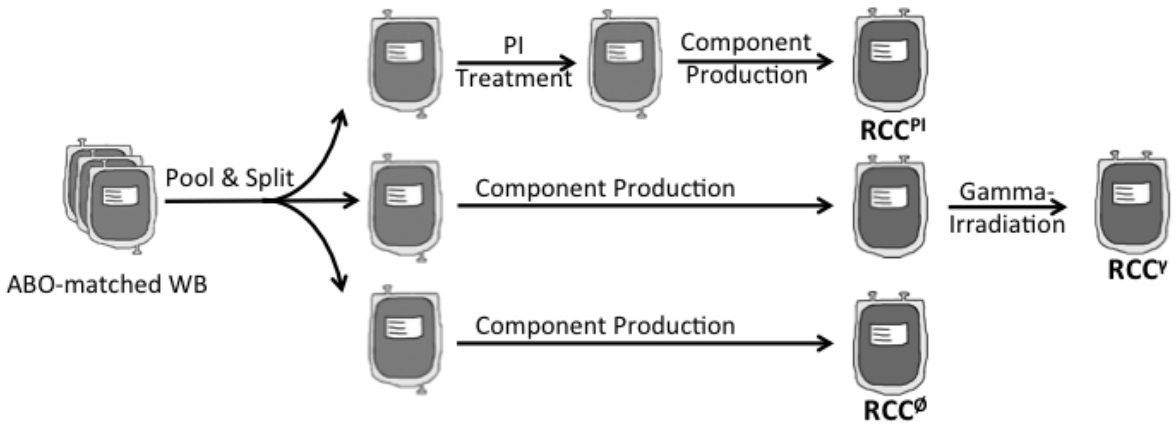

Figure 4.1 Study design schematic.

Three ABO-matched WB units were pooled and split into three identical units. One was treated with riboflavin and UV illumination and all three were kept on a cooling tray overnight prior to production into RCC. One of the two standard RCC derived from untreated pooled WB units was gamma-irradiated (25 Gy) immediately following production. This resulted in one WB PI-treated RCC (RCC^{PI}), one gamma-irradiated RCC (RCC^{γ}), and one standard untreated RCC ($RCC^{\varnothing}$). The study has six independent replicates (n = 6).

As expected, RMV formation paralleled closely hemolysis development (**Figure 4.2E**). RMV size appeared to increase gradually with storage time ($p < 0.01$). PI-treated RCC RMV exhibited a larger size ($p < 0.01$), while gamma-irradiated and untreated RCC produced RMV of comparable size ($p > 0.05$; **Figure 4.2F**). These changes in RMV size over time may contribute to the alteration in RBC osmotic fragility, a surrogate measure of membrane integrity. The ability of PI-treated RCC to resist changes in osmotic pressure declined significantly at day 42 ($p < 0.01$; **Figure 4.2G**).

Morphology scores decreased with increasing storage time ($p < 0.01$; **Figure 4.2H**). Both post-collection manipulations accelerated deterioration of RBC shape and membrane maintenance compared to untreated controls ($p < 0.0001$). ATP concentration over time followed a similar trend to morphology score ($r = 0.793$, $p < 0.0001$; **Figure 4.2**H, solid lines).

ATP of PI-treated and gamma-irradiated RCC hydrolyzed faster than untreated RCC, as further evidenced by their ADP and AMP accumulation patterns (**Figure 4.2I**, dashed and dotted lines, respectively), with PI-treated and gamma-irradiated RCC AMP levels higher than that of untreated RCC at expiry ($p < 0.01$).

The levels of 2, 3-BPG declined with time spent in storage without significant differences between treatments (**Figure 4.2J**). The percentage of annexin V positive RBC was not significantly different between the three study arms after 4 and 21 days of storage. RBC PS exposure was, however, significantly more pronounced in PI-treated RCC following 42 days of storage as compared to untreated RCC ($p < 0.05$; **Figure 4.2K**). As a positive control, RBC treated with ionomycin (0.1 μM for 15 min) showed significantly higher ($p < 0.01$) PS exposure (12.9 ± 1.2%; n = 3) as compared to untreated RBC (2.0 ± 0.4%; n = 3). Cytosolic calcium activity was determined using Fluo3 fluorescence in flow cytometry analysis. As illustrated in **Figure 4.2L**, Fluo3 fluorescence was significantly elevated in PI-treated RCC as compared to gamma-irradiated and untreated RCC, implying that increased cytosolic calcium activity contributes to enhanced PS externalization observed in PI-treated RCC after 42 days of storage. As a positive control, ionomycin treatment (0.1 μM for 15 min) showed significantly ($p < 0.001$) increased cytosolic calcium activity (3.8 ± 0.2 AU; n = 3) as compared to untreated RBC (1.0 ± 0.0 AU; n = 3).

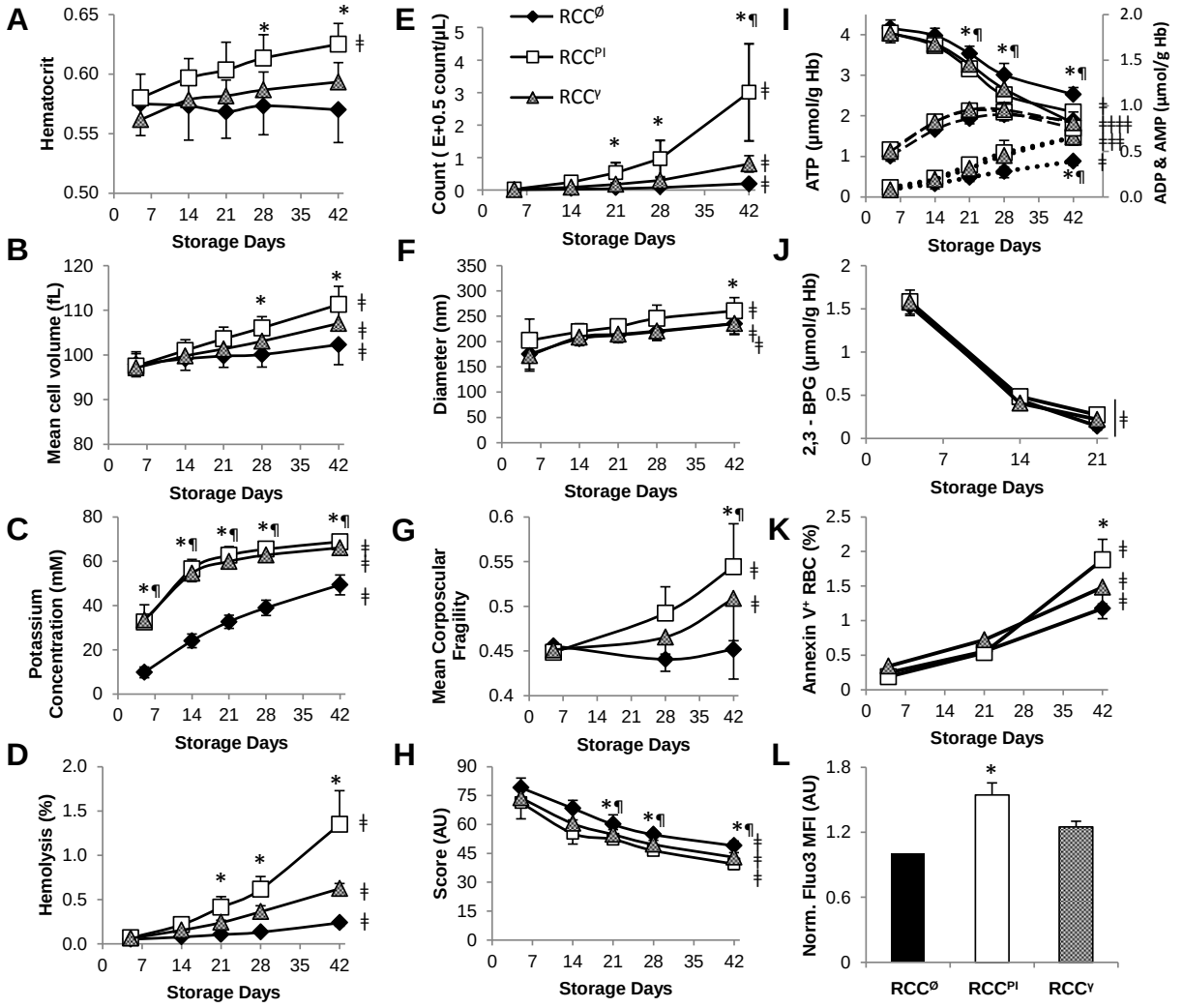

Figure 4.2. *In vitro* parameters of RCC^{Ø}, RCC^{Pl}, and RCC^{γ}

Graphs show mean ± S.D. of (A) HCT; (B) MCV; (C) extracellular potassium accumulation in the supernatant; (D) percentage hemolysis; (E) RMV count; (F) RMV size; (G) MCF; (H) morphology score; (I) intracellular ATP, ADP, and AMP concentrations (solid, dashed, and dotted lines, respectively); (J) 2,3-BPG levels; (K) PS exposure; and (L) normalized Fluo3 fluorescence of RCC^{Ø}, RCC^{Pl}, and RCC^{γ} during storage. All graphs show data from days 5, 14, 21, 28 and 42 of storage, except MCF which was measured on days 5, 28 and 42; 2, 3-BPG which was measured on days 4, 14, and 21, annexin V binding which was measured on days 4, 21, and 42, and normalized Fluo3 fluorescence at day 42. (* = RCC^{Pl} significantly different from RCC^{Ø}; ¶ = RCC^{γ} significantly different from RCC^{Ø}; ǂ = p<0.05 over time spent

in storage; n=6). Figure 1 from Chen D, Schubert P, Devine DV. Identification of potential protein quality markers in pathogen inactivated and gamma-irradiated red cell concentrates. Proteomics Clin. Appl. 2017; 11 (7-8):16600121. Page 5 of 9. Adapted with permission from publisher.

4.2.2 Proteomic Analysis of Ghost Fractions of Untreated, PI-treated, and Gamma-Irradiated Red Cell Concentrates

To gain further insights into post-collection manipulations-induced membrane alterations, we applied a quantitative proteomics approach using iTRAQ to assess the protein changes in the ghost fractions as a function of storage ($RCC^{Ø}$ D5 and $RCC^{Ø}$ D28) and as a function of post-collection manipulations ($RCC^{Ø}$ D28, RCC^{PI} D28, and $RCC^{γ}$ D28). This approach identified 100 proteins (**Table B.1**), with 53 shared between two independent experiments. This level of peptide overlap between two independent experiments lies in the range of technical replicates showing 35-60% repeatability [175] and is additionally impacted by the donor-to-donor variability. With the application of selection criteria of a fold-change of protein expression of either <0.5 or >1.5 for detection of biologically significant alterations [176], there were no significant membrane protein alterations over storage from day 5 to 28 ($RCC^{Ø}$ D5 and $RCC^{Ø}$ D28). Gamma-irradiation induced minor protein profile alterations at the RBC membrane but did not fulfill the selection criteria; however, 7 protein candidates reproducibly decreased in their respective concentrations with PI treatment (**Table 4.1**).

4.2.3 Validation of Proteomic Findings by Immunoblot Analyses

Changes in the levels of selected membrane-associated protein were assessed in independent ghost preparations to confirm protein changes identified in iTRAQ. Several identified proteins affected by post-collection manipulations are involved in oxidative stress response pathways; three of these were selected for orthogonal validation: peroxiredoxin-2,

catalase, and 20S proteasome, as they have been previously reported in the context of RCC storage quality. Representative immunoblots (**Figure 4.3 A-C**) confirmed significant decrease in PI-treated RCC day 28 ghost fractions as determined by iTRAQ. Spectrin, stomatin, and actin which were unchanged by post-collection manipulations (**Table B.**) were also evaluated via immunoblots (**Figure 4.3 D-F**) to verify the proteomic results.

Table 4.1 iTRAQ-identified protein candidates exhibiting expression differences in ghost fractions. Changes in membrane-associated protein level of $RCC^{Ø}$, RCC^{Y}, and RCC^{PI} on day 28 are displayed with respect to $RCC^{Ø}$ on day 5. Underlined proteins were verified by immunoblot analyses (see **Figure 4.3**). Table 1 from Chen D, Schubert P, Devine DV. Identification of potential protein quality markers in pathogen inactivated and gamma-irradiated red cell concentrates. Proteomics Clin. Appl. 2017; 11 (7-8):16600121. Page 6 of 9. Adapted with permission from publisher.

	iTRAQ #1			iTRAQ #2			Average		
Protein Name	$RCC^{Ø}$	RCC^{PI}	RCC^{Y}	$RCC^{Ø}$	RCC^{PI}	RCC^{Y}	$RCC^{Ø}$	RCC^{PI}	RCC^{Y}
Acylamino-acid-releasing enzyme (Fragment)	0.937	0.431	0.781	0.913	0.340	0.661	0.925	0.386	0.721
Catalase	1.118	0.490	0.911	0.873	0.284	0.502	0.996	0.387	0.707
Peroxiredoxin-2	1.302	0.404	0.944	1.033	0.320	0.655	1.168	0.362	0.800
Proteasome activator complex subunit 1	0.608	0.315	0.579	0.846	0.387	0.709	0.727	0.351	0.644
Proteasome subunit alpha type	0.453	0.317	0.457	0.972	0.581	0.903	0.712	0.449	0.680
Protocadherin-1 (Fragment)	0.642	0.427	0.558	1.082	0.521	0.672	0.862	0.474	0.615
Transitional endoplasmic reticulum ATPase	0.701	0.416	0.707	0.849	0.437	0.725	0.775	0.427	0.716

4.2.4 Correlation Between Membrane-Associated Protein Profile and Red Cell Concentrate Quality

In addition to the original samples assessed by iTRAQ, immunoblot analyses demonstrated that additional independent samples exhibited similar membrane-associated protein expression patterns. Since proteins involved in oxidative stress response are integral for RBC membrane maintenance and integrity, the relationship between observed alterations in membrane-associated protein profile and hemolysis were analyzed. Alterations in expression

levels of peroxiredoxin-2 (r = - 0.673; p = 0.006; **Figure 4.4A**), catalase (r = - 0.564; p = 0.029; **Figure 4.4B**), and proteasome (r = - 0.613; p = 0.015; **Figure 4.4C**) in ghost fractions of PI-treated, gamma-irradiated, and untreated RCC exhibited significant negative correlations with their respective hemolysis level at day 28. Additionally, membrane-associated peroxiredoxin-2 and catalase exhibit robust negative correlations (r = 0.881; $p < 0.001$), while no significant relationships were observed between peroxiredoxin-2 (r = 0.215; $p > 0.05$) or catalase and proteasome (r = -0.008; $p > 0.05$).

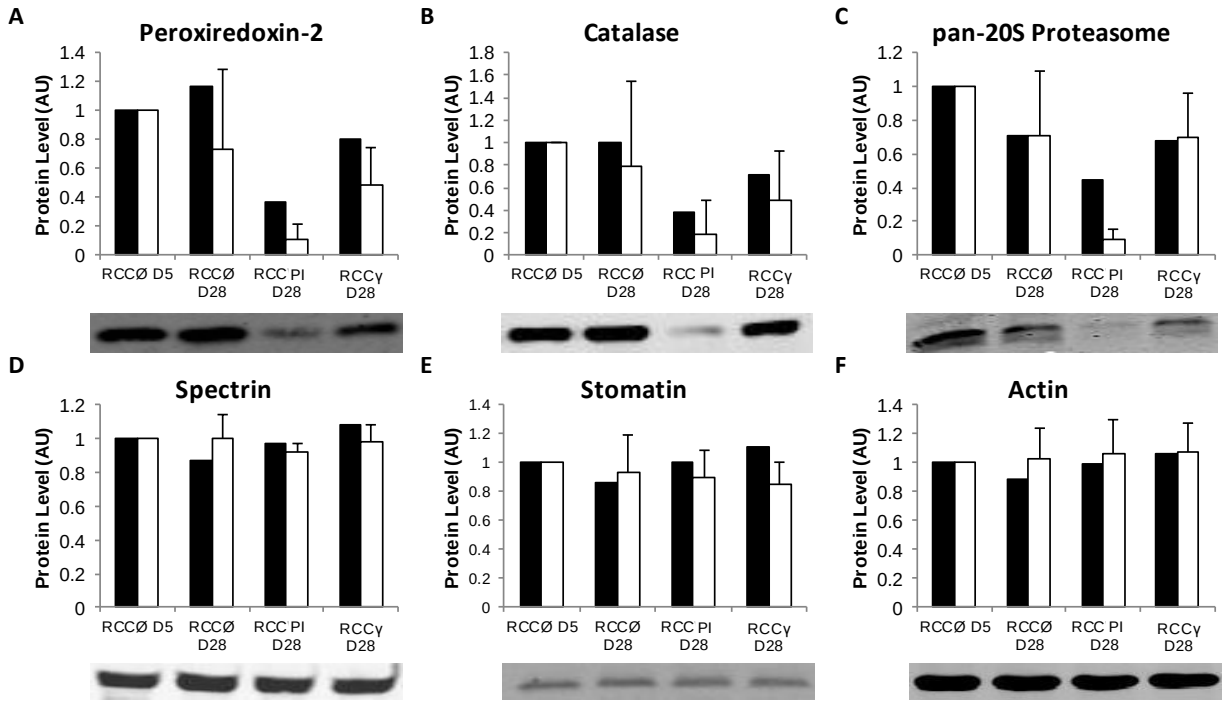

Figure 4.3 Immunoblot verification of selected iTRAQ-identified protein candidates

Column graphs displaying the ratio of protein changes of independent ghost fractions with respect to RCC^{Ø} day 5. (Solid bars = mean iTRAQ ratio change, n=2; open bars = mean ± S.D. of densitometry analysis of immunoblots, n=5). Representative immunoblots of RCC^{Ø}, RCC^{PI}, and RCC^{γ} day 28 ghost fractions on selected iTRAQ-identified protein candidates, including peroxiredoxin-2 (A), catalase (B), pan-20S proteasome (C), spectrin (D), stomatin (E), and actin (F). Figure 2 from Chen D, Schubert P, Devine DV. Identification of potential protein quality markers in pathogen inactivated and gamma-irradiated red cell concentrates. Proteomics Clin. Appl. 2017; 11 (7-8):16600121. Page 6 of 9. Adapted with permission from publisher.

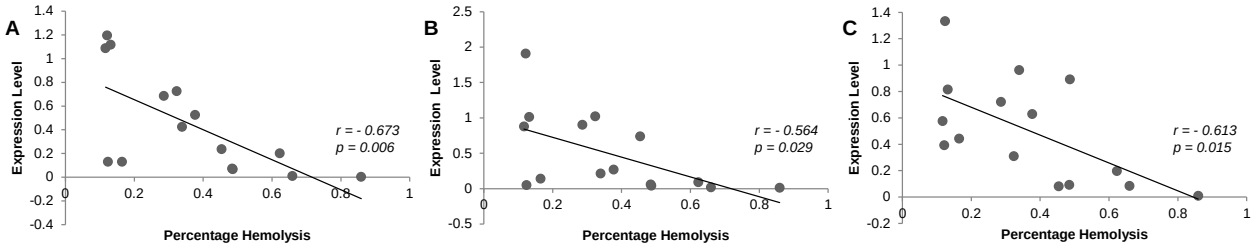

Figure 4.4 Correlation between hemolysis and immunoblot-verified protein candidates

Correlation graphs on all consolidated samples (n = 5) displaying robust negative linear relationships between hemolysis and expression of membrane peroxiredoxin (A), catalase (B), and pan-20 proteasome (C) at day 28 of storage in RCC^{Ø}, RCC^{PI}, and RCC^{γ}. Figure 3 from Chen D, Schubert P, Devine DV. Identification of potential protein quality markers in pathogen inactivated and gamma-irradiated red cell concentrates. Proteomics Clin. Appl. 2017; 11 (7-8):16600121. Page 6 of 9. Adapted with permission from publisher.

4.3 Discussion

Hemolysis is often attributed to mechanical rigidity and sheer stress; however, the mechanisms of hemolysis development remain poorly understood. Production and manufacturing processes can mechanically induce hemolysis[118,120,190], while prolonged hypothermic storage leads to the development of storage lesions[191]. The application of RCC post-collection manipulations augments storage lesion development, further accelerating the decline in product quality[144,189].

In our comparative analysis, all units were tested to the maximum 42 day storage of the controls. PI-treated RCC exhibited accelerated storage lesions development compared to untreated RCC with enhanced potassium accumulation, elevated hemolysis, higher RMV release, increased osmotic fragility, decreased morphology score, faster adenine nucleotide utilization, and subtle elevation of cytosolic calcium activity resulting in a small increase PS externalization. These *in vitro* changes were more pronounced in PI-treated RCC; the hemolysis

level exceeded the upper acceptable limit for transfusion (< 0.8% and < 1.0% for European/Canadian and US jurisdictions, respectively) at day 42 of storage with a striking amount of RMV in the supernatant, PS externalization was significantly higher than untreated RCC, and potassium levels were markedly elevated. RBC storage under blood bank conditions is known to potentiate cytosolic calcium concentration[64,192-194] which, in turn, stimulates the cell volume-regulatory calcium-sensitive potassium channels[195]. Activation of these channels drives the efflux of potassium ions and osmotically obliged water, leading to cell shrinkage[195]. Surprisingly, we observed that MCV of PI-treated RCC was increased at all time points measured and despite elevated PS exposure on day 42, the MCV remained significantly higher as compared to untreated RCC. It may be conjectured that the dissociation between cytosolic calcium activity and MCV alterations in PI-treated RCC is due to its inhibitory effect on cell volume regulatory ion channels[195]. These observations indicate that PI treatment may induce more severe alterations to regulated cellular processes at the membrane and may trigger cellular repair mechanisms in PI-treated RCC. While the mechanism of mean RMV size increase in PI-treated RCC over storage was not directly investigated, we speculate that this observation likely reflects the overall reduction in membrane stability and may be attributed to increased likelihood for lipid fusion events through chance collision, as we observed a marked increase in absolute number of PI-treated RCC RMV with time spent in storage. Additionally, the observed differences in *in vitro* quality parameters between PI-treated and gamma-irradiated RCC were likely influenced by the difference in total energy exposure. One previous study validated that PI treatment could as effectively ameliorate T cell proliferation as gamma-irradiation at a much lower dose (22 J/mL$_{RBC}$) than that employed in our study (80 J/mL$_{RBC}$)[188].

Lipoperoxidation and oxidative damage to membrane proteins occur with both storage [196-199] and post-collection manipulations [200] and efforts aimed to reduce the oxidative damage incurred over storage include blood product deoxygenation[201,202] and supplemental

antioxidants[203,204]. Pasini and colleagues demonstrated unexpected complexity of RBC membrane and cytosolic proteomes[16], and numerous subsequent RBC proteomic studies on standard RCC revealed time-dependent alterations in the post-translational modifications of Hb, markers of oxidation (protein carbonylation and malondialdehyde accumulation), stability of cytoskeletal membrane protein interactions, and protein phosphorylation status[113,114,205]. In the present study, iTRAQ was selected for its ability to directly compare and relatively quantify protein concentration of different samples in a single experiment. Our proteomic approach allowed the direct comparison of the membrane proteomes of PI-treated and gamma-irradiated RCC at day 28 of storage. The absence of reticulocyte-specific transferrin receptor and leukocyte- and platelet-specific glycoproteins identification by iTRAQ indicated an undetectable level of contaminating reticulocytes, white blood cells and/or platelets.

Because gamma-irradiated units have a limited regulatory shelf-life and PI-treated RCC are unlikely to be licensed for storage > 28 days owing to elevated hemolysis, we examined ghost fractions at days 5 and 28. No significant time-dependent alterations in membrane proteins were detected between days 5 and 28 of storage. This observation parallels that of osmotic fragility, suggesting that membrane integrity may not be severely compromised at day 28 of storage. Significant alterations of anti-oxidant membrane-associated protein levels were detected in PI-treated RCC [38,113,114]; however, we did not detect an accumulation in membrane-associated peroxiredoxin-2 in untreated RCC over storage (data not shown) as previously described [38], which was likely attributed to the differences in methodology during ghost fraction preparations. While acylamino-acid-releasing enzyme, protocadherin, and transitional endoplasmic reticulum ATPase have been previously identified in RBC membrane fractions[18,206,207], they were not further investigated as their physiological functions are poorly understood in RBCs. Whether these proteins did not translocate to the membrane or were destroyed by the treatment was not determined. PI-treated RCC showed strong decreases in

membrane-associated peroxiredoxin-2, catalase, and proteasome levels compared to that of gamma-irradiated and untreated RCC, which may reflect decreased capacity to defend against lipoperoxidation and protein oxidation, as well as ability to remove oxidized proteins to minimize their cytotoxicity[46]. This observation may further explain the accelerated deterioration of *in vitro* quality parameters of PI-treated RCC.

Numerous traditional quality indices of PI-treated RCC improved significantly during storage with oxygen reduction treatment [208], indicating that oxidative stress plays a significant role in the observed accelerated storage lesion development in PI-treated RCC. Our proteomic results support that PI treatment may indeed impact RCC through oxidative mechanisms. The peroxidase activity of peroxiredoxin-2 is crucial for RBC survival in mice, without which the animals exhibit hemolytic anemia, with extensive oxidation of RBC proteins[41,42]. Membrane-associated peroxiredoxin-2 was previously proposed as a biomarker for lipoperoxidation and oxidative stress in stored human RBC[38,119], further suggesting that biochemical changes induced by PI treatment may be mediated by oxidative injury. Similarly, the reduction in membrane-associated catalase further supports that PI treatment induces oxidative damage, as catalase plays an important role in neutralizing exogenous oxidative agents in RBC[33,46]. Proteasomes readily remove oxidized proteins in an ATP- and ubiquitin-independent manner, offering protection against oxidative damage[46]; their reduction in PI-treated RCC suggests a decrease in oxidative defense at the membrane. We identified a significant negative correlation between protein alterations in total membrane-associated peroxiredoxin-2, catalase, and 20S proteasome and percentage hemolysis, consolidating our proposal of their potential utility as RCC quality biomarkers. While membrane-associated peroxiredoxin-2 and catalase appeared to be closely related to one another and to percentage hemolysis, multivariate regression model (*percentage hemolysis = 0.661 – 0.119 peroxiredoxin-2 – 0.150 catalase – 0.329 proteasome*) suggests that when all three candidate proteins are taken into account, proteasome may be

more informative of percentage hemolysis development ($p < 0.01$) as it behaves differently from the other two candidate proteins.

Future studies are needed to interrogate the robustness of these potential protein biomarkers of RCC quality. Overall, insights into changes in *in vitro* parameters and membrane proteome as a function of post-collection manipulations may inform the development of efficient inventory management strategies and may offer alternative approaches to balance RCC safety and quality for our transfusion recipients.

Chapter 5: Modulating Process-Induced Hemolysis - Application of Identified Protein Quality Markers in Deoxygenated Red Cell Concentrates

5.1 Introduction

As further supported by data reported in the previous chapter, post-collection manipulations have been shown to exacerbate RBC oxidation through generation of ROS and result in reduced RBC survival *in vivo*[209,210]. Given that PI treatment is an emerging technology and currently under consideration for licensure in Canada, investigation into minimizing its negative impact on RCC *in vitro* quality is warranted. Previous efforts explored antioxidant supplementation or addition of precursor molecules to combat oxidative damage incurred over time spent in storage demonstrated reduction in hemolysis development, promoted GSH homeostasis, and slowed peroxiredoxin-2 oxidation[203,211,212]. An alternative approach to reduce oxidative stress is through deoxygenation; removal of oxygen at the beginning and throughout RCC storage appears to effectively slow the development of RBC storage lesions[156,157] through elimination of the primary substrate for the ROS-generating Fenton reaction and replenishment of high energy phosphates via Embden-Meyerhof pathway [158,159].

Using a pool-and-split study design (**Figure 5.1**), we explored the efficacy of deoxygenation treatment in rescuing deleterious effects induced by PI treatment. Moreover, we sought to further verify the utility of proposed candidate protein quality markers in these alternatively prepared RCCs, as membrane-associated proteins involved in oxidative response pathways appear to be central to overall RBC membrane integrity and, consequently, to their RCC storage quality. We predicted that deoxygenation treatment should successfully reduce hemolysis development and yield a concomitant increase in levels of candidate protein quality markers in units treated with PI.

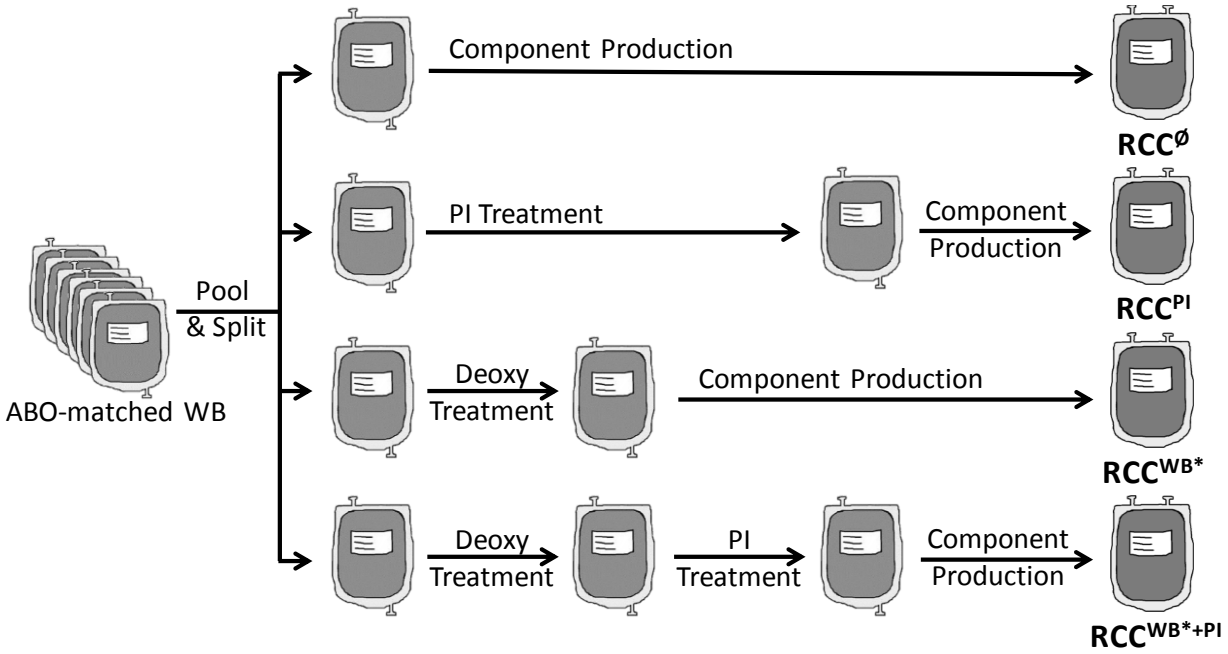

Figure 5.1 Study design schematic.

Six ABO-matched WB units were pooled and split into six identical units. For the purpose of this research chapter, only four treatment arms are displayed. One was treated with riboflavin and UV illumination; another was subjected to deoxygenation; and the third undergone deoxygenation treatment prior to PI. All four units were kept on a cooling tray overnight prior to production into RCC. This resulted in one standard untreated RCC, one WB PI-treated RCC (RCC^{PI}), one WB deoxygenated RCC (RCC^{WB*}), and one WB deoxygenated PI-treated RCC (RCC^{WB*+PI}). The study has five independent replicates (n = 5). Deoxygenation at the RCC level was omitted from this research chapter.

5.2 Results

5.2.1 Impact of Deoxygenation Treatment on Red Cell Concentrate *in vitro* Quality Parameters

Given that the plastic storage bags are gas-permeable, So_2 gradually increased with time in RCCs stored under conventional conditions ($p < 0.01$; **Figure 5.2A**), with PI-treated RCC exhibiting significantly lower So_2 than that of untreated RCC ($p < 0.05$). Deoxygenation

treatment successfully reduced So_2 at the beginning of storage and was able to maintain So_2 below 8% throughout storage ($p < 0.001$; **Figure 5.2A**). Percentage hemolysis increased temporally in all treatment arms as expected ($p < 0.01$), with WB deoxygenated and untreated RCC displaying comparable levels of hemolysis ($p > 0.05$). Deoxygenation treatment was able to dampen hemolysis development induced by PI treatment, as evidenced by the significantly reduced level in those that received WB deoxygenation treatment following PI treatment ($RCC^{WB^{*}+PI}$ compared to RCC^{PI}) ($p < 0.01$; **Figure 5.2B**). Moreover, RMV formation mirrored hemolysis development closely over storage ($p < 0.01$; **Figure 5.2C**).

While glucose consumption was similar between treatments ($p > 0.05$; **Figure 5.2D**), lactate showed higher accumulation in deoxygenated RCCs than in normoxic RCCs ($p < 0.01$; **Figure 5.2D**). RBC metabolism was reflected in a significant decrease in pH over storage in all treatment arms ($p < 0.01$; **Figure 5.2E**). In spite of similar pH between treatments ($p > 0.05$), deoxygenated RCCs ($RCC^{WB^{*}}$ and $RCC^{WB^{*}+PI}$) appeared to be better able to maintain ATP and 2, 3-BPG stores than normoxic RCCs ($RCC^{\varnothing}$ and RCC^{PI}) during storage ($p < 0.01$; **Figure 5.2F and G**). This observation reflected changes in osmotic fragility, as cellular integrity has been shown to depend on ATP level – RBC's ability to resist osmotic changes was significantly improved with deoxygenation treatment ($p < 0.01$; **Figure 5.2H**).

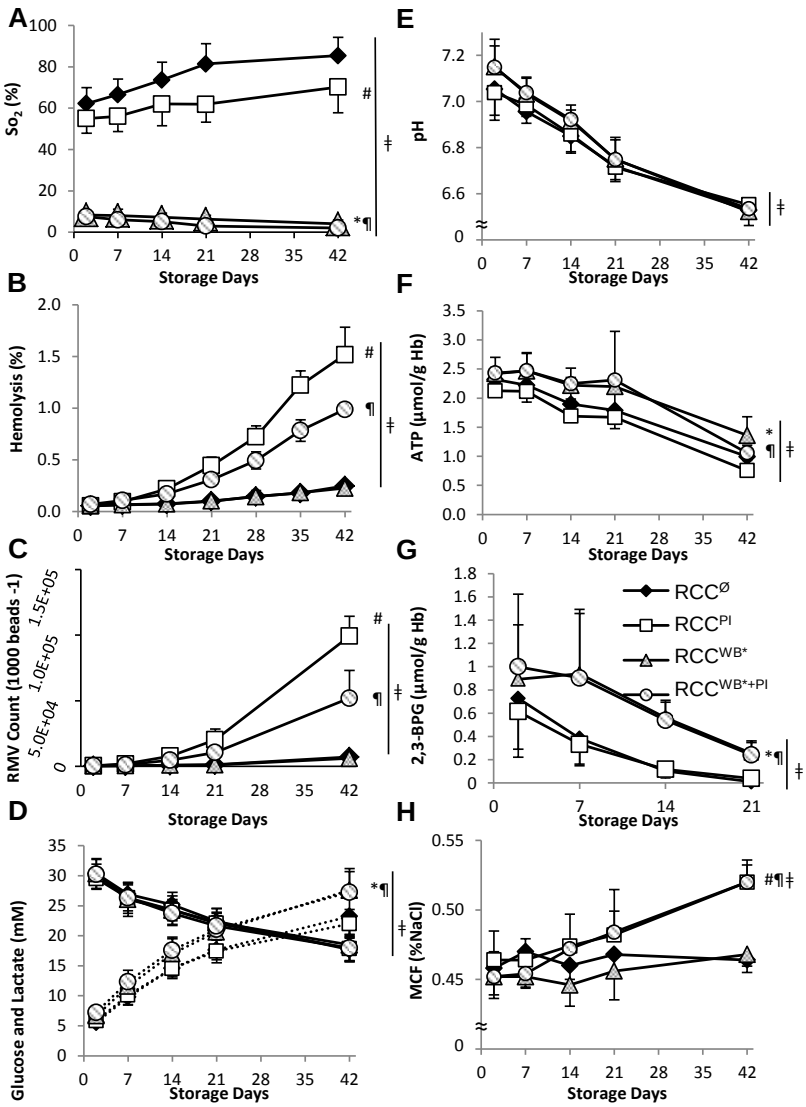

Figure 5.2. *In vitro* parameters of RCC^{Ø}, RCC^{PI}, RCC^{WB*}, and RCC^{WB*+PI}

Graphs show mean ± S.D. of (A) So_2; (B) percentage hemolysis; (C) RMV count; (D) glucose and lactate concentrations (solid and dotted line, respectively); (E) pH; (F) ATP concentration; (G) 2,3-BPG levels; and (H) mean corpuscular fragility of RCC^{Ø}, RCC^{PI}, RCC^{WB*}, and RCC^{WB*+PI} during storage. All graphs show data from days 2, 7, 14, 21, and 42 of storage, except percentage hemolysis which was measured weekly and 2, 3-BPG which was evaluated on days 2, 7, 14, and 21 of storage. (* = RCC^{WB*} significantly different from RCC^{Ø}; ¶ = RCC^{WB*+PI} significantly different from RCC^{PI}; ‡ = $p < 0.05$ over time spent in storage; n = 5). *In vitro* parameters were kindly provided by Dr. Peter Schubert to provide context for the application of candidate protein quality markers.

5.2.2 Application of Peroxiredoxin-2 and Catalase

To verify the utility of candidate membrane-associated protein quality markers identified in the studies described in earlier chapters, peroxiredoxin-2 and catalase were visualized in ghost fractions prepared on days 7, 21, and 42 of storage. In agreement with our previous study[179], marked reduction in protein levels was observed with PI treatment ($p < 0.01$) and there was no obvious change over storage ($p > 0.05$; **Figure 5.3**). With the exception of catalase on day 7, the magnitude of change in protein levels did not reach statistical significance between WB deoxygenated and untreated RCCs (RCC^{WB*} and $RCC^{Ø}$). However, both candidate proteins displayed a trend of increased protein level with deoxygenation treatment (**Figure 5.3**; $RCC^{Ø}$ and RCC^{WB*}). Surprisingly, there was no consistent change in candidate protein levels observed between RCC^{PI} and RCC^{WB*+PI}.

To glean insights into the utility of candidate protein quality markers, the relationship between percentage hemolysis and membrane-associated protein levels was analyzed. Altered expression levels of peroxiredoxin-2 (r = -0.504 and -0.094; $p > 0.05$; **Figure 5.4A and C**, respectively) and catalase (r = -0.179 and -0.265; $p > 0.05$; **Figure 5.4B and D**, respectively) in ghost fractions of $RCC^{Ø}$, RCC^{WB*}, RCC^{PI}, and RCC^{WB*+PI} did not reach significant correlation with their respective hemolysis level at day 7, nor when storage days 7, 21, and 42 were taken into account.

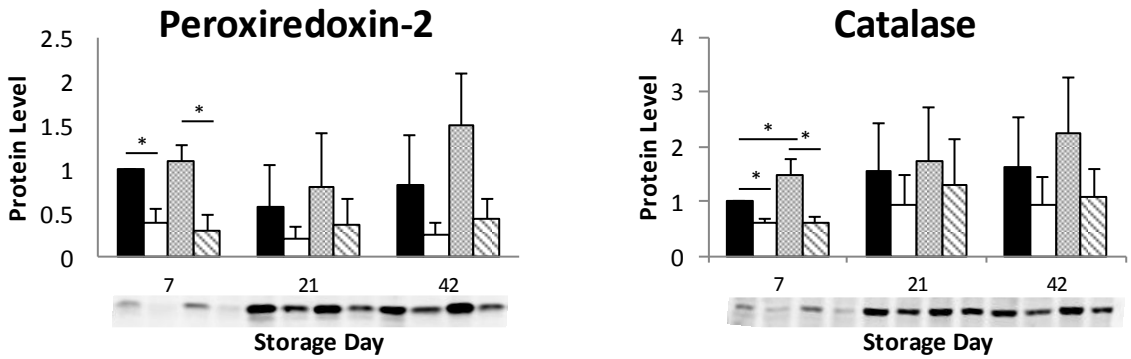

Figure 5.3 Immunoblot verification of proposed candidate protein quality markers

Column graphs displaying the ratio of protein changes of independent ghost fractions with respect to $RCC^{Ø}$ day 7 baseline (mean ± S.E.M. of densitometry analysis of immunoblots; n=3; solid bars = $RCC^{Ø}$; open bars = RCC^{PI}; shaded bars= RCC^{WB*}; lined bars = RCC^{WB*+PI}). Representative immunoblots of $RCC^{Ø}$, RCC^{PI}, RCC^{WB*}, and RCC^{WB*+PI} days 7, 21, and 42 ghost fractions on selected iTRAQ-identified protein candidates, including peroxiredoxin-2 (A) and catalase (B).* = $p < 0.05$.

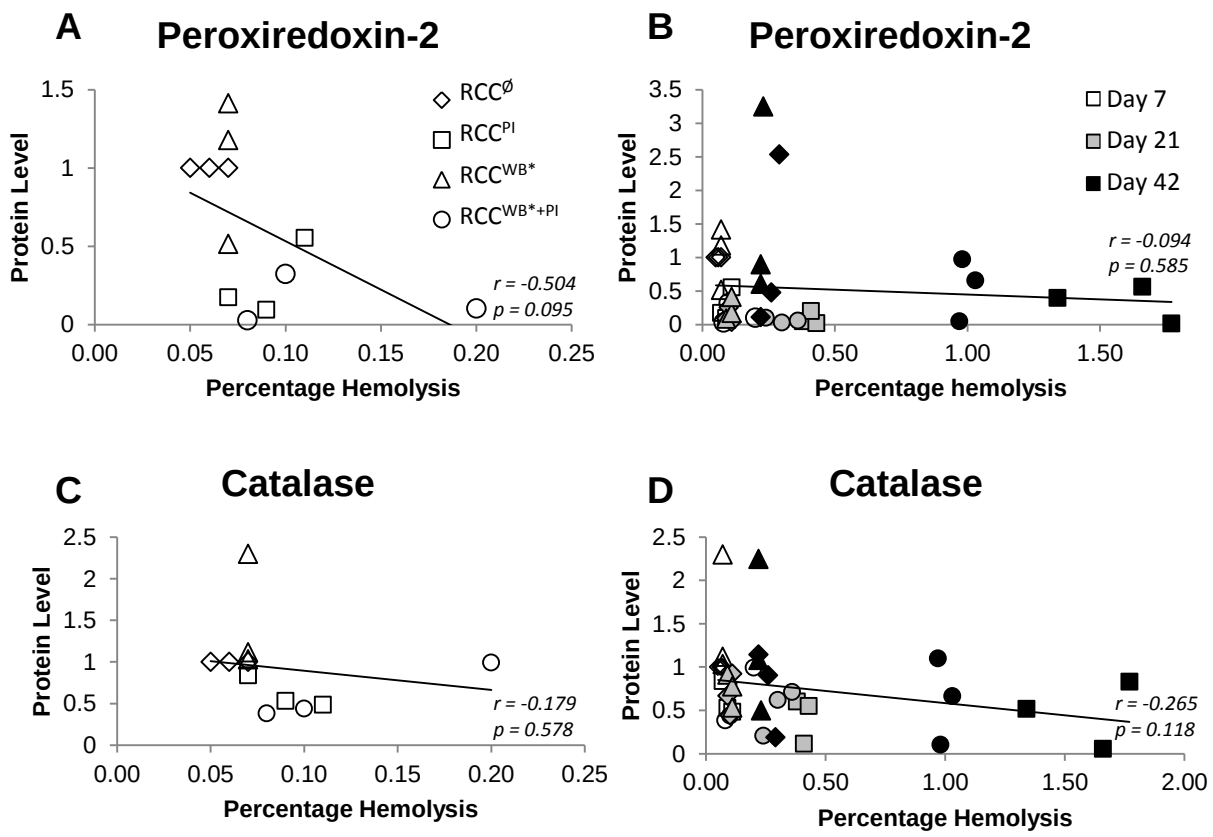

Figure 5.4 Lack of correlation between hemolysis and protein candidates

Correlation graphs on all consolidated samples (n=3) displaying no significant linear relationships between hemolysis and expression of membrane peroxiredoxin (A and B) and catalase (C and D) at day 7 and at days 7, 21, 42 of storage, respectively, in $RCC^{Ø}$, RCC^{Pl}, RCC^{WB*}, and RCC^{WB*+Pl}. The symbol for each treatment and shading for each storage day remain consistent throughout.

5.3 Discussion

Improving blood product quality is a continual quest for the transfusion community. Given that oxidative stress is a common feature of RBC storage lesions, deoxygenation treatment has been explored extensively to prevent accumulation of oxidative damage and to mitigate deterioration of product quality. The impacts of deoxygenation treatment on *in vitro*

quality parameters and candidate protein quality marker levels were evaluated in the context of PI treatment.

Deoxygenation treatment significantly reduced RCC oxygen content and successfully maintained a hypoxic environment throughout storage. Unlike previous reports, percentage hemolysis, RMV formation, and osmotic fragility were comparable between WB deoxygenated and untreated RCCs (RCC^{WB*} and $RCC^{Ø}$). This observation may be attributed to differences in the RCC additive solution and the gas composition used for deoxygenation treatment, as well as the stage of production process (WB versus RCC) in which the deoxygenation treatment was applied. Higher ATP and 2, 3-BPG maintenance were observed in WB deoxygenated RCC than that of untreated RCC, indicating that deoxygenation treatment was effective and modulated RBC metabolism as reported previously[213]. Notably, deoxygenation treatment successfully rescued the elevated hemolysis induced by PI treatment. As evidenced by higher accumulation of lactate and prolonged maintenance of ATP and 2, 3-BPG during storage in WB deoxygenated and PI-treated RCC compared to PI-treated RCC, the reduction in hemolysis level may be a result of enhanced glycolytic enzyme activity. In addition to minimizing oxidative damage during anaerobic storage, the high affinity of deoxygenated Hb for the N-terminal cytoplasmic domain of band 3 induces the release of bound-inhibited glycolytic enzymes, and thus diverts glucose from the pentose phosphate pathway to promote its conversion via the Embden-Meyerhof pathway [158,159]. This results in increased cellular access to ATP, which in turn supports the preservation of membrane integrity and resistance to osmotic stress. Alternatively, PI treatment efficacy may be compromised with the depletion of oxygen and thus induced less damage as assessed in various *in vitro* quality parameters; however, this was not directly assessed in the study. The presence of CO_2 was important in preventing alkylation of the additive solution[214], which may explain similar total glucose consumption between treatments, as it has been shown to be strongly pH-dependent[158].

In agreement with our hypothesis, deoxygenation treatment alone resulted in an increase in candidate protein levels with minor improvement in percentage hemolysis compared to untreated RCC at the early time point. However, Rinalducci *et al*. demonstrated disappearance of catalase and decreased migration of peroxiredoxin-2 to the membrane fraction with deoxygenation using a two-dimensional gel electrophoretic approach[38]. The discrepant observations between the two studies may be a result of differences in the timing of deoxygenation treatment and in cellular composition, with an additional 40 mL bolus of SAGM added to 60mL aliquot of RCC in their study design compared to a standard-issue RCC used in this study. Surprisingly, despite dramatic reduction in hemolysis level, deoxygenation treatment in combination with PI ($RCC^{WB^{*}+PI}$) did not result in significantly higher candidate protein levels compared to PI-treated RCC. The slight increasing trend of proposed membrane-associated protein markers in $RCC^{WB^{*}+PI}$ compared to RCC^{PI} suggests that these protein markers may not fully reflect the quality deterioration due to exposure of oxidative damage alone. There may be other underlying mechanisms contributing to the RBC storage lesions development triggered by the complex product manipulation, which the proposed protein quality markers are not sensitive enough in detecting. Correlation analysis suggests similar findings, with peroxiredoxin-2 levels at day 7 approaching a significant negative linear relationship with hemolysis development. This observation may provide further support for peroxiredoxin-2 protein level at early time point may be potentially predictive of hemolysis development over storage, as discussed earlier in **Chapter 3.3**. Due to compromised samples, the data regarding 20s proteasome levels at the membrane were unfortunately absent for analysis.

Historically, the preservation of human blood utilized glass containers [215]. So_2 decreases over time due to continuing cellular metabolism of residual white blood cells and the storage environment becomes increasingly hypoxic without gas exchange with the external environment. Aeration of RBCs stored in glass bottles improved various *in vitro* quality

parameters, including viscosity, osmotic fragility, storage hemolysis, pH, ATP and 2, 3-BPG maintenance[216], hinting at the importance of gas exchange during storage for maintenance of product quality. Gas-permeable storage containers for RBC preservation were introduced to improve blood product production and distribution logistics[217]. Storage hemolysis development in plastic storage bags was slowed compared to those stored in glass bottles[218]. However, product quality improvements associated with the use of gas-permeable plastic bags appeared to be independent of the oxygen content; *in vitro* quality parameters of RBCs stored in plastic bags were comparable in both normoxic or hypoxic (with the use of N_2) storage conditions [216]. This finding suggests that perhaps the elimination of CO_2 (which ultimately alters the rate of glycolysis) may play a more important role in influencing RBC quality than the level of oxygen tension during storage.

Taken together, our findings suggest that oxygen removal is an effective strategy in modulating storage lesions development and is able to reduce some of the deleterious impacts on *in vitro* quality parameters induced by PI treatment. The study also provides further evidence that the manifestation of hemolysis during storage is multifactorial, with oxidative stress playing an important role in its development. However, there may be other factors influencing the development of hemolysis and the migration of these proteins to the membrane.

Chapter 6: Conclusion

RBC transfusion is a life-saving intervention provided to patients undergoing major surgery, chemotherapy, or bone marrow transplant. RBC transfusions are also used to prevent hypovolemic shock in patients suffering acute massive hemorrhage or to restore oxygen-carrying capacity of the blood for patients living with RBC disorders, such as sickle cell anemia or thalassemia. In order to minimize risk to transfusion recipients, the safety and quality of blood products are of upmost importance. Rigorous donor screening, routine product testing, standardized manufacturing procedures, and ongoing process monitoring in accordance to regulatory guidelines are implemented to ensure a safe supply of quality blood products. However, the development of RBC storage lesions is inevitable within the allowable storage period and risk of post-transfusion adverse outcomes is not completely mitigated despite continual improvement and optimization of blood product collection, production, and storage conditions. Additionally, variability in blood donors also influences the RCC quality (**Figure 6.1**). Given that hemolysis is intricately related to membrane integrity and that RMV formation is governed by controlled cellular processes, we focused our research efforts in identifying potential membrane proteins as quality biomarkers for better donor and inventory management.

As the ultimate goal is to improve the ability of blood operators to monitor blood product storage quality, we first set out to examine the current active donor population at Canadian Blood Services for consistent molecular alterations that may be linked with elevated hemolysis development. As shown in **Chapter 3:**, variation in donor membrane protein levels was associated with storage hemolysis development. By comparing membrane protein profiles between high hemolyzers and their respective age- and sex-matched controls, membrane-associated peroxiredoxin-2, catalase, and 20s proteasome were proposed as candidate protein markers for RCC storage quality and may have potential utility as a donor and inventory management tool. While RBC morphology and osmotic fragility appeared normal, genetic and

biochemical abnormalities of donors were not directly assessed. Patients with G6PD deficiency exhibit enhanced oxidant sensitivity and an increased likelihood to undergo hemolysis. The underlying mechanism of oxidant susceptibility of G6PD deficient RBC is the decreased ability to catabolize H_2O_2, as the loss of G6PD results in an inability to regenerate NADPH for the recycling of NADPH-dependent antioxidant defenses via the pentose phosphate pathway[219,220]. The decrease in candidate protein levels at the membrane in high hemolyzers may suggest a corresponding decrease in antioxidant activity, which may offer a plausible explanation for the observed elevated hemolysis. Additional experiments such as protein activity, NADPH quantification, measurement of membrane protein carbonylation, lipoperoxidation, and metHb formation upon oxidative challenge may strengthen the results reported here. Moreover, donor genetic and biochemical variants testing would further illuminate the observed differences between the donor groups.

For vulnerable transfusion recipients, such as neonates, pregnant women, and those who are immunocompromised, additional processing manipulations are used to eliminate residual donor leukocytes and/or possible undetected/unknown pathogens to further minimize the risk of post-transfusion adverse outcomes. However, these treatments, such as gamma-irradiation and PI treatment, accelerate product *in vitro* quality deterioration in a time-dependent manner. While these RCCs are usually transfused shortly following treatment, attempts to mitigate the negative quality impacts induced by these treatments require thorough appraisal and understanding. In **Chapter 4**:, we investigated the interplay between membrane protein alterations and post-collection manipulations in the context of RCC storage quality using a pool-and-split study design. Again, peroxiredoxin-2, catalase, and 20s proteasome were identified as candidate markers via comparative membrane profile analysis of RCCs subjected to gamma-irradiation and PI treatment in reference to an untreated control. The protein level of these candidates at the membrane displayed a significant negative linear relationship with hemolysis

development, which augments our previous observation in the context of unique repeat donors (**Chapter 3:**) and lends further support for their potential utility as predictors of storage quality. The application of these candidate protein quality markers would first need to be evaluated in a larger donor population to establish “normal” distributions by important variables, such as age, sex, ethnicity, frequency of donations, and post-collection manipulations. Additionally, the sensitivity, specificity, and predictive power of these candidate protein quality markers must also be determined prior to the implementation of these biomarkers in the context of a RCC quality monitoring program.

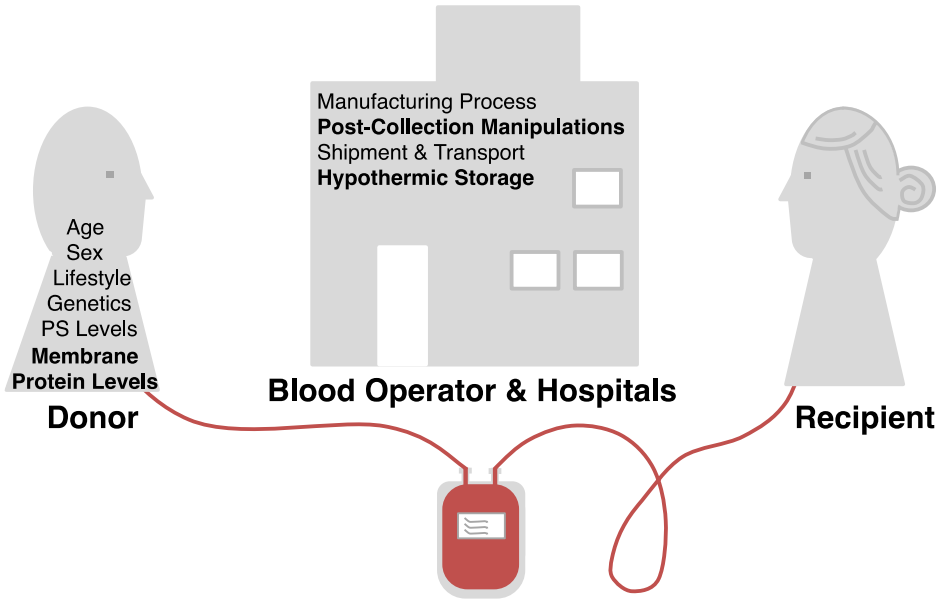

Figure 6.1 Factors influencing RCC Quality.

The illustration depicts various factors that may impact the quality of RCC before it reaches the transfusion recipient. Items in bold were directly investigated in this dissertation.

While markers of oxidative stress were not directly measured, the reduction in the levels of these potential protein markers in parallel with decreased *in vitro* quality parameters suggests

that oxidative stress driven deterioration critically impacts RCC quality. Although Hb auto-oxidation is slow, it is inevitable during storage. The accumulation of metHb may result in the formation of hemichromes, which undergo further denaturation leading to heme degradation and the release of iron by heme oxygenase-1 [221]. Free heme and molecular iron function as Fenton reagents and generate ROS, which results in lipid and protein peroxidation[222]. With declining RBC antioxidant defense with time spent in storage, these oxidative insults lead to a reduction in the membrane resilience against osmotic pressure, increased susceptibility to cation leaks, RMV formation, and hemolysis development. The alterations of membrane protein profiles may also be another feature or phenotype of stored RBCs and may reflect the changes in the *in vitro* quality parameters.

The marked reduction of candidate protein levels at the membrane may be attributed to oxidative modification of these proteins, which is accompanied by a loss of protein function. For example, the active form of peroxiredoxin-2 is monomeric and the enzyme acquires the inactive dimeric form when it becomes oxidized. Although peroxireodxin-2 is usually considered as a cytosolic protein, it can be associated with the membrane[18], where it could be involved in mechanisms of defense against lipid peroxidation and against the deleterious effects of membrane-bound Hb[223,224]. Some reports suggest that cytosolic peroxiredoxin-2 dimerizes in response to oxidative stress in a dose-dependent manner[38,40] and that the presence of the dimeric form in the cytoplasm is a prerequisite for its membrane-association[225]. Moreover, Rinalducci *et al*. has demonstrated that both monomeric and dimeric forms of peroxiredoxin-2 may be associated with membrane during storage [38]. The evidence presented in this report would be further strengthened, help delineate the conditions triggering molecular alterations of peroxiredoxin-2, and better inform the utility of peroxiredoxin-2 as a potential protein quality marker, should there be an evaluation of the redox state of these proteins at the membrane. Some of these modified or damaged proteins may become partially unfolded and in need of

assistance by chaperones for repair, while others may be bound for ATP- and ubiquitin-independent proteasome degradation[45,46]. For example, much evidence suggests that oxidatively damaged proteins are preferentially degraded by proteasome degradation[43,226]. This may also offer some explanation for the inconsistent protein levels with storage. Alternatively, these proteins may be removed from the membrane fraction through vesiculation[183,227], as damaged protein removal through proteasome-mediated degradation is progressively compromised by the continual release of proteasome components in the supernatant[181]. Additionally, secretory apolipoprotein J/Clusterin has been identified as a sensitive molecular marker of oxidative stress in RBCs and was shown to be actively involved in the vesiculation process to remove oxidized proteins and damaged molecules [228,229]. This mechanism may offer explanation for the observation of accumulation of antioxidant enzymes, such as peroxiredoxin-2, and other stress response chaperone proteins in the supernatant of RCC with storage[115]. The redox state of and/or the oxidative modification markers of these proteins released in the supernatant would help better inform the relationship between oxidative stress and their temporal movement during storage. Interestingly, the relationship between these protein markers and RCC storage quality appears to break down with more complex product manipulations, as was observed with deoxygenation in combination with PI treatment. This may reflect the inherent limitation of identified biomarkers due to the complexity of biological processes and indicate that multiple pathways may be implicated in the ultimate manifestation of hemolysis. This was exemplified in patients with acute kidney injury, whereby effective diagnostic and prognostic biomarkers identified in adults failed to translate in pediatric patients as a result of differences in age-related renal physiology and the many biologic pathways involved in kidney injury[230]. The underlying molecular mechanisms of hemolysis development may be altered with complex processing manipulations, rendering candidate protein quality markers less accurate. Excitingly, proposal of network biomarkers may be able to mitigate the

shortcoming of low biomarker accuracy with complex manipulations and should be further explored, where a set of protein biomarkers and their interactions are taken into account in predicting the hemolysis development. This approach was successful in the model of cardiovascular disease, with pair-biomarker and multi-biomarker successfully distinguishing two patient populations more accurately than current single ones without consideration for biological molecular interactions[231]. The results reported herein would be enhanced with direct measurements of candidate protein activities and determination of protein-protein interactions. Moreover, the membrane-associated protein candidate selection criteria was stringent to optimize the identification of biologically significant differences with respect to hemolysis development; however, this approach may have excluded other potentially relevant membrane or membrane-associated protein candidates in predicting product quality.

6.1 Future Directions

As demonstrated in **Chapter 3:**, donors may exhibit molecular signatures that relate to storage hemolysis development. Continual identification of these repeat donors exhibiting high hemolysis would allow us to better understand our current donor population and the resultant RCC inventory. Longitudinal study of these high hemolyzers with repeated RCC donations may inform the reliability of these candidate protein quality markers and illuminate the effects of donation frequency on RCC quality in a prospective approach. Additionally, information about donor genetics and biochemical variants would allow us to better control for key confounding variables and may offer alternative and/or complementary explanations for elevated hemolysis. This work also suggests that there may be other donor subpopulations that share similar RCC quality features over time spent in storage and that our definition of what constitute a healthy volunteer blood donor may require further evaluation in the context of product quality.

Identified candidate protein quality markers displaying significant alterations in relation to hemolysis development are membrane-associated cytosolic proteins, indicating that the role of soluble proteins in hemolysis development may be underappreciated in the research presented here. Metabolomics is a powerful approach to glean insight into cytosolic enzymatic functions as supported by the production and consumption of small molecule metabolites. Numerous studies revealed descriptive metabolic transition signatures over RCC storage[114,232-234], with evidence suggesting RBC metabolism switching from energy production to producing metabolites involved in anti-oxidant responses during storage. Additionally, eight unique metabolites were identified as potential biomarkers for distinguishing metabolic stages of stored RBCs[235]. The metabolic shift to the oxidative phase of the pentose phosphate pathway aims to restore reducing equivalents to counteract oxidative stress to functional proteins; however, this metabolic alteration does not seem sufficient as oxidized small molecules accumulate in supernatant over time [115,183,236,237]. We speculate that the observed alterations of membrane protein profiles may follow the shift in RBC metabolism, which may exhibit a different temporal pattern with additional post-collection manipulations, in an attempt to achieve redox homeostasis. While metabolomics studies revealed rich information regarding metabolic phenotypes of stored RBCs, their relationships to product quality, such as percentage hemolysis, remain elusive. REDS-III Omics[238] and other similar initiatives will shed light on this knowledge gap in the coming years and offer insights into how best to monitor product quality. Moreover, combining metabolomics and proteomic data may offer a more in-depth, comprehensive understanding of RBC physiology during storage and allow us to discover more accurate quality markers for product monitoring.

Given the high correlation with hemolysis development, RMV formation and enumeration may also serve as a potential biomarker for quality assessment and to inform inventory management. GPI-anchored proteins, such as acetylcholinesterase (AChE) and decay

accelerating factor (DAF), are preferentially released from the RBC during vesiculation[239,240]. Erythrocyte membrane AChE is involved in the NO signal pathway; in the presence of ACh, the natural substrate of the membrane AChE, are able to release NO[241]. The NO released from endothelial cells to the lumen is scavenged by the erythrocytes through the band 3 protein, providing a route for an NO influx to, and an efflux from, erythrocytes [242,243]. Depletion of membrane AChE could result in challenges in maintaining vascular tone. DAF serves an important role in protecting RBCs from lysis via complement[244]. Thus, RBCs depleted of DAF as a result of RMV formation during storage may be more susceptible to complement induced lysis and be preferentially removed *in vivo*; the role of RMV formation, RMV composition over storage, as well as their impact on product quality and efficacy requires further investigations.

Future work may also involve evaluation of how the levels of these candidate protein quality markers correlate with post-transfusion recipient outcome in different patient populations; it would be helpful to further elucidate the relationship between *in vitro* quality (e.g., hemolysis at time of transfusion) and product efficacy.

6.2 Significance

Taken together, the findings indicate that hemolysis development is a multifaceted process; while oxidative stress incurred during storage plays an important role in hemolysis development, there are additional mechanisms at play. As research in the field of transfusion evolve, we become more aware of the impacts of various factors that influence RCC storage quality as well as their interrelationships in the context of RBC physiology. The identified candidate protein quality markers may help inform strategies for donor recruitment, as well as potential inventory management, such as differential outdate, with aims to provide high quality and efficacious products for transfusion recipients.

References

1. Pennell RB. In the red blood cell. 2 ed. New York: Academic Press, 1974.
2. Singer SJ, Nicolson GL. The fluid mosaic model of the structure of cell membranes. Science 1972;**175**: 720-31.
3. Verkleij AJ, Zwaal RF, Roelofsen B, *et al*. The asymmetric distribution of phospholipids in the human red cell membrane. A combined study using phospholipases and freeze-etch electron microscopy. Biochim Biophys Acta 1973;**323**: 178-93.
4. Kamata K, Manno S, Ozaki M, Takakuwa Y. Functional evidence for presence of lipid rafts in erythrocyte membranes: Gsalpha in rafts is essential for signal transduction. Am J Hematol 2008;**83**: 371-5.
5. Contreras F, Sanchez-Magraner L, Alonso A, Goni FM. Transbilayer (flip-flop) lipid motion and lipid scrambling in membranes. FEBS Letters 2009;**584**: 1779-86.
6. Bevers EM, Comfurius P, Zwaal RF. Regulatory mechanisms in maintenance and modulation of transmembrane lipid asymmetry: pathophysiological implications. Lupus 1996;**5**: 480-7.
7. Williamson P, Schlegel RA. Transbilayer phospholipid movement and the clearance of apoptotic cells. Biochim Biophys Acta 2002;**1585**: 53-63.
8. Fadok VA, Bratton DL, Rose DM, *et al*. A receptor for phosphatidylserine-specific clearance of apoptotic cells. Nature 2000;**405**: 85-90.
9. Setty BN, Kulkarni S, Stuart MJ. Role of erythrocyte phosphatidylserine in sickle red cell-endothelial adhesion. Blood 2002;**99**: 1564-71.
10. Kuypers FA. Membrane lipid alterations in hemoglobinopathies. Hematology Am Soc Hematol Educ Program 2007: 68-73.

11. Chasis JA, Mohandas N. Erythrocyte membrane deformability and stability: two distinct membrane properties that are independently regulated by skeletal protein associations. J Cell Biol 1986;**103**: 343-50.

12. Bennett V. Proteins involved in membrane--cytoskeleton association in human erythrocytes: spectrin, ankyrin, and band 3. Methods Enzymol 1983;**96**: 313-24.

13. Salomao M, Zhang X, Yang Y, *et al*. Protein 4.1R-dependent multiprotein complex: new insights into the structural organization of the red blood cell membrane. Proc Natl Acad Sci U S A 2008;**105**: 8026-31.

14. Khan AA, Hanada T, Mohseni M, *et al*. Dematin and adducin provide a novel link between the spectrin cytoskeleton and human erythrocyte membrane by directly interacting with glucose transporter-1. J Biol Chem 2008;**283**: 14600-9.

15. An X, Guo X, Sum H, *et al*. Phosphatidylserine binding sites in erythroid spectrin: location and implications for membrane stability. Biochemistry 2004;**43**: 310-5.

16. Pasini EM, Kirkegaard M, Mortensen P, *et al*. In-depth analysis of the membrane and cytosolic proteome of red blood cells. Blood 2006;**108**: 791-801.

17. Pesciotta EN, Sriswasdi S, Tang HY, *et al*. A label-free proteome analysis strategy for identifying quantitative changes in erythrocyte membranes induced by red cell disorders. J Proteomics 2012;**76 Spec No.**: 194-202.

18. Low TY, Seow TK, Chung MC. Separation of human erythrocyte membrane associated proteins with one-dimensional and two-dimensional gel electrophoresis followed by identification with matrix-assisted laser desorption/ionization-time of flight mass spectrometry. Proteomics 2002;**2**: 1229-39.

19. Rose IA. Regulation of human red cell glycolysis: a review. Exp Eye Res 1971;**11**: 264-72.

20. van Wijk R, van Solinge WW. The energy-less red blood cell is lost: erythrocyte enzyme abnormalities of glycolysis. Blood 2005;**106**: 4034-42.

21. Benga G. Water transport in red blood cell membranes. Prog Biophys Mol Biol 1988;**51**: 193-245.

22. Kuchel PW, Benga G. Why does the mammalian red blood cell have aquaporins? Biosystems 2005;**82**: 189-96.

23. Tosteson DC, Hoffman JF. Regulation of cell volume by active cation transport in high and low potassium sheep red cells. J Gen Physiol 1960;**44**: 169-94.

24. Joiner CH. Cation transport and volume regulation in sickle red blood cells. Am J Physiol 1993;**264**: C251-70.

25. Lew VL, Bookchin RM. Volume, pH, and ion-content regulation in human red cells: analysis of transient behavior with an integrated model. J Membr Biol 1986;**92**: 57-74.

26. Davies KJ. Oxidative stress: the paradox of aerobic life. Biochem Soc Symp 1995;**61**: 1-31.

27. Webster SH. Heinz body phenomenon in erythrocytes; a review. Blood 1949;**4**: 479-97.

28. Das SK, Nair RC. Superoxide dismutase, glutathione peroxidase, catalase and lipid peroxidation of normal and sickled erythrocytes. Br J Haematol 1980;**44**: 87-92.

29. Scott MD, Eaton JW, Kuypers FA, Chiu DT, Lubin BH. Enhancement of erythrocyte superoxide dismutase activity: effects on cellular oxidant defense. Blood 1989;**74**: 2542-9.

30. Cohen G, Hochstein P. Glutathione peroxidase: the primary agent for the elimination of hydrogen peroxide in erythrocytes. Biochemistry 1963;**2**: 1420-8.

31. Gaetani GF, Galiano S, Canepa L, Ferraris AM, Kirkman HN. Catalase and glutathione peroxidase are equally active in detoxification of hydrogen peroxide in human erythrocytes. Blood 1989;**73**: 334-9.

32. Scott MD, Lubin BH, Zuo L, Kuypers FA. Erythrocyte defense against hydrogen peroxide: preeminent importance of catalase. J Lab Clin Med 1991;**118**: 7-16.

33. Mueller S, Riedel HD, Stremmel W. Direct evidence for catalase as the predominant H2O2 -removing enzyme in human erythrocytes. Blood 1997;**90**: 4973-8.

34. Kirkman HN, Gaetani GF. Catalase: a tetrameric enzyme with four tightly bound molecules of NADPH. Proc Natl Acad Sci U S A 1984;**81**: 4343-7.

35. Kirkman HN, Galiano S, Gaetani GF. The function of catalase-bound NADPH. J Biol Chem 1987;**262**: 660-6.

36. Peskin AV, Low FM, Paton LN, *et al*. The high reactivity of peroxiredoxin 2 with H(2)O(2) is not reflected in its reaction with other oxidants and thiol reagents. J Biol Chem 2007;**282**: 11885-92.

37. Chae HZ, Kim HJ, Kang SW, Rhee SG. Characterization of three isoforms of mammalian peroxiredoxin that reduce peroxides in the presence of thioredoxin. Diabetes Res Clin Pract 1999;**45**: 101-12.

38. Rinalducci S, D'Amici GM, Blasi B, *et al*. Peroxiredoxin-2 as a candidate biomarker to test oxidative stress levels of stored red blood cells under blood bank conditions. Transfusion 2011;**51**: 1439-49.

39. Nagababu E, Mohanty JG, Friedman JS, Rifkind JM. Role of peroxiredoxin-2 in protecting RBCs from hydrogen peroxide-induced oxidative stress. Free Radic Res 2013;**47**: 164-71.

40. Bayer SB, Hampton MB, Winterbourn CC. Accumulation of oxidized peroxiredoxin 2 in red blood cells and its prevention. Transfusion 2015;**55**: 1909-18.

41. Lee TH, Kim SU, Yu SL, *et al*. Peroxiredoxin II is essential for sustaining life span of erythrocytes in mice. Blood 2003;**101**: 5033-8.

42. Johnson RM, Ho YS, Yu DY, *et al*. The effects of disruption of genes for peroxiredoxin-2, glutathione peroxidase-1, and catalase on erythrocyte oxidative metabolism. Free Radic Biol Med 2010;**48**: 519-25.

43. Pacifici RE, Salo DC, Davies KJ. Macroxyproteinase (M.O.P.): a 670 kDa proteinase complex that degrades oxidatively denatured proteins in red blood cells. Free Radic Biol Med 1989;**7**: 521-36.

44. Salo DC, Pacifici RE, Lin SW, Giulivi C, Davies KJ. Superoxide dismutase undergoes proteolysis and fragmentation following oxidative modification and inactivation. J Biol Chem 1990;**265**: 11919-27.

45. Pickering AM, Davies KJ. Degradation of damaged proteins: the main function of the 20S proteasome. Prog Mol Biol Transl Sci 2012;**109**: 227-48.

46. Davies KJ. Degradation of oxidized proteins by the 20S proteasome. Biochimie 2001;**83**: 301-10.

47. Flegel WA, Natanson C, Klein HG. Does prolonged storage of red blood cells cause harm? Br J Haematol 2014;**165**: 3-16.

48. Bosman GJ, Werre JM, Willekens FL, Novotný VM. Erythrocyte ageing in vivo and in vitro: structural aspects and implications for transfusion. Transfus Med 2008;**18**: 335-47.

49. Zimrin AB, Hess JR. Current issues relating to the transfusion of stored red blood cells. Vox Sang 2009;**96**: 93-103.

50. Hess JR. Red cell storage. J Proteomics 2010;**73**: 368-73.

51. Stan A, Zsigmond E. The restoration in vivo of 2,3-diphosphoglycerate (2,3-DPG) in stored red cells, after transfusion. The levels of red cells 2,3-DPG. Rom J Intern Med 2009;**47**: 173-7.

52. Matthes G, Strunk S, Siems W, Grune T. Posttransfusional changes of 2,3-diphosphoglycerate and nucleotides in CPD-SAGM-preserved erythrocytes. Infusionsther Transfusionsmed 1993;**20**: 89-92.

53. Smith HM, Farrow SJ, Ackerman JD, Stubbs JR, Sprung J. Cardiac arrests associated with hyperkalemia during red blood cell transfusion: a case series. Anesth Analg 2008;**106**: 1062-9, table of contents.

54. Hall TL, Barnes A, Miller JR, Bethencourt DM, Nestor L. Neonatal mortality following transfusion of red cells with high plasma potassium levels. Transfusion 1993;**33**: 606-9.

55. Bull BS, Herrmann PC. Morphology of the Erythron. 8 ed. New York, NY: Williams Hematlogy, 2010.

56. Nakao M, Nakao T, Yamazoe S. Adenosine triphosphate and maintenance of shape of the human red cells. Nature 1960;**187**: 945-6.

57. Greenwalt TJ. The how and why of exocytic vesicles. Transfusion 2006;**46**: 143-52.

58. Rubin O, Canellini G, Delobel J, Lion N, Tissot JD. Red blood cell microparticles: clinical relevance. Transfus Med Hemother 2012;**39**: 342-7.

59. Jy W, Ricci M, Shariatmadar S, *et al*. Microparticles in stored red blood cells as potential mediators of transfusion complications. Transfusion 2011;**51**: 886-93.

60. Fischer D, Büssow J, Meybohm P, *et al*. Microparticles from stored red blood cells enhance procoagulant and proinflammatory activity. Transfusion 2017;**57**: 2701-2711

61. Tinmouth A, Chin-Yee I. The clinical consequences of the red cell storage lesion. Transfus Med Rev 2001;**15**: 91-107.

62. Card RT, Mohandas N, Mollison PL. Relationship of post-transfusion viability to deformability of stored red cells. Br J Haematol 1983;**53**: 237-40.

63. Relevy H, Koshkaryev A, Manny N, Yedgar S, Barshtein G. Blood banking-induced alteration of red blood cell flow properties. Transfusion 2008;**48**: 136-46.

64. Koshkaryev A, Zelig O, Manny N, Yedgar S, Barshtein G. Rejuvenation treatment of stored red blood cells reverses storage-induced adhesion to vascular endothelial cells. Transfusion 2009;**49**: 2136-43.

65. Izumida Y, Seiyama A, Maeda N. Erythrocyte aggregation: bridging by macromolecules and electrostatic repulsion by sialic acid. Biochim Biophys Acta 1991;**1067**: 221-6.

66. Barshtein G, Manny N, Yedgar S. Circulatory risk in the transfusion of red blood cells with impaired flow properties induced by storage. Transfus Med Rev 2011;**25**: 24-35.

67. Karon BS, Hoyer JD, Stubbs JR, Thomas DD. Changes in Band 3 oligomeric state precede cell membrane phospholipid loss during blood bank storage of red blood cells. Transfusion 2009;**49**: 1435-42.

68. Kay MM. Generation of senescent cell antigen on old cells initiates IgG binding to a neoantigen. Cell Mol Biol (Noisy-le-grand) 1993;**39**: 131-53.

69. Wagner GM, Chiu DT, Qju JH, Heath RH, Lubin BH. Spectrin oxidation correlates with membrane vesiculation in stored RBCs. Blood 1987;**69**: 1777-81.

70. Hess JR. Conventional blood banking and blood component storage regulation: opportunities for improvement. Blood Transfus 2010;**8 Suppl 3**: s9-15.

71. Lee JS, Gladwin MT. Bad blood: The risk of red cell storage. Nature Medicine 2010;**16**: 381-2.

72. Reiter CD, Wang X, Tanus-Santos JE, *et al*. Cell-free hemoglobin limits nitric oxide bioavailability in sickle-cell disease. Nat Med 2002;**8**: 1383-9.

73. Donadee C, Raat NJ, Kanias T, *et al*. Nitric oxide scavenging by red blood cell microparticles and cell-free hemoglobin as a mechanism for the red cell storage lesion. Circulation 2011;**124**: 465-76.

74. Morris CR, Gladwin MT, Kato GJ. Nitric oxide and arginine dysregulation: a novel pathway to pulmonary hypertension in hemolytic disorders. Curr Mol Med 2008;**8**: 620-32.

75. Kim-Shapiro DB, Lee J, Gladwin MT. Storage lesion: role of red blood cell breakdown. Transfusion 2011;**51**: 844-51.

76. Luten M, Roerdinkholder-Stoelwinder B, Schaap NP, *et al*. Survival of red blood cells after transfusion: a comparison between red cells concentrates of different storage periods. Transfusion 2008;**48**: 1478-85.

77. Thomsen JH, Etzerodt A, Svendsen P, Moestrup SK. The haptoglobin-CD163-heme oxygenase-1 pathway for hemoglobin scavenging. Oxid Med Cell Longev 2013;**2013**: 523652.

78. Rapido F, Brittenham GM, Bandyopadhyay S, *et al*. Prolonged red cell storage before transfusion increases extravascular hemolysis. J Clin Invest 2017;**127**: 375-82.

79. Hod EA, Spitalnik SL. Stored red blood cell transfusions: Iron, inflammation, immunity, and infection. Transfus Clin Biol 2012;**19**: 84-9.

80. Belotti A, Duca L, Borin L, *et al*. Non transferrin bound iron (NTBI) in acute leukemias throughout conventional intensive chemotherapy: kinetics of its appearance and potential predictive role in infectious complications. Leuk Res 2015;**39**: 88-91.

81. Solomon SB, Wang D, Sun J, *et al*. Mortality increases after massive exchange transfusion with older stored blood in canines with experimental pneumonia. Blood 2013;**121**: 1663-72.

82. Wang D, Cortés-Puch I, Sun J, *et al*. Transfusion of older stored blood worsens outcomes in canines depending on the presence and severity of pneumonia. Transfusion 2014;**54**: 1712-24.

83. van de Watering L. Pitfalls in the current published observational literature on the effects of red blood cell storage. Transfusion 2011;**51**: 1847-54.

84. Dzik W. Fresh blood for everyone? Balancing availability and quality of stored RBCs. Transfus Med 2008;**18**: 260-5.

85. Vamvakas EC. Meta-analysis of clinical studies of the purported deleterious effects of "old" (versus "fresh") red blood cells: are we at equipoise? Transfusion 2010;**50**: 600-10.

86. Fergusson D, Hutton B, Hogan DL, *et al*. The age of red blood cells in premature infants (ARIPI) randomized controlled trial: study design. Transfus Med Rev 2009;**23**: 55-61.

87. Fergusson DA, Hébert P, Hogan DL, *et al*. Effect of fresh red blood cell transfusions on clinical outcomes in premature, very low-birth-weight infants: the ARIPI randomized trial. JAMA 2012;**308**: 1443-51.

88. Lacroix J, Hébert PC, Fergusson DA, *et al*. Age of transfused blood in critically ill adults. N Engl J Med 2015;**372**: 1410-8.

89. Steiner ME, Assmann SF, Levy JH, *et al*. Addressing the question of the effect of RBC storage on clinical outcomes: the Red Cell Storage Duration Study (RECESS) (Section 7). Transfus Apher Sci 2010;**43**: 107-16.

90. Steiner ME, Ness PM, Assmann SF, *et al*. Effects of red-cell storage duration on patients undergoing cardiac surgery. N Engl J Med 2015;**372**: 1419-29.

91. Kor DJ, Kashyap R, Weiskopf RB, *et al*. Fresh red blood cell transfusion and short-term pulmonary, immunologic, and coagulation status: a randomized clinical trial. Am J Respir Crit Care Med 2012;**185**: 842-50.

92. Kaukonen KM, Bailey M, Ady B, *et al*. A randomised controlled trial of standard transfusion versus fresher red blood cell use in intensive care (TRANSFUSE): protocol and statistical analysis plan. Crit Care Resusc 2014;**16**: 255-61.

93. Heddle NM, Cook RJ, Arnold DM, *et al*. Effect of Short-Term vs. Long-Term Blood Storage on Mortality after Transfusion. N Engl J Med 2016;**375**: 1937-45.

94. Tchir JD, Acker JP, Holovati JL. Rejuvenation of ATP during storage does not reverse effects of the hypothermic storage lesion. Transfusion 2013;**53**: 3184-91.

95. D'Amici GM, Rinalducci S, Zolla L. Proteomic analysis of RBC membrane protein degradation during blood storage. J Proteome Res 2007;**6**: 3242-55.

96. D'Alessandro A, Temkov T, Blair A, *et al*. Anaerobic storage Condition enhances GSH Levels while Maintaining Pentose Phosphate Pathway Activity. Transfusion 2016;**56**: SP25.

97. Horowitz B, Stryker MH, Waldman AA, *et al*. Stabilization of red blood cells by the plasticizer, diethylhexylphthalate. Vox Sang 1985;**48**: 150-5.

98. Ho J, Sibbald WJ, Chin-Yee IH. Effects of storage on efficacy of red cell transfusion: when is it not safe? Crit Care Med 2003;**31**: S687-97.

99. Han V, Serrano K, Devine DV. A comparative study of common techniques used to measure haemolysis in stored red cell concentrates. Vox Sang 2010;**98**: 116-23.

100. Hemoglobin. In: Shinton N, ed. Desk Reference for Hematology. Boca Raton, FL: Taylor & Francis Group, 2008:399-405.

101. Kakhniashvili DG, Bulla LA, Goodman SR. The human erythrocyte proteome: analysis by ion trap mass spectrometry. Mol Cell Proteomics 2004;**3**: 501-9.

102. Hegedűs T, Chaubey PM, Várady G, *et al*. Inconsistencies in the red blood cell membrane proteome analysis: generation of a database for research and diagnostic applications. Database (Oxford) 2015;**2015**: bav056.

103. Simó C, Bachi A, Cattaneo A, *et al*. Performance of combinatorial peptide libraries in capturing the low-abundance proteome of red blood cells. 1. Behavior of mono- to hexapeptides. Anal Chem 2008;**80**: 3547-56.

104. Bachi A, Simó C, Restuccia U, *et al*. Performance of combinatorial peptide libraries in capturing the low-abundance proteome of red blood cells. 2. Behavior of resins containing individual amino acids. Anal Chem 2008;**80**: 3557-65.

105. Roux-Dalvai F, Gonzalez de Peredo A, Simó C, *et al*. Extensive analysis of the cytoplasmic proteome of human erythrocytes using the peptide ligand library technology and advanced mass spectrometry. Mol Cell Proteomics 2008;**7**: 2254-69.

106. Goodman SR, Kurdia A, Ammann L, Kakhniashvili D, Daescu O. The human red blood cell proteome and interactome. Exp Biol Med (Maywood) 2007;**232**: 1391-408.

107. D'Alessandro A, Righetti PG, Zolla L. The red blood cell proteome and interactome: an update. J Proteome Res 2010;**9**: 144-63.

108. Goodman SR, Daescu O, Kakhniashvili DG, Zivanic M. The proteomics and interactomics of human erythrocytes. Exp Biol Med (Maywood) 2013;**238**: 509-18.

109. Bordbar A, Jamshidi N, Palsson BO. iAB-RBC-283: A proteomically derived knowledge-base of erythrocyte metabolism that can be used to simulate its physiological and patho-physiological states. BMC Syst Biol 2011;**5**: 110.

110. D'Alessandro A, Kriebardis AG, Rinalducci S, *et al*. An update on red blood cell storage lesions, as gleaned through biochemistry and omics technologies. Transfusion 2015;**55**: 205-19.

111. Pallotta V, Rinalducci S, Zolla L. Red blood cell storage affects the stability of cytosolic native protein complexes. Transfusion 2015;**55**: 1927-36.

112. Walpurgis K, Kohler M, Thomas A, *et al*. Storage-induced changes of the cytosolic red blood cell proteome analyzed by 2D DIGE and high-resolution/high-accuracy MS. Proteomics 2012;**12**: 3263-72.

113. Bosman GJ, Lasonder E, Luten M, *et al*. The proteome of red cell membranes and vesicles during storage in blood bank conditions. Transfusion 2008;**48**: 827-35.

114. D'Alessandro A, D'Amici GM, Vaglio S, Zolla L. Time-course investigation of SAGM-stored leukocyte-filtered red bood cell concentrates: from metabolism to proteomics. Haematologica 2012;**97**: 107-15.

115. D'Alessandro A, Dzieciatkowska M, Hill RC, Hansen KC. Supernatant protein biomarkers of red blood cell storage hemolysis as determined through an absolute quantification proteomics technology. Transfusion 2016;**56**: 1329-39.

116. Hess JR. Scientific problems in the regulation of red blood cell products. Transfusion 2012;**52**: 1827-35.

117. Williamson LM, Devine DV. Challenges in the management of the blood supply. Lancet 2013;**381**: 1866-75.

118. Jordan A, Chen D, Yi QL, *et al*. Assessing the influence of component processing and donor characteristics on quality of red cell concentrates using quality control data. Vox Sang 2016; **111**: 8-15

119. Tzounakas VL, Kriebardis AG, Papassideri IS, Antonelou MH. Donor-variation effect on red blood cell storage lesion: A close relationship emerges. Proteomics Clin Appl 2016; **10**: 791-804.

120. Hess JR, Sparrow RL, van der Meer PF, *et al*. Red blood cell hemolysis during blood bank storage: using national quality management data to answer basic scientific questions. Transfusion 2009;**49**: 2599-603.

121. Van 't Erve TJ, Wagner BA, Martin SM, *et al*. The heritability of hemolysis in stored human red blood cells. Transfusion;**55**: 1178-85.

122. Hess JR. Scientific problems in the regulation of red blood cell products. Transfusion 2012;**52**: 1827-35.

123. Schuetz AN, Hillyer KL, Roback JD, Hillyer CD. Leukoreduction filtration of blood with sickle cell trait. Transfus Med Rev 2004;**18**: 168-76.

124. Stroncek DF, Byrne KM, Noguchi CT, Schechter AN, Leitman SF. Increasing hemoglobin oxygen saturation levels in sickle trait donor whole blood prevents hemoglobin S polymerization and allows effective white blood cell reduction by filtration. Transfusion 2004;**44**: 1293-9.

125. Stroncek DF, Rainer T, Sharon V, *et al*. Sickle Hb polymerization in RBC components from donors with sickle cell trait prevents effective WBC reduction by filtration. Transfusion 2002;**42**: 1466-72.

126. Glass GA, Gershon D, Gershon H. Some characteristics of the human erythrocyte as a function of donor and cell age. Exp Hematol 1985;**13**: 1122-6.

127. Zimring JC, Smith N, Stowell SR, *et al*. Strain-specific red blood cell storage, metabolism, and eicosanoid generation in a mouse model. Transfusion 2014;**54**: 137-48.

128. Tarasev M, Alfano K, Chakraborty S, *et al*. Similar donors-similar blood? Transfusion 2014;**54**: 933-41.

129. Raval JS, Waters JH, Seltsam A, *et al*. Menopausal status affects the susceptibility of stored RBCs to mechanical stress. Vox Sang 2011;**100**: 418-21.

130. Swank RL. Changes in blood of dogs and rabbits by high fat intake. Am J Physiol 1959;**196**: 473-7.

131. Johnson V, Freeman LW, Longini J. Erythrocyte damage by lipemic serum in normal man and in pernicious anemia JAMA, 1944:1250-4

132. Swank RL, Roth ES. Hemolysis and alimentary anemia: Effects of incubation, heparin, and protamine. Blood 1954;**9**: 348-61.

133. Bashir S, Wiltshire M, Cardigan R, Thomas S. Lipaemic plasma induces haemolysis in resuspended red cell concentrate. Vox Sang 2013;**104**: 218-24.

134. Kanias T, Lanteri M, Keating S, *et al*. of Age, Sex or Frequent Blood Donations on Donors' Ferritin Levels and Red Blood Cell Storage Stability. Transfusion 2016;**56**: S89-040C.

135. Dinkla S, Peppelman M, Van Der Raadt J, *et al*. Phosphatidylserine exposure on stored red blood cells as a parameter for donor-dependent variation in product quality. Blood Transfus 2014;**12**: 204-9.

136. Calderón-Salinas JV, Muñoz-Reyes EG, Guerrero-Romero JF, *et al*. Eryptosis and oxidative damage in type 2 diabetic mellitus patients with chronic kidney disease. Mol Cell Biochem 2011;**357**: 171-9.

137. Brubaker DB. Transfusion-associated graft-versus-host disease. Hum Pathol 1986;**17**: 1085-8.

138. Juji T, Takahashi K, Shibata Y, *et al*. Post-transfusion graft-versus-host disease in immunocompetent patients after cardiac surgery in Japan. N Engl J Med 1989;**321**: 56.

139. Pelszynski MM, Moroff G, Luban NL, Taylor BJ, Quinones RR. Effect of gamma irradiation of red blood cell units on T-cell inactivation as assessed by limiting dilution analysis: implications for preventing transfusion-associated graft-versus-host disease. Blood 1994;**83**: 1683-9.

140. Xu D, Peng M, Zhang Z, *et al*. Study of damage to red blood cells exposed to different doses of γ-ray irradiation. Blood Transfus 2012;**10**: 321-30.

141. Leitner GC, Neuhauser M, Weigel G, *et al*. Altered intracellular purine nucleotides in gamma-irradiated red blood cell concentrates. Vox Sang 2001;**81**: 113-8.

142. Anand AJ, Dzik WH, Imam A, Sadrzadeh SM. Radiation-induced red cell damage: role of reactive oxygen species. Transfusion 1997;**37**: 160-5.

143. Moreira OC, Oliveira VH, Benedicto LB, *et al*. Effects of gamma-irradiation on the membrane ATPases of human erythrocytes from transfusional blood concentrates. Ann Hematol 2008;**87**: 113-9.

144. Serrano K, Chen D, Hansen AL, *et al*. The effect of timing of gamma-irradiation on hemolysis and potassium release in leukoreduced red cell concentrates stored in SAGM. Vox Sang 2014;**106**: 379-81.

145. Katharia R, Chaudhary R, Agarwal P. Prestorage gamma irradiation induces oxidative injury to red cells. Transfus Apher Sci 2013;**48**: 39-43.

146. Salunkhe V, van der Meer PF, de Korte D, Seghatchian J, Gutiérrez L. Development of blood transfusion product pathogen reduction treatments: a review of methods, current applications and demands. Transfus Apher Sci 2015;**52**: 19-34.

147. Tonnetti L, Thorp AM, Deisting B, *et al*. Babesia microti seroprevalence in Minnesota blood donors. Transfusion 2013;**53**: 1698-705.

148. O'Brien SF, Delage G, Scalia V, *et al*. Seroprevalence of Babesia microti infection in Canadian blood donors. Transfusion 2016;**56**: 237-43.

149. Picker SM. Current methods for the reduction of blood-borne pathogens: a comprehensive literature review. Blood Transfus 2013;**11**: 343-8.

150. Goodrich RP, Doane S, Reddy HL. Design and development of a method for the reduction of infectious pathogen load and inactivation of white blood cells in whole blood products. Biologicals 2010;**38**: 20-30.

151. Reddy HL, Doane SK, Keil SD, Marschner S, Goodrich RP. Development of a riboflavin and ultraviolet light-based device to treat whole blood. Transfusion 2013;**53 Suppl 1**: 131S-6S.

152. Henschler R, Seifried E, Mufti N. Development of the S-303 Pathogen Inactivation Technology for Red Blood Cell Concentrates. Transfus Med Hemother 2011;**38**: 33-42.

153. Mufti NA, Erickson AC, North AK, *et al*. Treatment of whole blood (WB) and red blood cells (RBC) with S-303 inactivates pathogens and retains in vitro quality of stored RBC. Biologicals 2010;**38**: 14-9.

154. Webert KE, Cserti CM, Hannon J, *et al*. Proceedings of a Consensus Conference: pathogen inactivation-making decisions about new technologies. Transfus Med Rev 2008;**22**: 1-34.

155. Dumont LJ, Yoshida T, AuBuchon JP. Anaerobic storage of red blood cells in a novel additive solution improves in vivo recovery. Transfusion 2009;**49**: 458-64.

156. Yoshida T, Shevkoplyas SS. Anaerobic storage of red blood cells. Blood Transfus 2010;**8**: 220-36.

157. Burns JM, Yoshida T, Dumont LJ, *et al*. Deterioration of red blood cell mechanical properties is reduced in anaerobic storage. Blood Transfus 2016;**14**: 80-8.

158. Messana I, Orlando M, Cassiano L, *et al*. Human erythrocyte metabolism is modulated by the O2-linked transition of hemoglobin. FEBS Lett 1996;**390**: 25-8.

159. Chu H, Breite A, Ciraolo P, Franco RS, Low PS. Characterization of the deoxyhemoglobin binding site on human erythrocyte band 3: implications for O2 regulation of erythrocyte properties. Blood 2008;**111**: 932-8.

160. D'Alessandro A, Gevi F, Zolla L. Red blood cell metabolism under prolonged anaerobic storage. Mol Biosyst 2013;**9**: 1196-209.

161. Dunham A, Yoshida T, Cordero R, Keegan P, Hemanext: device and method for establishing and maintaining controlled oxygen environment for storage of red blood cells. Vox Sang 2016;**111**: 53.

162. Harboe M. A method for determination of hemoglobin in plasma by near-ultraviolet spectrophotometry. Scand J Clin Lab Invest 1959;**11**: 66-70.

163. Noe DA, Weedn V, Bell WR. Direct spectrophotometry of serum hemoglobin: an Allen correction compared with a three-wavelength polychromatic analysis. Clin Chem 1984;**30**: 627-30.

164. Crescentini G, Stocchi V. Fast reversed-phase high-performance liquid chromatographic determination of nucleotides in red blood cells. J Chromatogr 1984;**290**: 393-9.

165. Usry RT, Moore GL, Manalo FW. Morphology of stored, rejuvenated human erythrocytes. Vox Sang 1975;**28**: 176-83.

166. Dodge JT, Mitchell C, Hanahan DJ. The preparation and chemical characteristics of hemoglobin-free ghosts of human erythrocytes. Arch Biochem Biophys 1963;**100**: 119-30.

167. Aggarwal K, Choe LH, Lee KH. Shotgun proteomics using the iTRAQ isobaric tags. Brief Funct Genomic Proteomic 2006;**5**: 112-20.

168. Rappsilber J, Ishihama Y, Mann M. Stop and go extraction tips for matrix-assisted laser desorption/ionization, nanoelectrospray, and LC/MS sample pretreatment in proteomics. Anal Chem 2003;**75**: 663-70.

169. Van 't Erve TJ, Wagner BA, Martin SM, *et al*. The heritability of hemolysis in stored human red blood cells. Transfusion 2015;**55**: 1178-85.

170. Bandyopadhyay S, Hod E, Francis R, *et al*. Refrigerator-stored red cells from iron deficient donor mice have reduced 24-hour post-transfusion recovery. Transfusion 2015;**55**: P5-030A.

171. Dinkla S, Peppelman M, Van Der Raadt J, *et al*. Phosphatidylserine exposure on stored red blood cells as a parameter for donor-dependent variation in product quality. Blood Transfus 2014;**12**: 204-9.

172. Greenwalt TJ, McGuinness CG, Dumaswala UJ. Studies in red blood cell preservation: 4. Plasma vesicle hemoglobin exceeds free hemoglobin. Vox Sang 1991;**61**: 14-7.

173. Hess JR. Red cell changes during storage. Transfus Apher Sci 2010;**43**: 51-9.

174. Chen D, Serrano K, Devine DV. Introducing the red cell storage lesion. ISBT Science Series. 2016;**11**: 26-33.

175. Tabb DL, Vega-Montoto L, Rudnick PA, *et al*. Repeatability and reproducibility in proteomic identifications by liquid chromatography-tandem mass spectrometry. J Proteome Res 2010;**9**: 761-76.

176. Schubert P, Culibrk B, Karwal S, Goodrich RP, Devine DV. Protein translation occurs in platelet concentrates despite riboflavin/UV light pathogen inactivation treatment. Proteomics Clin Appl 2016.

177. Karp NA, Huber W, Sadowski PG, *et al*. Addressing accuracy and precision issues in iTRAQ quantitation. Mol Cell Proteomics 2010;**9**: 1885-97.

178. Burkhart JM, Vaudel M, Zahedi RP, Martens L, Sickmann A. iTRAQ protein quantification: a quality-controlled workflow. Proteomics 2011;**11**: 1125-34.

179. Chen D, Schubert P, Devine DV. Identification of potential protein quality markers in pathogen inactivated and gamma-irradiated red cell concentrates. Proteomics Clin Appl 2017; **11** : 201600121.

180. Nikolovski Z, De La Torre C, *et al*. Alterations of the erythrocyte membrane proteome and cytoskeleton network during storage--a possible tool to identify autologous blood transfusion. Drug Test Anal 2012;**4**: 882-90.

181. Geng Q, Romero J, Saini V, Patel MB, Majetschak M. Extracellular 20S proteasomes accumulate in packed red blood cell units. Vox Sang 2009;**97**: 273-4.

182. Reisz JA, Wither MJ, Dzieciatkowska M, *et al*. Oxidative modifications of glyceraldehyde 3-phosphate dehydrogenase regulate metabolic reprogramming of stored red blood cells. Blood 2016;**128**: e32-42.

183. Wither M, Dzieciatkowska M, Nemkov T, *et al*. Hemoglobin oxidation at functional amino acid residues during routine storage of red blood cells. Transfusion 2016;**56**: 421-6.

184. Harper VM, Oh JY, Stapley R, *et al*. Peroxiredoxin-2 recycling is inhibited during erythrocyte storage. Antioxid Redox Signal 2015;**22**: 294-307.

185. Raval JS, Waters JH, Seltsam A, *et al*. The use of the mechanical fragility test in evaluating sublethal RBC injury during storage. Vox Sang 2010;**99**: 325-31.

186. Anderson KC, Weinstein HJ. Transfusion-associated graft-versus-host disease. N Engl J Med 1990;**323**: 315-21.

187. Treleaven J, Gennery A, Marsh J, *et al*. Guidelines on the use of irradiated blood components prepared by the British Committee for Standards in Haematology blood transfusion task force. Br J Haematol 2011;**152**: 35-51.

188. Fast LD, Nevola M, Tavares J, *et al*. Treatment of whole blood with riboflavin plus ultraviolet light, an alternative to gamma irradiation in the prevention of transfusion-associated graft-versus-host disease? Transfusion 2013;**53**: 373-81.

189. Schubert P, Culibrk B, Karwal S, *et al*. Whole blood treated with riboflavin and ultraviolet light: quality assessment of all blood components produced by the buffy coat method. Transfusion 2015;**55**: 815-23.

190. Sowemimo-Coker SO. Red blood cell hemolysis during processing. Transfus Med Rev 2002;**16**: 46-60.

191. Antonelou MH, Kriebardis AG, Stamoulis KE, *et al*. Red blood cell aging markers during storage in citrate-phosphate-dextrose-saline-adenine-glucose-mannitol. Transfusion 2010;**50**: 376-89.

192. Kucherenko YV, Bernhardt I. Natural antioxidants improve red blood cell "survival" in non-leukoreduced blood samples. Cell Physiol Biochem 2015;**35**: 2055-68.

193. Larsson A, Hult A, Nilsson A, Olsson M, Oldenborg PA. Red blood cells with elevated cytoplasmic Ca(2+) are primarily taken up by splenic marginal zone macrophages and CD207+ dendritic cells. Transfusion 2016;**56**: 1834-44.

194. Lang E, Pozdeev VI, Xu HC, *et al*. Storage of Erythrocytes Induces Suicidal Erythrocyte Death. Cell Physiol Biochem 2016;**39**: 668-76.

195. Lang F, Qadri SM. Mechanisms and significance of eryptosis, the suicidal death of erythrocytes. Blood Purif 2012;**33**: 125-30.

196. Wolfe LC. Oxidative injuries to the red cell membrane during conventional blood preservation. Semin Hematol 1989;**26**: 307-12.

197. Chiu D, Kuypers F, Lubin B. Lipid peroxidation in human red cells. Semin Hematol 1989;**26**: 257-76.

198. Hebbel RP, Leung A, Mohandas N. Oxidation-induced changes in microrheologic properties of the red blood cell membrane. Blood 1990;**76**: 1015-20.

199. Kriebardis AG, Antonelou MH, Stamoulis KE, *et al*. Progressive oxidation of cytoskeletal proteins and accumulation of denatured hemoglobin in stored red cells. J Cell Mol Med 2007;**11**: 148-55.

200. Kim YK, Kwon EH, Kim DH, *et al*. Susceptibility of oxidative stress on red blood cells exposed to gamma rays: hemorheological evaluation. Clin Hemorheol Microcirc 2008;**40**: 315-24.

201. Zolla L, D'Alessandro A. An efficient apparatus for rapid deoxygenation of erythrocyte concentrates for alternative banking strategies. J Blood Transfus 2013;**2013**: 896537.

202. Yoshida T, AuBuchon JP, Dumont LJ, *et al*. The effects of additive solution pH and metabolic rejuvenation on anaerobic storage of red cells. Transfusion 2008;**48**: 2096-105.

203. Pallotta V, Gevi F, D'alessandro A, Zolla L. Storing red blood cells with vitamin C and N-acetylcysteine prevents oxidative stress-related lesions: a metabolomics overview. Blood Transfus 2014;**12**: 376-87.

204. Arun P, Padmakumaran Nair KG, Manojkumar V, *et al*. Decreased hemolysis and lipid peroxidation in blood during storage in the presence of nicotinic acid. Vox Sang 1999;**76**: 220-5.

205. Longo V, Marrocco C, Zolla L, Rinalducci S. Label-free quantitation of phosphopeptide changes in erythrocyte membranes: towards molecular mechanisms underlying deformability alterations in stored red blood cells. Haematologica 2014;**99**: e122-5.

206. Fujino T, Watanabe K, Beppu M, Kikugawa K, Yasuda H. Identification of oxidized protein hydrolase of human erythrocytes as acylpeptide hydrolase. Biochim Biophys Acta 2000;**1478**: 102-12.

207. De Palma A, Roveri A, Zaccarin *et al*. Extraction methods of red blood cell membrane proteins for Multidimensional Protein Identification Technology (MudPIT) analysis. J Chromatogr A 2010;**1217**: 5328-36.

208. Schubert P, Culibrk B, Serrano K, *et al*. Improvement of Red Cell Quality upon Pathogen Inactivation of Whole Blood using Riboflavin/UV light by Deoxygenation. Transfusion 2016;**56**: SP42.

209. Moroff G, Holme S, AuBuchon JP, *et al*. Viability and in vitro properties of AS-1 red cells after gamma irradiation. Transfusion 1999;**39**: 128-34.

210. Cancelas JA, Rugg N, Fletcher D, *et al*. In vivo viability of stored red blood cells derived from riboflavin plus ultraviolet light-treated whole blood. Transfusion 2011;**51**: 1460-8.

211. Grinberg L, Fibach E, Amer J, Atlas D. N-acetylcysteine amide, a novel cell-permeating thiol, restores cellular glutathione and protects human red blood cells from oxidative stress. Free Radic Biol Med 2005;**38**: 136-45.

212. Amen F, Machin A, Touriño C, *et al*. N-acetylcysteine improves the quality of red blood cells stored for transfusion. Arch Biochem Biophys 2017;**621**: 31-7.

213. Yoshida T, AuBuchon JP, Tryzelaar L, Foster KY, Bitensky MW. Extended storage of red blood cells under anaerobic conditions. Vox Sang 2007;**92**: 22-31.

214. Dumont LJ, D'Alessandro A, Szczepiorkowski ZM, Yoshida T. CO_2 -dependent metabolic modulation in red blood cells stored under anaerobic conditions. Transfusion 2016;**56**: 392-403.

215. Robertson OH. Transfusion with preserved red blood cells. Br Med J 1918;**1**: 691-5.

216. Sasakawa S, Tokunaga E. Physical and chemical changes of ACD-preserved blood: a comparison of blood in glass bottles and plastic bags. Vox Sang 1976;**31?-73**: 199-210.

217. Walter CW, Murphy WP. A closed gravity technique for the preservation of whole blood in ACD solution utilizing plastic equipment. Surg Gynecol Obstet 1952;**94**: 687-92.

218. Loiselle JM, Hudon F. The presevation of human blood in glass and plastic containers: an in vitro evaluation. Can Anaesth Soc J 1960;**7**: 60-3.

219. Scott MD, Zuo L, Lubin BH, Chiu DT. NADPH, not glutathione, status modulates oxidant sensitivity in normal and glucose-6-phosphate dehydrogenase-deficient erythrocytes. Blood 1991;**77**: 2059-64.

220. Scott MD, Wagner TC, Chiu DT. Decreased catalase activity is the underlying mechanism of oxidant susceptibility in glucose-6-phosphate dehydrogenase-deficient erythrocytes. Biochim Biophys Acta 1993;**1181**: 163-8.

221. Rachmilewitz EA, Peisach J, Blumberg WE. Studies on the stability of oxyhemoglobin A and its constituent chains and their derivatives. J Biol Chem 1971;**246**: 3356-66.

222. Karon BS, van Buskirk CM, Jaben EA, Hoyer JD, Thomas DD. Temporal sequence of major biochemical events during blood bank storage of packed red blood cells. Blood Transfus 2012;**10**: 453-61.

223. Lim YS, Cha MK, Yun CH, *et al*. Purification and characterization of thiol-specific antioxidant protein from human red blood cell: a new type of antioxidant protein. Biochem Biophys Res Commun 1994;**199**: 199-206.

224. Cha MK, Yun CH, Kim IH. Interaction of human thiol-specific antioxidant protein 1 with erythrocyte plasma membrane. Biochemistry 2000;**39**: 6944-50.

225. Rocha S, Costa E, Coimbra S, *et al*. Linkage of cytosolic peroxiredoxin 2 to erythrocyte membrane imposed by hydrogen peroxide-induced oxidative stress. Blood Cells Mol Dis 2009;**43**: 68-73.

226. Salo DC, Lin SW, Pacifici RE, Davies KJ. Superoxide dismutase is preferentially degraded by a proteolytic system from red blood cells following oxidative modification by hydrogen peroxide. Free Radic Biol Med 1988;**5**: 335-9.

227. Delobel J, Prudent M, Rubin O, *et al*. Subcellular fractionation of stored red blood cells reveals a compartment-based protein carbonylation evolution. J Proteomics 2012;**76 Spec No.**: 181-93.

228. Antonelou MH, Kriebardis AG, Stamoulis KE, Trougakos IP, Papassideri IS. Apolipoprotein J/clusterin in human erythrocytes is involved in the molecular process of defected material disposal during vesiculation. PLoS One 2011;**6**: e26033.

229. Antonelou MH, Kriebardis AG, Stamoulis KE, Trougakos IP, Papassideri IS. Apolipoprotein J/Clusterin is a novel structural component of human erythrocytes and a biomarker of cellular stress and senescence. PLoS One 2011;**6**: e26032.

230. Greenberg JH, Parikh CR. Biomarkers for Diagnosis and Prognosis of AKI in Children: One Size Does Not Fit All. Clin J Am Soc Nephrol 2017; **12**: 1551-7.

231. Jin G, Zhou X, Wang H, *et al*. The knowledge-integrated network biomarkers discovery for major adverse cardiac events. J Proteome Res 2008;**7**: 4013-21.

232. Paglia G, Sigurjónsson Ó, Bordbar A, *et al*. Metabolic fate of adenine in red blood cells during storage in SAGM solution. Transfusion 2016;**56**: 2538-47.

233. Gevi F, D'Alessandro A, Rinalducci S, Zolla L. Alterations of red blood cell metabolome during cold liquid storage of erythrocyte concentrates in CPD-SAGM. J Proteomics 2012;**76 Spec No.**: 168-80.

234. Bordbar A, Johansson PI, Paglia G, *et al*. Identified metabolic signature for assessing red blood cell unit quality is associated with endothelial damage markers and clinical outcomes. Transfusion 2016;**56**: 852-62.

235. Paglia G, D'Alessandro A, Rolfsson Ó, *et al*. Biomarkers defining the metabolic age of red blood cells during cold storage. Blood 2016;**128**: e43-50.

236. Rinalducci S, Marrocco C, Zolla L. Thiol-based regulation of glyceraldehyde-3-phosphate dehydrogenase in blood bank-stored red blood cells: a strategy to counteract oxidative stress. Transfusion 2015;**55**: 499-506.

237. Fu X, Felcyn JR, Odem-Davis K, Zimring JC. Bioactive lipids accumulate in stored red blood cells despite leukoreduction: a targeted metabolomics study. Transfusion 2016;**56**: 2560-70.

238. Kleinman S, Busch MP, Murphy EL, *et al.* The National Heart, Lung, and Blood Institute Recipient Epidemiology and Donor Evaluation Study (REDS-III): a research program striving to improve blood donor and transfusion recipient outcomes. Transfusion 2014;**54**: 942-55.

239. Bütikofer P, Kuypers FA, Xu CM, Chiu DT, Lubin B. Enrichment of two glycosyl-phosphatidylinositol-anchored proteins, acetylcholinesterase and decay accelerating factor, in vesicles released from human red blood cells. Blood 1989;**74**: 1481-5.

240. Butikofer P, Chiu DT, Lubin B, Kuypers FA. Preferential Release of Glycosyl-Phosphatidylinositol Anchored Proteins from Human Red Blood Cells during Vesiculation.: Springer, 1990; 29-41.

241. Almeida, JP, Carvalho F, Martins-Silva J, Saldanha C. The modulation o f cyclic nucleotide levels and PKC activity by acetylcholinesterase effectors in human erythrocytes. Acta Bioquímica 2008;**9**: 111–4.

242. Vaughn MW, Huang KT, Kuo L, Liao JC. Erythrocytes possess an intrinsic barrier to nitric oxide consumption. J Biol Chem 2000;**275**: 2342-8.

243. Huang KT, Han TH, Hyduke DR,*et al*. Modulation of nitric oxide bioavailability by erythrocytes. Proc Natl Acad Sci U S A 2001;**98**: 11771-6.

244. Sun X, Funk CD, Deng C, *et al.* Role of decay-accelerating factor in regulating complement activation on the erythrocyte surface as revealed by gene targeting. Proc Natl Acad Sci U S A 1999;**96**: 628-33.

Appendices

Appendix A Supplementary Data for Chapter 3

Table A.1. Comparative summary of two study donor population characteristics.

	RCC^{HH}	RCC^{Ctrl}	P value
Number of Donations (past 12 months)	3.90 ± 0.60	3.10 ± 0.48	*> 0.05*
ABO Distribution			*< 0.01*
O	0	3	
A	0	6	
B	7	1	
AB	3	0	
Age at time of Donation	48.30 ± 4.46	47.70 ± 4.45	*> 0.05*
RCC Volume	314.00 ± 6.79	299.10 ± 8.94	*> 0.05*
Production Method			*> 0.05*
Buffy Coat	2	4	
Whole Blood Filtration	8	6	

Table A.2 Summary of two independent iTRAQ experiements showing the changes in protein level at the RBC membrane.

Highlighted proteins are included in **Table 3.2,** as they meet the inclusion criteria. Ratios/changes of RCC^{HH} day 5, RCC^{HH} day 42, and RCC^{Ctrl} day 42 ghost fractions (isotype label 114, 115, and 117, respectively) relative to the RCC^{Ctrl} day 5 ghost fractions (isotype label 116) are displayed. Protein candidates mutual to both experiments were considered for further analyses. The average of the iTRAQ results are shown.

	iTRAQ #1 (Donor Pair #3)			iTRAQ #2 (Donor Pair #8)			Mutual		
Description	114/116	115/116	117/116	114/116	115/116	117/116	114/116	115/116	117/116
26S proteasome non-ATPase regulatory subunit 11 (Fragment)				0.589	0.781	0.829			
26S proteasome non-ATPase regulatory subunit 3				0.243	0.610	0.509			
55 kDa erythrocyte membrane protein (Fragment)	0.910	0.738	0.884	0.843	0.878	0.953	0.877	0.808	0.919
Actin, cytoplasmic 1	0.945	0.790	0.938	0.897	1.007	0.958	0.921	0.899	0.948
Acylamino-acid-releasing enzyme (Fragment)	0.106	0.080	1.047						
Alpha-adducin	0.733	0.607	0.875	0.586	0.828	0.675	0.659	0.717	0.775
Ammonium transporter Rh type A	1.096	0.644	0.836						
Ankyrin repeat domain-containing protein 24 (Fragment)	1.175	0.810	1.314	0.933	1.019	1.009	1.054	0.915	1.162
Ankyrin-1	1.009	0.738	0.960	0.903	0.986	1.032	0.956	0.862	0.996
Aquaporin-1	0.922	0.652	0.952	1.039	1.106	0.999	0.981	0.879	0.976
Arginase-1	1.147	0.703	0.766	1.665	0.863	0.817	1.406	0.783	0.791
ATP-binding cassette sub-family B member 6, mitochondrial (Fragment)	0.815	0.620	0.824	1.026	1.108	1.041	0.920	0.864	0.932
ATP-citrate synthase	0.415	0.519	1.352	0.791	1.058	1.256	0.603	0.789	1.304
Band 3 anion transport protein	1.064	0.973	0.978	0.973	1.040	0.945	1.018	1.007	0.962
Basal cell adhesion molecule (Fragment)	1.016	0.665	0.926	0.872	0.897	1.006	0.944	0.781	0.966
Basigin (Fragment)	1.128	0.728	1.036	1.096	1.075	1.038	1.112	0.901	1.037
Beta-adducin	0.768	0.595	0.873	0.608	0.786	0.677	0.688	0.691	0.775
C-1-tetrahydrofolate synthase, cytoplasmic	0.706	0.329	0.506	1.431	0.695	0.637	1.068	0.512	0.571
Calmodulin	0.769	0.851	1.053						
Calnexin (Fragment)	1.107	0.852	1.000						
Calpain-5				1.322	1.430	1.042			
Calpastatin (Fragment)	1.054	0.844	0.644						

Description	iTRAQ #1 (Donor Pair #3)			iTRAQ #2 (Donor Pair #8)			Mutual		
	114/116	115/116	117/116	114/116	115/116	117/116	114/116	115/116	117/116
Calreticulin				1.471	1.572	1.051			
Catalase	0.169	0.139	1.193	0.068	0.135	0.360	0.118	0.137	0.777
CB1 cannabinoid receptor-interacting protein 1				1.018	0.778	0.813			
CD44 antigen (Fragment)	1.017	0.762	1.051	1.055	1.108	0.896	1.036	0.935	0.974
CD59 glycoprotein	1.068	0.585	1.268	0.912	0.881	1.011	0.990	0.733	1.140
Cell division control protein 42 homolog (Fragment)	0.634	0.590	0.851	0.684	1.052	0.890	0.659	0.821	0.871
Cytochrome b reductase 1	1.359	0.938	0.802	0.759	0.699	0.584	1.059	0.818	0.693
Dematin	1.278	0.997	1.047	0.926	0.978	0.897	1.102	0.987	0.972
Elongation factor 1-alpha 1				1.495	1.260	0.814			
Endonuclease domain-containing 1 protein	0.721	0.590	0.830	1.109	1.282	1.122	0.915	0.936	0.976
Equilibrative nucleoside transporter 1	1.178	0.888	0.831	0.907	0.993	0.893	1.042	0.941	0.862
Erythrocyte band 7 integral membrane protein	1.073	0.712	0.907	0.964	0.928	0.959	1.018	0.820	0.933
Erythrocyte membrane protein band 4.2	0.949	0.711	0.906	1.054	1.127	1.004	1.001	0.919	0.955
Erythroid membrane-associated protein	0.474	0.376	0.920	0.893	0.938	1.085	0.684	0.657	1.003
Fibrous sheath-interacting protein 2	0.956	0.737	1.088						
Flotillin-1	0.851	0.674	0.939	1.043	1.037	1.081	0.947	0.856	1.010
Flotillin-2	0.914	0.678	1.015	1.007	1.054	1.065	0.961	0.866	1.040
Fructose-bisphosphate aldolase	1.947	1.250	0.948	4.008	1.809	1.718	2.977	1.530	1.333
Glutaminyl-peptide cyclotransferase (Fragment)	0.645	0.948	0.429						
Glyceraldehyde-3-phosphate dehydrogenase	1.117	0.784	0.928	2.109	1.559	1.249			
Glycophorin Erik I-IV				1.038	1.043	0.858	1.038	1.043	0.858
Glycophorin-C	0.995	0.704	0.849	0.978	0.878	0.845	0.987	0.791	0.847
Golgi-associated plant pathogenesis-related protein 1	1.111	0.845	1.001	0.744	0.806	1.031	0.928	0.826	1.016
Guanine nucleotide-binding protein G(I)/G(S)/G(O) subunit gamma-5	1.156	0.783	0.869						
Guanine nucleotide-binding protein G(I)/G(S)/G(T) subunit beta-2	1.178	0.834	0.917	0.901	0.930	0.902	1.040	0.882	0.910
Heat shock cognate 71 kDa protein	0.445	0.822	1.590	0.531	1.166	0.843	0.488	0.994	1.217
Hemoglobin subunit alpha	0.774	1.543	0.926	0.533	0.732	0.726	0.653	1.137	0.826
Hemoglobin subunit beta	0.645	1.094	0.973						

Description	iTRAQ #1 (Donor Pair #3)			iTRAQ #2 (Donor Pair #8)			Mutual		
	114/116	115/116	117/116	114/116	115/116	117/116	114/116	115/116	117/116
Hemoglobin subunit delta	2.551	4.343	1.014	2.455	1.116	0.886	2.503	2.730	0.950
Ig gamma-1 chain C region (Fragment)				0.465	1.117	0.448			
Kell blood group glycoprotein				0.953	0.996	0.975			
Kinesin-like protein				0.923	1.018	1.047			
Leukocyte surface antigen CD47	0.948	0.654	0.935	0.791	0.925	1.063	0.870	0.789	0.999
Membrane transport protein XK	0.859	0.625	0.850	1.079	1.074	0.921	0.969	0.849	0.885
Peroxiredoxin-2	0.041	0.035	1.051	0.040	0.157	0.419	0.040	0.096	0.735
Phosphatidylinositol 5-phosphate 4-kinase type-2 alpha	0.723	0.735	1.108	0.400	0.889	0.587	0.562	0.812	0.847
Plasma membrane calcium-transporting ATPase 4	1.073	0.855	0.934	0.936	1.002	1.093	1.005	0.929	1.014
Polypyrimidine tract-binding protein 1 (Fragment)	1.295	1.003	0.886						
Protease serine 1	0.910	0.924	0.674						
Proteasome activator complex subunit 1	0.070	0.059	0.952	0.031	0.285	0.379	0.050	0.172	0.665
Proteasome activator complex subunit 2	0.124	0.096	1.004						
Proteasome subunit alpha type	0.118	0.090	0.905	0.167	0.406	0.506	0.143	0.248	0.706
Proteasome subunit alpha type-1				0.072	0.351	0.427			
Proteasome subunit alpha type-3				0.354	0.577	0.511			
Proteasome subunit alpha type-5	0.180	0.198	0.921	0.119	0.371	0.466	0.150	0.284	0.694
Proteasome subunit alpha type-7	0.125	0.097	0.900						
Proteasome subunit beta type-1	0.567	0.285	0.941	0.114	0.350	0.436	0.341	0.318	0.688
Proteasome subunit beta type-2	0.112	0.089	0.894	0.042	0.339	0.380	0.077	0.214	0.637
Proteasome subunit beta type-3				0.074	0.285	0.383			
Proteasome subunit beta type-4	0.133	0.095	0.744	0.097	0.345	0.481	0.115	0.220	0.612
Proteasome subunit beta type-6 (Fragment)				0.148	0.371	0.475			
Proteasome subunit beta type-7	0.191	0.156	0.926	0.133	0.369	0.455	0.162	0.262	0.690
Protein 4.1	0.964	0.775	0.973	0.960	1.025	0.964	0.962	0.900	0.969
Protein argonaute-2	0.758	0.582	0.926	0.981	0.978	0.953	0.870	0.780	0.939
Protein Jade-3 (Fragment)	0.983	0.792	0.945	1.237	0.992	1.102	1.110	0.892	1.023
Proteolipid protein 2				0.985	1.169	0.970			

Description	iTRAQ #1 (Donor Pair #3)			iTRAQ #2 (Donor Pair #8)			Mutual		
	114/116	115/116	117/116	114/116	115/116	117/116	114/116	115/116	117/116
Protocadherin-1 (Fragment)	0.180	0.248	0.612	0.701	0.822	0.593	0.441	0.535	0.602
Ras homolog gene family, member C	0.804	0.665	0.956						
Ras-related C3 botulinum toxin substrate 1	1.006	0.583	1.017						
Ras-related protein Rab-10				1.084	1.105	1.094			
Ras-related protein Rab-21				1.101	1.103	1.021			
Ras-related protein Ral-A				0.723	0.882	0.837			
Ras-related protein Rap-1a	0.988	0.710	0.864						
Ras-related protein Rap-1b				0.661	0.606	0.746			
Ras-related protein Rap-2a				0.820	0.691	0.872			
Ras-related protein Rap-2b	0.953	0.614	0.878						
Solute carrier family 2, facilitated glucose transporter member 1	1.128	0.821	0.970	1.119	1.167	0.991	1.123	0.994	0.981
Solute carrier family 43 member 3 (Fragment)				1.132	1.352	1.674			
Sorbitol dehydrogenase	1.023	0.733	0.846	2.516	1.972	1.146	1.769	1.352	0.996
Spectrin alpha chain, erythrocytic 1	1.059	0.769	1.060	1.025	1.063	1.019	1.042	0.916	1.040
Spectrin beta chain, erythrocytic	1.084	0.786	1.041	1.062	1.082	1.016	1.073	0.934	1.029
Sulfotransferase (Fragment)	1.002	0.807	0.968	0.786	0.862	0.923	0.894	0.835	0.945
Syntaxin-7	0.987	0.805	1.043	0.807	1.242	0.932	0.897	1.024	0.988
T-complex protein 1 subunit alpha	0.561	0.401	0.854						
T-complex protein 1 subunit delta	0.205	0.184	1.092						
T-complex protein 1 subunit eta (Fragment)	0.161	0.216	0.975						
Thioredoxin (Fragment)				1.462	1.472	1.013			
Transitional endoplasmic reticulum ATPase	0.106	0.083	0.946	0.121	0.426	0.428	0.114	0.255	0.687
Tropomodulin-1	0.955	0.744	0.890	0.953	1.054	0.976	0.954	0.899	0.933
Tropomyosin 1 (Alpha), isoform CRA_m	0.463	0.451	0.908	0.326	0.500	0.424	0.395	0.476	0.666
Tropomyosin alpha-3 chain	0.727	0.581	0.821	0.567	0.678	0.575	0.647	0.629	0.698
Ubiquitin-60S ribosomal protein L40 (Fragment)	0.618	0.453	0.791	1.051	0.954	0.835	0.834	0.704	0.813
Uncharacterized protein (Fragment)				0.983	1.129	0.834			
UPF0317 protein C14orf159, mitochondrial (Fragment)	1.132	0.698	1.161	1.054	1.104	1.020	1.093	0.901	1.090

Description	iTRAQ #1 (Donor Pair #3)			iTRAQ #2 (Donor Pair #8)			Mutual		
	114/116	115/116	117/116	114/116	115/116	117/116	114/116	115/116	117/116
Urea transporter 1 (Fragment)	0.922	0.760	0.799	0.862	0.940	0.415	0.892	0.850	0.607
Zinc finger protein 40 (Fragment)	0.692	0.558	0.818	0.544	0.645	0.564	0.618	0.601	0.691

Appendix B Supplementary Data for Chapter 4

Table B.1 Summary of two independent iTRAQ experiments showing the changes in protein level at the RBC membrane

Highlighted proteins are included in **Table 4.1**, as they meet the inclusion criteria. Ratios/changes of $RCC^{Ø}$, RCC^{PI}, and RCC^{Y} ghost fractions on day 28 (isotype label 115, 116, and 117, respectively) relative to the $RCC^{Ø}$ day 5 ghost fractions (isotype label 114) on day 5 are displayed. Protein candidates mutual to both experiments were considered for further analyses. The averages of the iTRAQ results are shown.

	iTRAQ #1			iTRAQ #2			Mutual		
Description	115/114	116/114	117/114	115/114	116/114	117/114	115/114	116/114	117/114
2',3'-cyclic-nucleotide 3'-phosphodiesterase (Fragment)	0.828	0.958	1.062						
26S proteasome non-ATPase regulatory subunit 11 (Fragment)				0.857	0.685	0.893			
55 kDa erythrocyte membrane protein	0.880	1.051	1.145	0.920	1.165	1.260	0.900	1.108	1.202
Actin, cytoplasmic 1	0.908	1.091	1.130	0.857	0.902	0.999	0.883	0.997	1.065
Acylamino-acid-releasing enzyme (Fragment)	0.937	0.431	0.781	0.913	0.340	0.661	0.925	0.386	0.721
Alpha-adducin	0.722	0.805	0.944	0.720	0.725	0.816	0.721	0.765	0.880
Alpha-trypsin chain 2 (Fragment)	0.952	1.117	1.246						
Ammonium transporter Rh type A	0.887	1.707	1.477						
Ankyrin-1	0.894	1.056	1.152	0.826	0.926	1.049	0.860	0.991	1.100
Aquaporin-1	0.924	1.135	1.203	0.970	1.121	1.261	0.947	1.128	1.232
Arginase-1	0.530	0.591	0.739	1.018	1.080	1.350	0.774	0.836	1.045
ATP-binding cassette sub-family B member 6, mitochondrial (Fragment)				0.755	0.933	1.029			
ATP-citrate synthase (Fragment)	1.137	1.270	1.455	1.130	1.174	1.456	1.134	1.222	1.455
Band 3 anion transport protein	0.895	1.053	1.131	0.846	0.924	1.024	0.870	0.989	1.078
Basal cell adhesion molecule (Fragment)				0.861	0.888	1.023			
Beta-adducin	0.737	0.840	0.956	0.675	0.776	0.908	0.706	0.808	0.932
Blood group Rh(CE) polypeptide	0.848	1.222	1.211						
C-1-tetrahydrofolate synthase, cytoplasmic				0.616	0.776	0.840			

	iTRAQ #1			iTRAQ #2			Mutual		
Description	115/114	116/114	117/114	115/114	116/114	117/114	115/114	116/114	117/114
Calpain-5				0.796	0.822	0.946			
Calreticulin (Fragment)	0.873	0.976	1.112	0.791	0.811	0.938	0.832	0.894	1.025
Catalase	1.118	0.490	0.911	0.873	0.284	0.502	0.996	0.387	0.707
Cathepsin E				1.124	1.374	1.112			
CB1 cannabinoid receptor-interacting protein 1	0.915	1.466	1.259						
CD59 glycoprotein	0.959	1.020	1.174	0.886	0.954	1.148	0.922	0.987	1.161
CDGSH iron-sulfur domain-containing protein 2	0.901	1.031	1.124						
Cell division control protein 42 homolog (Fragment)	0.725	0.954	0.929	0.679	0.730	0.861	0.702	0.842	0.895
Cytochrome b reductase 1	0.823	0.965	1.057	0.357	0.386	0.815	0.590	0.675	0.936
Dematin	0.987	1.225	1.163	0.960	1.219	1.280	0.974	1.222	1.221
Endonuclease domain-containing 1 protein	0.808	0.861	0.979	0.841	0.805	0.910	0.825	0.833	0.944
Equilibrative nucleoside transporter 1	1.002	1.477	1.513	0.669	0.886	0.994	0.835	1.181	1.254
Erythrocyte band 7 integral membrane protein	0.927	1.158	1.236	0.805	0.855	0.984	0.866	1.006	1.110
Erythrocyte membrane protein band 4.2	0.919	1.292	1.287	0.816	0.884	1.031	0.867	1.088	1.159
Erythroid membrane-associated protein	1.064	1.248	1.294	0.801	0.886	1.021	0.932	1.067	1.157
Fibrous sheath-interacting protein 2	0.931	1.059	1.175	0.883	0.943	1.096	0.907	1.001	1.136
Flotillin-1	0.850	1.036	1.094	0.858	0.891	1.017	0.854	0.964	1.056
Flotillin-2	0.914	1.009	1.066	0.808	0.926	1.036	0.861	0.968	1.051
Fructose-bisphosphate aldolase C	0.698	0.621	0.812	1.095	1.120	1.379	0.896	0.870	1.096
Fructose-bisphosphate aldolase	0.769	0.794	0.919	1.131	1.385	1.694	0.950	1.090	1.306
Glutaminyl-peptide cyclotransferase (Fragment)	0.920	2.075	1.761						
Glyceraldehyde-3-phosphate dehydrogenase	0.673	0.786	0.862	1.345	1.760	1.991	1.009	1.273	1.427
Glycophorin Erik I-IV	1.461	2.798	2.126						
Glycophorin-C	0.854	1.060	1.119	0.806	0.767	0.918	0.830	0.913	1.018
Golgi-associated plant pathogenesis-related protein 1	0.861	0.902	1.021	0.957	0.952	1.065	0.909	0.927	1.043
Guanine nucleotide-binding protein G(I)/G(S)/G(T) subunit beta-1	0.907	0.976	1.055						
Guanine nucleotide binding protein (G protein), beta polypeptide 1 (Fragment)				0.725	0.855	1.136			
Heat shock cognate 71 kDa protein (Fragment)	0.627	0.734	0.819						

	iTRAQ #1			iTRAQ #2			Mutual		
Description	115/114	116/114	117/114	115/114	116/114	117/114	115/114	116/114	117/114
Heat shock protein 75 kDa, mitochondrial (Fragment)	0.642	0.544	0.699						
Heat shock protein HSP 90-alpha				0.957	0.478	0.795			
Hemoglobin subunit alpha	0.883	0.914	1.010	0.641	0.779	0.968	0.762	0.847	0.989
Hemoglobin subunit beta	0.976	1.225	1.225						
Hemoglobin subunit delta (Fragment)	0.955	1.326	1.202	0.837	0.915	1.029	0.896	1.120	1.115
Kell blood group glycoprotein	0.859	0.944	1.047	0.964	0.750	0.929	0.912	0.847	0.988
Keratin, type II cytoskeletal 1				0.276	0.782	0.566			
Leukocyte surface antigen CD47	0.904	1.181	1.269	0.946	1.012	1.161	0.925	1.097	1.215
LVV-hemorphin-7 (Fragment)				0.696	0.764	0.930			
Membrane transport protein XK				0.769	0.849	0.892			
Peroxiredoxin-2	1.302	0.404	0.944	1.033	0.320	0.655	1.168	0.362	0.800
Peroxisomal membrane protein 11A				0.817	0.966	0.956			
Phosphatidylinositol 5-phosphate 4-kinase type-2 alpha				0.855	0.756	0.943			
Plasma membrane calcium-transporting ATPase 1	0.879	0.995	1.116	0.793	0.961	1.044	0.836	0.978	1.080
Proteasome activator complex subunit 1	0.608	0.315	0.579	0.846	0.387	0.709	0.727	0.351	0.644
Proteasome subunit alpha type	0.453	0.317	0.457	0.972	0.581	0.903	0.712	0.449	0.680
Proteasome subunit alpha type-5				0.978	0.544	0.910			
Proteasome subunit beta type-1				0.833	0.444	0.699			
Proteasome subunit beta type-7				0.846	0.468	0.766			
Protein 4.1	0.912	1.101	1.181	0.838	0.958	1.063	0.875	1.030	1.122
Protein argonaute-2	0.814	0.944	1.056	0.897	0.908	1.039	0.855	0.926	1.048
Protein Jade-3 (Fragment)	0.875	1.163	1.183						
Protein XRP2	0.892	1.013	1.074						
Proteolipid protein 2				0.877	1.057	1.140			
Protocadherin-1 (Fragment)	0.642	0.427	0.558	1.082	0.521	0.672	0.862	0.474	0.615
Ras-related C3 botulinum toxin substrate 3 (Fragment)	0.836	0.944	1.054	0.863	0.914	1.021	0.849	0.929	1.037
Ras-related protein Rab-10	0.973	0.918	1.019						
Ras-related protein Rab-35 (Fragment)	0.946	1.356	1.421						

	iTRAQ #1			iTRAQ #2			Mutual		
Description	115/114	116/114	117/114	115/114	116/114	117/114	115/114	116/114	117/114
Ras-related protein Ral-A (Fragment)				0.744	0.710	0.880			
Ras-related protein Rap-1b (Fragment)	0.746	0.978	0.984	0.695	0.766	0.889	0.721	0.872	0.936
Ras-related protein Rap-2a	0.786	0.800	0.937						
Ras-related protein Rap-2b				0.748	0.806	1.005			
Rho GDP-dissociation inhibitor 3 (Fragment)				0.606	0.395	0.680			
Rootletin				0.928	1.020	1.196			
Selenoprotein W				0.923	0.798	0.962			
Small integral membrane protein 5	0.904	1.696	1.420						
Small VCP/p97-interacting protein	0.938	1.118	1.213						
Solute carrier family 2, facilitated glucose transporter member 1	0.909	1.226	1.200	0.667	0.688	1.049	0.788	0.957	1.124
Solute carrier family 43 member 3 (Fragment)				0.895	1.237	1.824			
Spectrin alpha chain, erythrocytic 1	0.910	1.062	1.156	0.842	0.892	1.028	0.876	0.977	1.092
Spectrin beta chain, erythrocytic	0.904	1.071	1.152	0.819	0.843	0.982	0.862	0.957	1.067
Spermatogenesis-associated protein 16	0.861	0.960	1.096						
Sulfotransferase (Fragment)	0.967	1.159	1.283	0.839	1.025	1.156	0.903	1.092	1.220
Syntaxin-7				1.190	1.026	1.171			
Transitional endoplasmic reticulum ATPase	0.701	0.416	0.707	0.849	0.437	0.725	0.775	0.427	0.716
Tropomodulin-1	0.702	0.772	0.875	0.822	0.903	0.991	0.762	0.838	0.933
Tropomyosin 1 (Alpha), isoform CRA_m	0.602	0.529	0.715	0.655	0.530	0.676	0.629	0.529	0.696
Tropomyosin alpha-3 chain	0.658	0.764	0.826	0.649	0.623	0.762	0.653	0.694	0.794
Tudor domain-containing protein 5 (Fragment)	1.039	2.394	2.090						
Ubiquitin (Fragment)				0.775	1.003	1.072			
Ubiquitin-60S ribosomal protein L40 (Fragment)	0.887	1.336	1.413						
Uncharacterized protein (Fragment)	0.982	1.091	1.125	0.907	0.797	1.049	0.945	0.944	1.087
UPF0317 protein C14orf159, mitochondrial (Fragment)	0.894	1.074	1.208	0.901	0.909	1.089	0.898	0.991	1.148
Urea transporter 1	0.813	1.092	1.127	0.706	1.281	1.036	0.760	1.187	1.081